

UC San Diego

UC San Diego Electronic Theses and Dissertations

Title

Disturbance Cancellation by State Derivative Feedback with Application to Ramp-Connected Surface Effect Ships

Permalink

<https://escholarship.org/uc/item/2db004s6>

Author

Basturk, Halil I.

Publication Date

2013

Peer reviewed|Thesis/dissertation

UNIVERSITY OF CALIFORNIA, SAN DIEGO

**Disturbance Cancellation by State Derivative Feedback with
Application to Ramp-Connected Surface Effect Ships**

A dissertation submitted in partial satisfaction of the
requirements for the degree
Doctor of Philosophy

in

Engineering Sciences (Mechanical Engineering)

by

Halil I. Basturk

Committee in charge:

Professor Miroslav Krstic, Chair
Professor Thomas Bewley
Professor Raymond A. de Callafon
Professor Joel P. Conte
Professor Michael D. Todd

2013

Copyright
Halil I. Basturk, 2013
All rights reserved.

The dissertation of Halil I. Basturk is approved, and it is acceptable in quality and form for publication on microfilm and electronically:

Chair

University of California, San Diego

2013

DEDICATION

To my parents and my wife.

TABLE OF CONTENTS

Signature Page		iii
Dedication		iv
Table of Contents		v
List of Figures		vii
List of Tables		x
Acknowledgements		xi
Vita		xiii
Abstract of the Dissertation		xv
Chapter 1	Introduction	1
Chapter 2	Adaptive Cancellation of Unknown Sinusoidal Disturbances for Known LTI Systems by State Derivative Feedback	5
	2.1 Matched Unknown Sinusoidal Disturbance	6
	2.1.1 Problem Statement and Adaptive Controller Design	6
	2.1.2 Stability Proof	8
	2.1.3 Simulation Results	17
	2.2 Unmatched and Unknown Sinusoidal Disturbance	18
	2.2.1 Problem Statement and Backstepping Adaptive Controller Design	18
	2.2.2 Stability Proof	20
	2.2.3 Simulation Results	25
	2.3 Summary	26
Chapter 3	State Derivative Feedback for Adaptive Cancellation of Un- matched Disturbances in Unknown Strict-Feedback LTI Systems	28
	3.1 Problem Statement	29
	3.2 Main Result–Design and Stability Statement	30
	3.2.1 Disturbance Observer	31
	3.2.2 Reciprocal State-Space Representation	33
	3.2.3 Main Controller and Stability Statement	35
	3.3 Stability Proof	37
	3.4 Simulation Results	44
	3.5 Summary	44

Chapter 4	Adaptive Wave Cancelation by Acceleration Feedback for Ramp-Connected Air Cushion-Actuated Surface Effect Ships	47
4.1	Mathematical Model of System Dynamics	48
4.1.1	SES Heave Model	48
4.1.2	Pressure dynamics for single chamber air-cushion	48
4.2	Control Design for Heave	50
4.2.1	Disturbance Representation	52
4.2.2	Reciprocal State Space Representation	53
4.2.3	Adaptive Backstepping Control Design	54
4.2.4	Stability Proof	60
4.3	Simulation	65
4.3.1	Configuration and Parameters	66
4.3.2	Sea States and Wave Modeling for Simulation	66
4.4	Results	68
4.5	Conclusion	71
Chapter 5	Simultaneous Heave and Pitch Control of Two-Chamber Air-Cushion Surface Effect Ship	79
5.1	Mathematical Model of System Dynamics	80
5.1.1	SES Pitch Model	80
5.1.2	Pressure dynamics for two chambers air-cushion	80
5.2	Simultaneous Control Design for Heave and Pitch	82
5.3	Adaptive Ramp Pitch Control in Bow to Stern Configuration	89
5.4	Results	92
Chapter 6	Implementation of the Developed Controller on a Scale Model Surface Effect Ship	97
6.1	Scale Model SES - AirCat	97
6.2	Control Design	99
6.2.1	Controller	99
6.2.2	Dead-Zone Modification	103
6.3	Experiment Setup and Results	104
Bibliography	108

LIST OF FIGURES

Figure 2.1:	Closed loop system's response for the simulation example where the system parameters are known and the unknown disturbance is matched.	16
Figure 2.2:	Disturbance estimation for the simulation example where the system parameters are known and the unknown disturbance is matched.	17
Figure 2.3:	Closed loop system's response for the simulation example where the system parameters are known and the unknown disturbance is unmatched.	25
Figure 2.4:	Disturbance estimation for the simulation example where the system parameters are known and the unknown disturbance is unmatched.	26
Figure 3.1:	Closed loop system's response for the simulation example where the system parameters are unknown and the unknown disturbance is unmatched.	45
Figure 3.2:	Disturbance estimation for the simulation example where the system parameters are unknown and the unknown disturbance is unmatched.	46
Figure 4.1:	Illustration of the chamber of the air cushion of a surface effect ship. The symbol A_L denotes louver area which is used as the control input.	50
Figure 4.2:	The structure of the control problem. The overall system consists of two dynamics, wave disturbances, fan and louver maps.	51
Figure 4.3:	3D Rhino model of hulls of large, medium-speed, roll-on/roll-off (LMSR) and surface effect ship (SES).	66
Figure 4.4:	Top view of a bow to stern configuration. Bow of an SES is connected to stern of an LMSR by a ramp.	66
Figure 4.5:	The structure of the control problem for simultaneous input actuation. The fan and louver system are used simultaneously to regulate air-flow rate.	69
Figure 4.6:	The wave disturbance estimation in heave in SS4. Figure 4.6(a) shows the wave disturbance and its estimation. Figure 4.6(b) presents the error between actual wave disturbance and its estimation	72
Figure 4.7:	Heave of SES for different sea states with and without control in head seas. Figure 4.7(a) presents the heave of SES when the controller is turned on at 300 seconds.	73
Figure 4.8:	Heave, excess pressure inside the air-cushion and louver area of SES between 662 - 680 seconds.	74

Figure 4.9:	Relative vertical motion of the ramp edge at SES with respect to the edge at LMSR in SS4, the controller is turned on at 300 seconds.	75
Figure 4.10:	Heave of SES in SS4 for heading angle 200 degrees (bow seas), the controller is turned on at 300 seconds.	76
Figure 4.11:	The comparison of heave of SES in SS4 between louver only control and fan+louver simultaneous control. The controller is turned on at 250 seconds.	77
Figure 4.12:	Louver area and rpm coefficient of SES between 600–700 seconds. Louver area and rpm coefficient are saturated at 0, 2500 ft^2 and $-3, 3$, respectively.	78
Figure 5.1:	Illustration of a two-chamber air-cushion model. The symbol A_{1L} and A_{2L} denotes louver area which is used as the control input.	81
Figure 5.2:	Side view of a bow to stern configuration. Bow of an SES, A , is connected to stern of an LMSR, B , by a ramp.	90
Figure 5.3:	Pitch of SES in SS4 with and without controller. The controller is turned on at 250 seconds.	93
Figure 5.4:	Heave of SES in SS4 with and without controller. The controller is turned on at 250 seconds.	94
Figure 5.5:	Louver area, A_{1L} , and rpm coefficient, α_1 , of the chamber one of SES between 600–700 seconds. Louver area, A_{1L} , and rpm coefficient, α_1 , are saturated at 0, 1250 ft^2 and $-3, 3$, respectively.	95
Figure 5.6:	Simulation results for tracking algorithm by state feedback. Both with and without control results are shown. The developed tracking algorithm provides significant stability on the ramp.	96
Figure 6.1:	Top view with blower and system box, side view and general view of AirCat are presented with air-cushion at the bottom.	99
Figure 6.2:	System box of AirCat. It has microcontroller inside with sensors and actuator driver. The box is placed in the scale model.	100
Figure 6.3:	Picture of the wave tank located in Hydrodynamic Lab at Florida Atlantic University.	105
Figure 6.4:	Picture of the AirCat taken in the wave tank while heading to the wave generator.	105
Figure 6.5:	Illustration of the experiment setup located in Hydrodynamic Lab at Florida Atlantic University.	106
Figure 6.6:	Heave of AirCat in the wave tank. The controller is turned on at 40 seconds.	106

Figure 6.7: Heave response of AirCat in frequency domain. First figure in the plot represents the response heave when the control is off (0-40 sec), the second figure represents the steady state response of heave when the controller is on (100-250 sec). 107

LIST OF TABLES

Table 4.1:	The vessel parameters of the surface effect ship (SES) and large, medium-speed, roll-on/roll-off (LMSR).	67
Table 4.2:	Description of sea states from 2 to 4 in terms of important wave and wind values.	68
Table 6.1:	Dimensions of the scale model SES, named AirCat are given in millimeter (mm)	98

ACKNOWLEDGEMENTS

Many people deserve thanks for helping me reach this point in my academic career, and this small section is, by no means, adequate to express my sincere gratitude. But it is a start.

First and foremost, I would like to thank my advisor Professor Miroslav Krstic for his constant support. This work would not have happened without the guidance and expertise of him. I am grateful for his mentorship, direction and leadership.

I would like to thank my committee members, Prof. Thomas Bewley, Prof. Raymond de Callafon, Prof. Joel Conte and Prof. Michael Todd, for their time, assistance and advice. I also wish to thank Prof. Emre Kose from Bogazici University for being a great advisor during my B.S. and M.S. education.

I would also like to thank Prof. Manhar Dhanak and his students Michael Kindel and Quintin Du Plessis from Florida Atlantic University for being so helpful during our collaboration and allowing me to use their lab instruments.

I would like to extend a sincere thank to my lab mates: Nima Ghods, Paul Frihauf, Joe Doblack, James Krieger and Nikos Bekiaris-Liberis for both showing me the ropes and making the lab enjoyable place to work; Azad Ghaffari, Gideon Prior and James Gray for being helpful; Beibei Ren for being a great post-doc; Alex Scheinker for occasionally gracing us with his presence when he is not in Los Alamos; and David Ryan and Shuxia Tang for gracefully accepting the baton from those of us leaving the lab.

Last but not least, I would like to thank my parents Necmettin and Sehure and my wife Elif and my daughter Hilal for all their love, support and encouragement.

The research contained in this dissertation was partially funded by a Office of Naval Research (ONR) grant.

This dissertation includes reprints or adaptations of the following papers:

- H. I. Basturk and M. Krstic, “Adaptive cancelation of matched unknown sinusoidal disturbances for LTI systems by state derivative feedback,” *ASME*

Journal of Dynamic Systems, Measurement, and Control, vol. 153, paper 014501-2, 2013. (Section 2.1 in Chapter 2)

- H. I. Basturk and M. Krstic, “Adaptive backstepping cancelation of *unmatched* unknown sinusoidal disturbances for LTI systems by state derivative feedback,” *ASME Dynamic Systems and Control Conference*, 2012. (Section 2.2 in Chapter 2)
- H. I. Basturk and M. Krstic, “Adaptive backstepping cancelation of *unmatched* unknown sinusoidal disturbances for *unknown* LTI systems by state derivative feedback,” *IEEE Conference on Decision and Control*, 2012. (Chapter 3)
- H. I. Basturk and M. Krstic, “Adaptive wave cancelation by acceleration feedback for ramp-connected air-cushion actuated surface effect ships,” *Automatica*, to appear. (Chapter 4)

The dissertation author is the primary investigator and author of these works.

VITA

2005–2006	Product Engineering Intern , Mercedes-Benz Turk, Istanbul, Turkey
2006	B.S. in Mechanical Engineering, Bogazici University, Istanbul, Turkey
2007–2008	Production Engineer, Arcelik Inc., Istanbul, Turkey
2008	M.S. in Mechanical Engineering, Bogazici University, Istanbul, Turkey
2009	Teaching Assistant, Department of Mechanical and Aerospace Engineering, University of California, San Diego, La Jolla, CA
2009–2013	Research Assistant, Department of Mechanical and Aerospace Engineering, University of California, San Diego, La Jolla, CA
2013	Ph.D. in Engineering Sciences (Mechanical Engineering), University of California, San Diego, La Jolla, CA

PUBLICATIONS

Journal Articles

1. H. I. Basturk and M. Krstic, “Adaptive cancelation of matched unknown sinusoidal disturbances for LTI systems by state derivative feedback,” *ASME Journal of Dynamic Systems, Measurement, and Control*, vol. 153, paper 014501-2, 2013.
2. H. I. Basturk and M. Krstic, “Adaptive wave cancelation by acceleration feedback for ramp-connected air-cushion actuated surface effect ships,” *Automatica*, to appear.

Conference Proceedings

1. H. I. Basturk and M. Krstic, “Adaptive backstepping cancelation of *unmatched* unknown sinusoidal disturbances for *unknown* LTI systems by state derivative feedback,” *IEEE Conference on Decision and Control*, 2012.
2. H. I. Basturk and M. Krstic, “Adaptive backstepping cancelation of *unmatched* unknown sinusoidal disturbances for LTI systems by state derivative feedback,” *ASME Dynamic Systems and Control Conference*, 2012.

3. H. I. Basturk and M. Krstic, “Adaptive cancelation of matched unknown sinusoidal disturbances for *unknown* LTI systems by state derivative feedback,” *American Control Conference*, 2012.
4. H. I. Basturk and M. Krstic, “Adaptive cancelation of matched unknown sinusoidal disturbances for LTI systems by state derivative feedback,” *ASME Dynamic Systems and Control Conference*, 2011.
5. H. I. Basturk, J. Doblack, and M. Krstic, “Air cushion adaptive disturbance cancelation for the reduction of wave induced motion of ramp-connected ships,” 11th *International Conference on Fast Sea Transportation*, 2011.
6. J. Doblack, H. I. Basturk, A. Chakirov, and M. Krstic, “Air cushion active control for the reduction of wave induced motion of ramp-connected ships,” *Grand Challenges Conference in Modeling and Simulation*, 2010.
7. M. Krstic, J. Doblack, J. Toubi, A. Veksler, H. I. Basturk, “Optimization of wave-induced motion of ramp-interconnected craft for cargo transfer,” *Grand Challenges Conference in Modeling and Simulation*, 2009.

ABSTRACT OF THE DISSERTATION

**Disturbance Cancellation by State Derivative Feedback with
Application to Ramp-Connected Surface Effect Ships**

by

Halil I. Basturk

Doctor of Philosophy in Engineering Sciences (Mechanical Engineering)

University of California, San Diego, 2013

Professor Miroslav Krstic, Chair

This dissertation develops a theory to design a controller which estimates and cancels unknown sinusoidal disturbances forcing a linear time-invariant system by using only measurement of state-derivatives of the system. Our design is based on the following steps; parametrization of the sinusoidal disturbance as the output of a known feedback system with an unknown output vector that depends on both unknown disturbance parameters and unknown plant parameters, design of an adaptive disturbance observer, and finally design of an adaptive controller. We extend the results for unmatched disturbances by using a backstepping procedure.

We employ the developed controller to solve the problem of cargo transfer in high sea states over a ramp from a large, medium-speed, roll-on/roll-off (LMSR)

vessel to a smaller connector vessel of a surface effect ship (SES) type. Our aim is to reduce ramp motion between the LMSR and SES in order to provide a safer environment for cargo transfer. We design an air cushion actuated controller to estimate and cancel the wave disturbance and stabilize the heave of the SES via heave acceleration feedback with actuation of the louver area for the case where the hydrodynamic and other parameters of the SES are not known a priori and the pressure dynamics of the air-cushion contains nonlinearly parameterized unknown terms. We also consider a two-chamber air-cushion SES model and design an adaptive controller to regulate heave and pitch simultaneously. In addition a tracking algorithm is proposed to keep the ramp stationary during the cargo transfer. We demonstrate the effects of our control designs in simulations in a time-domain seakeeping code, named AEGIR.

We also implement the developed controller on a scale model SES. We perform several experiments in a wave tank to test the performance of the controller. It is shown that the experimental results we have obtained are consistent with the developed theory.

Chapter 1

Introduction

The problem of cancelling sinusoidal disturbances in dynamical systems is a fundamental control problem, with many applications such as vibrating structures [42], active noise control [43] and rotating mechanisms control [44]. The common method to approach this problem is the internal model principle for which a general solution is given in [9], [10] in the case of linear systems. In the internal model approach, the disturbance is modeled as the output of a linear dynamic system which is called an exosystem. Then the effect of the disturbance on the plant response can be completely compensated by adding a replica of the exosystem model in the feedback loop.

The output regulation problem for minimum phase, uncertain nonlinear systems is solved in [4], [5], [19] and extended for non-minimum phase plants in [20]. Moreover, designs for nonlinear systems are proposed in [28], [29], [46], [47]. The regulation of a linear time-varying system for unknown exosystem is considered in [30]. Disturbance cancelation and output regulation designs also exist for continuous-time LTI systems [1], [6], [21], [31], [38], [40] and discrete-time LTI systems [41]. In all of these references, the controllers are designed by using measurement of state or an output.

In the last decade, the state derivative feedback control has been considered by many researchers [48]–[32] due to its various advantages in applications. In most practical systems, using accelerometers as sensors is easier, cheaper and more reliable than using position sensors. As an application example, the heave

dynamics of a surface effect ship (SES) which has air cushion chamber underneath the deck, is given as a second order mass-spring-damper system which is driven by sinusoidal wave disturbances and pressure of the air cushion chamber in [2]. The model can be represented in the controllable canonical state space form by considering heave and heave rate as states. Besides, the pressure dynamics can be modeled either as a linear system [2], [11] or as a nonlinear system for control design purpose.

An SES offers a high quality and more efficient ride in heavy sea states compared to conventional catamarans. One of its main operational requirements is the transfer of cargo from a large, medium-speed, roll-on/roll-off (LMSR), to nearby land targets [3]. An SES has two modes of operation: It is either supported entirely by twin hulls resembling a catamaran, or by an air cushion that uses a bag system and fans to fill a pocket of air to lift the craft towards the surface of the water.

There is an ongoing effort on the improvement of modeling of such ships, with a number of highly complex and coupled interactions that increase the difficulty. References [25] and [37] present mathematical models of various marine vehicles and their applications. In addition to the synthesis of equations of motion, there is also an effort to analyze and simulate these ships [7], [8].

There are control approaches to increase the ride quality of a marine vessel. In [2], the wave equation is considered to yield a more general equation for spatial change of the pressure of air cushion in time and design a ride control system using dissipative control. Reference [11] proposes a decoupled cushion control to reduce the effect of the two main resonant modes for air cushion catamarans. The main objective of the proposed controllers in the given references is to keep the pressure of the air cushion stable and avoid cobble stone effect. The dynamic model and control scheme for under-actuated and fully actuated marine surface vessels are given in [23] and [24] respectively. Reference [33] proposes a model predictive control design to prevent dynamic stall and increase the effectiveness of ship fin stabilizers. The various techniques to control of roll motions of ships are summarized in [34].

One of the main aim is to reduce ramp motion between an LMSR and SES operating in moderate sea states in order to provide a safer environment for cargo transfer. The oscillation of an LMSR is relatively low with respect to an SES, due to its heavy structure. Therefore, it is reasonable to focus on the stabilization of the heave mode of SES.

Despite of all simplification in the model, designing a controller for an SES presents significant challenges. Difficulties arise from unmeasured sinusoidal wave disturbances, inaccurate system parameters such as mass and hydrodynamic terms, indirect actuation of the air cushion pressure, nonlinearly parameterized model of the air cushion pressure dynamics and the difficulty of measuring the position of each vessel precisely.

In Chapter 2 by employing an approach inspired by [39] and [38], we design an adaptive controller to estimate and cancel the matched and unmatched unknown sinusoidal disturbances forcing LTI systems with known system parameters by using measurement of state-derivative of system and the state of input dynamics. We solve the problem for the case where the parameters of the system are unknown, in Chapter 3. We prove that the equilibrium of closed loop is stable and state of the LTI system goes to zero as $t \rightarrow \infty$ with perfect disturbance estimation. In Chapter 4 we develop an adaptive backstepping wave cancelation algorithm by using the measurement of pressure, heave rate and acceleration with actuation of the louver area to tackle all combinations of the mentioned challenges. We consider a two-chamber air-cushion SES and design an adaptive controller to regulate heave and pitch simultaneously in Chapter 5. We use existing software, named AEGIR, to model the system and simulate it with and without control. AEGIR is a time-domain seakeeping code that uses an advanced, high-order boundary element method (BEM) to solve the three-dimensional, potential and-flow, and wave flow problems and automatically calculates the water line intersection to determine the wetted and dry surface areas as the vessel moves through waves [7]. With the proposed controller, we estimate the unknown wave disturbance and cancel its effect to the system. Simulation results demonstrate significant reduction in heave and pitch of SES. Thus, we achieve to reduce ramp oscillation and provide safer

environment for cargo transfer over the ramp. The implementation of the developed algorithm on a scale model SES and the result of the experiments which has been performed in a wave tank are given in Chapter 6.

Chapter 2

Adaptive Cancellation of Unknown Sinusoidal Disturbances for Known LTI Systems by State Derivative Feedback

We develop an adaptive controller to estimate and cancel the matched and unmatched unknown sinusoidal disturbances forcing LTI systems with known system parameters by using measurement of state-derivative of system and the state of input dynamics. Our design is based on the parametrization of the sinusoidal disturbance as the output of a known feedback system with an unknown output vector that depends on unknown disturbance parameters. This parametrization allows us to design an observer and convert the problem to an adaptive control design. We also propose a design for unmatched disturbance by using a backstepping procedure. We prove that the equilibrium of the closed-loop adaptive system is stable and state of the system goes to zero as $t \rightarrow \infty$ with perfect disturbance estimation. The effectiveness of the controllers are illustrated with simulation examples.

This chapter is organized as follows: We state the problem for the case where the disturbance and the system input are matched and propose our design with

stability proof and numerical example in Section 2.1. In Section 2.2 we develop an adaptive controller for unmatched disturbance by using backstepping design. The stability of the proof with a numerical example are also given in the same section. Section 2.3 summarizes the results.

2.1 Matched Unknown Sinusoidal Disturbance

2.1.1 Problem Statement and Adaptive Controller Design

We consider the multi-input LTI system

$$\dot{x}(t) = Ax(t) + B(u(t) + \nu(t)), \quad (2.1)$$

with the state $x(t) \in \mathbb{R}^n$, input $u(t) \in \mathbb{R}$, and sinusoidal disturbance $\nu(t) \in \mathbb{R}$ given by

$$\nu(t) = \sum_{i=1}^q g_i \sin(\omega_i t + \phi_i), \quad (2.2)$$

where $i \neq j \Rightarrow \omega_i \neq \omega_j$, $\omega \in \mathbb{Q}$, $g_i, \phi_i \in \mathbb{R}$.

The sinusoidal disturbance ν can be represented as the output of a linear exosystem,

$$\dot{w}(t) = Sw(t) \quad (2.3)$$

$$\nu(t) = h^T w(t) \quad (2.4)$$

where $w \in \mathbb{R}^{2q}$ and the choice of $S \in \mathbb{R}^{2q \times 2q}$ and $h \in \mathbb{R}^{2q}$ is not unique.

We make the following assumptions regarding the plant (2.1) and the exosystem (2.3)–(2.4):

Assumption 2.1 *A is invertible.*

Assumption 2.2 *The pair (A, B) is controllable.*

Assumption 2.3 *x and ν are not measured but \dot{x} is measured.*

Assumption 2.4 *The pair (h^T, S) is observable.*

Assumption 2.5 *The eigenvalues of S are imaginary, distinct and rational.*

Assumption 2.6 *q is known.*

Assumption 2.7 *S and h are unknown.*

Assumption 2.8 *$g_i \neq 0$ for all $i \in \{1, \dots, q\}$.*

Under Assumptions 2.1 and 2.2, there exists a control gain $K \in \mathbb{R}^{1 \times n}$ such that $(A^{-1} + A^{-1}BK)$ is Hurwitz [48].

We state now our adaptive controller with a disturbance observer. In Section 2.1.2 we analyze the stability properties of the closed-loop system.

The adaptive controller for the system (2.1), (2.3), (2.4) is given by

$$u = -K\dot{x} - \hat{\theta}^T \xi, \quad (2.5)$$

the update law for $\hat{\theta}(t)$ is given by

$$\dot{\hat{\theta}} = -\gamma \xi (A^{-1}B)^T P \dot{x}, \quad \gamma > 0, \quad (2.6)$$

with the positive definite matrix P which is a solution of the matrix equation

$$(A^{-1} + A^{-1}BK)^T P + P(A^{-1} + A^{-1}BK) = -2I. \quad (2.7)$$

The disturbance observer is given by

$$\dot{\eta} = G(\eta + N(\dot{x} - Bu)) - NA\dot{x} \quad (2.8)$$

$$\xi = \eta + N(\dot{x} - Bu), \quad (2.9)$$

where G is a $2q \times 2q$ Hurwitz matrix with distinct poles and constitutes a controllable pair with a chosen vector $l \in \mathbb{R}^{2q}$ and N is a $2q \times n$ matrix which is given by

$$N = \frac{1}{B^T B} l B^T, \quad (2.10)$$

where the given N is one of the many solutions of the following equation

$$NB = l. \quad (2.11)$$

Since the matrices G and S have disjoint spectra, the pair (h^T, S) is observable, and the pair (G, l) is controllable, the Sylvester equation

$$MS - GM = lh^T, \quad (2.12)$$

has a unique solution[13]. This fact is exploited in the proof of our stability result (Lemma 2.1).

We first state a theorem describing our main stability result and then we prove it using a series of technical lemmas in Section 2.1.2.

Theorem 2.1 *Consider the closed-loop system consisting of the plant (2.1) forced by the unknown sinusoidal disturbance (2.2), the disturbance observer (2.8),(2.9) and the adaptive controller (2.5),(2.6). Under Assumptions 2.1–2.7, the system’s solution $x(t) \equiv 0$, $\hat{\theta}(t) \equiv (MS)^{-T}h$, $\eta(t) \equiv GMw(t)$ is globally uniformly asymptotically stable and locally exponentially stable. Furthermore, $\hat{\theta}^T(t)\xi(t) - \nu(t) \rightarrow 0$ exponentially as $t \rightarrow \infty$, namely, perfect estimation of the disturbance is achieved.*

2.1.2 Stability Proof

The following lemma enables us to represent the unknown sinusoidal disturbance as the output of a linear system whose input is the disturbance itself, whose state and input matrices are known, and whose output matrix is unknown.

Lemma 2.1 *Let $G \in \mathbb{R}^{2q \times 2q}$ be a Hurwitz matrix with distinct eigenvalues and let (G, l) be a controllable pair. Then, ν can be represented as the output of the model*

$$\dot{z} = Gz + l\nu \quad (2.13)$$

$$\nu = \theta^T \dot{z} \quad (2.14)$$

$$\theta^T = h^T (MS)^{-1}. \quad (2.15)$$

Proof This result and its proof are inspired by [39]. To establish (2.13) from (2.3), consider

$$z = Mw. \quad (2.16)$$

Differentiating (2.16), we obtain

$$\dot{z} = MSw. \quad (2.17)$$

Using (2.12), we have

$$\dot{z} = MSw = GMw + lh^T w. \quad (2.18)$$

Substituting (2.4) and (2.16) into (2.18) yields (2.13). Substituting $w = (MS)^{-1}\dot{z}$ into (2.4), we obtain (2.14) and (2.15). ■

The previous lemma enables us to write the unknown external disturbance ν as the product of an unknown constant θ and the vector \dot{z} . However, \dot{z} is not accessible, since the signal ν can not be measured. To overcome this problem, we design the observer (2.8)–(2.9).

The following lemma establishes the properties of the observer.

Lemma 2.2 *The inaccessible disturbance ν can be represented in the form*

$$\nu = \theta^T \xi + \theta^T \delta, \quad (2.19)$$

where $\delta \in R^q$ obeys the equation

$$\dot{\delta} = G\delta. \quad (2.20)$$

Proof Differentiating (2.13), we obtain

$$\ddot{z} = G\dot{z} + l\dot{\nu} \quad (2.21)$$

By defining the estimation error, we get

$$\delta = \dot{z} - \xi. \quad (2.22)$$

Differentiating δ with respect to time and in view of (2.13), (2.8) and (2.9), we get

$$\dot{\delta} = G\dot{z} + l\dot{\nu} - G(\eta + N(\dot{x} - Bu)) + NA\dot{x} - NA\dot{x} - NB\dot{\nu}. \quad (2.23)$$

Substituting (2.9) into (2.23), using (2.22) and the fact that $ND = l$, we get (2.20).

Using (2.14), (2.22), we obtain (2.19). ■

Lemmas 2.1 and 2.2 convert the problem from cancelation of an unknown sinusoidal disturbance to an adaptive control problem.

The following lemma is used in the proof of the main theorem.

Lemma 2.3 *There exists $\rho > 0$ such that for all $t_0 \geq 0$, the following holds*

$$Q_p(\rho, t_0) = \int_{t_0}^{t_0+\rho} \xi(t)\xi^T(t) dt - \frac{1}{\rho} \int_{t_0}^{t_0+\rho} \xi(t) dt \int_{t_0}^{t_0+\rho} \xi^T(t) dt > 0. \quad (2.24)$$

Proof By differentiating (2.22) with respect to time and using (2.20) and (2.21), the estimate ξ can be represented as the solution of

$$\dot{\xi} = G\xi + l\dot{\nu}, \quad (2.25)$$

where

$$\dot{\nu} = \sum_{i=1}^q \bar{g}_i \cos(\omega_i t + \phi_i), \quad (2.26)$$

with $\bar{g}_i = g_i \omega_i$.

By solving (2.25), we get

$$\xi(\tau) = e^{G\tau} \xi(0) + \int_0^\tau e^{G(\tau-\sigma)} l \dot{\nu} d\sigma. \quad (2.27)$$

Since G has distinct eigenvalues and is Hurwitz, it is diagonalizable. Using a Jordan decomposition of the matrix G , we can write

$$G = L\Lambda L^{-1}, \quad (2.28)$$

where L is the square $2q \times 2q$ matrix whose i^{th} column is the i^{th} eigenvector of G and Λ is the diagonal matrix whose diagonal elements are the corresponding eigenvalues of G .

Defining $L^{-1}l = \bar{l}$, substituting (2.28) into (2.27) and using the property $e^{L\Lambda L^{-1}} = Le^\Lambda L^{-1}$, we get

$$\xi(\tau) = Le^{\Lambda\tau} L^{-1} \xi(0) + Le^{\Lambda\tau} \int_0^\tau e^{-\Lambda\sigma} \bar{l} \dot{\nu} d\sigma. \quad (2.29)$$

By computing the integral in (2.29), we obtain

$$\xi(\tau) = L (e^{\Lambda\tau} C_c + \Psi(\tau)), \quad (2.30)$$

where $\Psi \in R^{2q}$ is the vector whose j^{th} row is

$$\sum_{i=1}^q \frac{\bar{l}_j \bar{g}_i}{\lambda_j^2 + \omega_i^2} (-\lambda_j \cos(\omega_i \tau + \phi_i) + \omega_i \sin(\omega_i \tau + \phi_i)), \quad (2.31)$$

and

$$C_c = L^{-1} \xi(0) - \Psi(0). \quad (2.32)$$

Since $\dot{\nu}$ is a sufficiently rich signal order of $2q$ and (G, l) is a controllable pair, ξ is persistently exciting [18]. Therefore, there exist positive ρ^* and α_0 such that for all $\rho > \rho^*$ and $t_0 \geq 0$ the following holds

$$\int_{t_0}^{t_0+\rho} \xi(t) \xi^T(t) dt \geq \rho \alpha_0 I. \quad (2.33)$$

Under Assumption 2.5, the frequencies of $\dot{\nu}$ can be represented as

$$\omega_i = \frac{\text{num}(\omega_i)}{\text{den}(\omega_i)}, \quad \text{num}(\omega_i), \text{den}(\omega_i) \in \mathbb{Z}^+, \quad i = 1 \dots q.$$

Then ρ that given by

$$\rho = \vartheta \text{lcm}(\text{num}(\omega_1), \dots, \text{num}(\omega_q)) \times \text{lcm}(\text{den}(\omega_1), \dots, \text{den}(\omega_q)) 2\pi > \rho^*, \quad (2.34)$$

where lcm is the abbreviation of the least common multiple, satisfies (2.33) if $\vartheta \in \mathbb{Z}^+$ is chosen sufficiently large for given ρ^* and $\omega_1, \dots, \omega_q$. Since $\Psi(t)$ defined by (2.31) has a period ρ and incorporates only zero-mean functions, it follows that

$$\int_{t_0}^{t_0+\rho} \Psi(t) dt = 0. \quad (2.35)$$

Substituting (2.30)–(2.35) into (2.24), we get

$$Q_p(\rho, t_0) \geq L \Theta L^T, \quad (2.36)$$

where

$$\Theta = \rho \bar{\alpha}_0 I - \frac{1}{\rho} \Gamma(\rho) \Gamma^T(\rho), \quad (2.37)$$

$\bar{\alpha}_0 > 0$ satisfies $\alpha_0 I - \bar{\alpha}_0 L L^T > 0$,

$$\Gamma(\rho) = \begin{bmatrix} c_1 e^{\lambda_1 t_0} (e^{\lambda_1 \rho} - 1) \\ \vdots \\ c_{2q} e^{\lambda_{2q} t_0} (e^{\lambda_{2q} \rho} - 1) \end{bmatrix}, \quad (2.38)$$

and c_i denotes the i^{th} row of the vector C_c/λ_i .

Since L is full rank, Q_p satisfies the inequality (2.24) if $\mu^T \Theta \mu > 0$ for all nonzero $\mu \in R^{2q}$. Using (2.37), we have

$$\begin{aligned} \mu^T \Theta \mu = & \rho \bar{\alpha}_0 (\mu_1^2 + \dots + \mu_{2q}^2) - \frac{1}{\rho} \left(\mu_1 c_1 e^{\lambda_1 t_0} (e^{\lambda_1 \rho} - 1) \right. \\ & \left. + \dots + \mu_{2q} c_{2q} e^{\lambda_{2q} t_0} (e^{\lambda_{2q} \rho} - 1) \right)^2. \end{aligned} \quad (2.39)$$

By using Cauchy-Schwarz's inequality and by noting that $\lambda_i < 0$, $|e^{\lambda_i \rho} - 1| \leq 1$, we have

$$\begin{aligned} \mu^T \Theta \mu \geq & \rho \bar{\alpha}_0 (\mu_1^2 + \dots + \mu_{2q}^2) - \frac{1}{\rho} (\mu_1^2 + \dots + \mu_{2q}^2) \left((c_1 e^{\lambda_1 t_0} (e^{\lambda_1 \rho} - 1))^2 \right. \\ & \left. + \dots + (c_{2q} e^{\lambda_{2q} t_0} (e^{\lambda_{2q} \rho} - 1))^2 \right) \\ \geq & (\mu_1^2 + \dots + \mu_{2q}^2) \left(\rho \bar{\alpha}_0 - \frac{1}{\rho} \left((c_1 e^{\lambda_1 t_0})^2 + \dots + (c_{2q} e^{\lambda_{2q} t_0})^2 \right) \right). \end{aligned} \quad (2.40)$$

Since $\rho \bar{\alpha}_0$ is monotonically increasing and $\frac{1}{\rho} \left((c_1 e^{\lambda_1 t_0})^2 + \dots + (c_{2q} e^{\lambda_{2q} t_0})^2 \right)$ is monotonically decreasing with respect to ρ for all fixed t_0 , one can find a ρ using (2.34) such that for all $t_0 \geq 0$, (2.24) holds. \blacksquare

Proof of Theorem 2.1: We represent the closed-loop system as a linear time-varying (LTV) system which is given by

$$\dot{\zeta} = E(t)\zeta + F(t)\delta, \quad (2.41)$$

where

$$E(t) = \begin{bmatrix} A_{cl} & \underline{B}\xi^T \\ \gamma\xi(A^{-1}B)^T P A_{cl} & \gamma\xi(A^{-1}B)^T P \underline{B}\xi^T \end{bmatrix} \quad (2.42)$$

$$F(t) = \begin{bmatrix} \underline{B}\theta^T \\ \gamma\xi(A^{-1}B)^T P \underline{B}\theta^T \end{bmatrix} \quad (2.43)$$

$$\zeta = \begin{bmatrix} x^T, & \tilde{\theta}^T \end{bmatrix}^T \quad (2.44)$$

$$\tilde{\theta} = \theta - \hat{\theta}, \quad (2.45)$$

with

$$A_{cl} = (A^{-1} + A^{-1}BK)^{-1} \quad (2.46)$$

$$\underline{B} = A_{cl}A^{-1}B. \quad (2.47)$$

We first show that the equilibrium $\zeta = 0$ of the homogenous part of the LTV system (2.41) is exponentially stable. Towards that end, we choose the following Lyapunov function

$$V = \frac{1}{2}\zeta^T P_c \zeta, \quad (2.48)$$

where

$$P_c = \begin{bmatrix} P & 0 \\ 0 & \frac{1}{\gamma}I \end{bmatrix}. \quad (2.49)$$

Taking the derivative of V , we get

$$\dot{V} = \frac{1}{2}\zeta^T \begin{bmatrix} A_{cl}^T P + P A_{cl} & (A_{cl}^T P A_{cl}^{-1} + P) \underline{B} \xi^T \\ \xi \underline{B}^T (A_{cl}^T P A_{cl}^{-1} + P)^T & \xi \underline{B}^T (A_{cl}^{-T} P + P A_{cl}^{-1}) \underline{B} \xi^T \end{bmatrix} \zeta. \quad (2.50)$$

By pre and post multiplying (2.7) by A_{cl}^T and A_{cl} and using the fact that $A_{cl} = (A^{-1} + A^{-1}BK)^{-1}$, we obtain

$$A_{cl}^T P + P A_{cl} = -2A_{cl}^T A_{cl}. \quad (2.51)$$

Pre-multiplying (2.7) by A_{cl}^T , we get

$$A_{cl}^T P A_{cl}^{-1} + P = -2A_{cl}^T. \quad (2.52)$$

Post-multiplying (2.7) by A_{cl} , we get

$$P + A_{cl}^{-T} P A_{cl} = -2A_{cl}. \quad (2.53)$$

Substituting (2.7), (2.51)–(2.53) into (2.50), we get

$$\dot{V} = -\zeta^T \begin{bmatrix} A_{cl}^T A_{cl} & A_{cl}^T \underline{B} \xi^T \\ \xi \underline{B}^T A_{cl} & \xi \underline{B}^T \underline{B} \xi^T \end{bmatrix} \zeta. \quad (2.54)$$

Defining

$$C^T(t) = \begin{bmatrix} A_{cl} & \underline{B}\xi^T \end{bmatrix}, \quad (2.55)$$

we get

$$\dot{V} = \frac{1}{2}\zeta^T (E^T(t)P_c + P_cE(t)) \zeta = -\zeta^T C(t)C(t)^T \zeta. \quad (2.56)$$

Therefore, it follows that P_c , as defined in (2.49), satisfies the following inequality

$$E^T(t)P_c + P_cE(t) + \alpha C^T(t)C(t) \leq 0 \quad (2.57)$$

for some $\alpha > 0$.

The equilibrium $\zeta = 0$ of the homogenous part of (2.41) is exponentially stable if $(C(t), E(t))$ is a uniformly completely observable (UCO) pair [26]. For a bounded $H(t)$, the pairs $(C(t), E(t))$ and $(C(t), E(t) + H(t)C(t)^T)$ have the same UCO property [26]. Choosing

$$H(t) = \begin{bmatrix} -I \\ -\xi(A^{-1}\underline{B})^T P \end{bmatrix}, \quad (2.58)$$

we write the system corresponding to the pair $(C, E + HC^T)$ as

$$\dot{Y} = 0 \quad (2.59)$$

$$y = C^T(t)Y. \quad (2.60)$$

The state transition matrix of (2.59) is $\Phi = I$. Therefore, $(C, E + HC^T)$ is a UCO pair if there exist positive constants α_1, α_2, ρ such that the observability Gramian satisfies

$$\alpha_2 I \geq \int_{t_0}^{t_0+\rho} C(t)C^T(t) dt \geq \alpha_1 I, \quad (2.61)$$

for all $t_0 \geq 0$. Since ξ is bounded, recalling (2.55), the upper bound of (2.61) is satisfied. We now prove the lower bound in (2.61). Calculating the integral in (2.61), we get

$$\begin{aligned} X &= \int_{t_0}^{t_0+\rho} C(t)C^T(t) dt \\ &= \begin{bmatrix} A_{cl}^T A_{cl} \rho & A_{cl}^T \underline{B} \int_{t_0}^{t_0+\rho} \xi^T dt \\ \int_{t_0}^{t_0+\rho} \xi dt \underline{B}^T A_{cl} & \int_{t_0}^{t_0+\rho} \xi \underline{B}^T \underline{B} \xi^T dt \end{bmatrix}. \end{aligned} \quad (2.62)$$

Let S_h be the Schur complement of $A_{cl}^T A_{cl} \rho$ in X , where

$$\begin{aligned} S_h &= \int_{t_0}^{t_0+\rho} \xi \underline{B}^T \underline{B} \xi^T dt - \frac{1}{\rho} \int_{t_0}^{t_0+\rho} \xi dt \underline{B}^T A_{cl} A_{cl}^{-1} A_{cl}^{-T} A_{cl}^T \underline{B} \int_{t_0}^{t_0+\rho} \xi^T dt \\ &= \underline{B}^T \underline{B} \left(\int_{t_0}^{t_0+\rho} \xi \xi^T dt - \frac{1}{\rho} \int_{t_0}^{t_0+\rho} \xi dt \int_{t_0}^{t_0+\rho} \xi^T dt \right). \end{aligned} \quad (2.63)$$

Since $A_{cl}^T A_{cl} \rho$ is positive definite, X is positive definite if and only if S_h is positive definite. Since $\underline{D}^T \underline{D}$ is a positive scalar, according to Lemma 2.3 there exists a positive ρ such that for all $t_0 > 0$, $S_h > 0$. Hence, $(C, E + HC^T)$ is UCO, which implies that (C, E) is UCO. Therefore, the state transition matrix $\Phi(t, t_0)$ corresponding to $E(t)$ in (2.41) satisfies

$$\|\Phi(t, t_0)\| \leq \kappa_0 e^{-\gamma_0(t-t_0)} \quad (2.64)$$

for some positive constants κ_0, γ_0 . Since G is Hurwitz, we have that

$$|\delta(t)| = |e^{G(t-t_0)} \delta(0)| \leq \kappa_1 e^{-\gamma_1(t-t_0)} |\delta(0)| \quad (2.65)$$

for some positive constants κ_1, γ_1 . The solution of (2.41) is written as

$$\zeta(t) = \Phi(t, 0) \zeta(0) + \int_0^t \Phi(t, \tau) F(\tau) \delta(\tau) d\tau. \quad (2.66)$$

Using (2.64)–(2.66), we get

$$\begin{aligned} |\zeta(t)| &\leq \kappa_0 e^{-\gamma_0 t} |\zeta(0)| + \int_0^t \kappa_0 e^{-\gamma_0(t-\tau)} |F(\tau)| \kappa_1 e^{-\gamma_1 \tau} |\delta(0)| d\tau \\ &\leq \kappa_0 e^{-\gamma_0 t} |\zeta(0)| + \kappa_1 \kappa_0 e^{-\gamma_0 t} |\delta(0)| \sup_{0 \leq \tau \leq t} |F(\tau)| \int_0^t e^{(\gamma_0 - \frac{1}{2} \min\{\gamma_0, \gamma_1\})\tau} d\tau \\ &= \kappa_0 e^{-\gamma_0 t} |\zeta(0)| + \frac{\kappa_1 \kappa_0 \sup_{0 \leq \tau \leq t} |F(\tau)|}{\left(\gamma_0 - \frac{1}{2} \min\{\gamma_0, \gamma_1\}\right)} |\delta(0)| e^{-\gamma_0 t} \left(e^{(\gamma_0 - \frac{1}{2} \min\{\gamma_0, \gamma_1\})t} - 1 \right) \\ &= \kappa_0 e^{-\gamma_0 t} |\zeta(0)| + \frac{\kappa_1 \kappa_0 \sup_{0 \leq \tau \leq t} |F(\tau)|}{\left(\gamma_0 - \frac{1}{2} \min\{\gamma_0, \gamma_1\}\right)} |\delta(0)| \left(e^{-\frac{1}{2} \min\{\gamma_0, \gamma_1\}t} - e^{-\gamma_0 t} \right) \\ &\leq \kappa_0 e^{-\gamma_0 t} |\zeta(0)| + \frac{\kappa_1 \kappa_0 \sup_{0 \leq \tau \leq t} |F(\tau)|}{\left(\gamma_0 - \frac{1}{2} \min\{\gamma_0, \gamma_1\}\right)} |\delta(0)| e^{-\frac{1}{2} \min\{\gamma_0, \gamma_1\}t}. \end{aligned} \quad (2.67)$$

Substituting (2.17) into (2.22), we get

$$\xi(t) = MSw(t) - \delta(t). \quad (2.68)$$

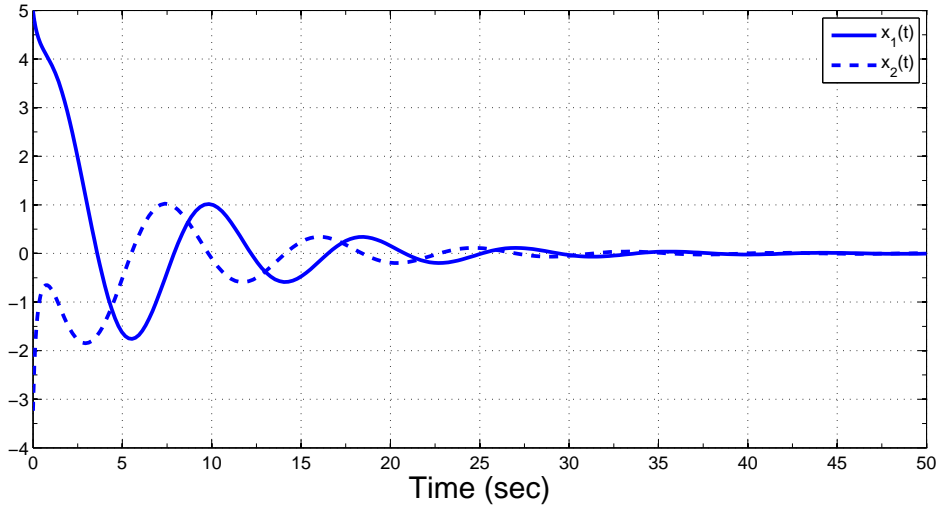


Figure 2.1: Closed loop system's response for the simulation example where the system parameters are known and the unknown disturbance is matched.

Substituting (2.68) into (2.9) and using (2.12) and the fact that $\dot{x} - Bu = Ax + Bv$ and $NB = l$, we obtain

$$\eta(t) - GMw(t) = -NAx(t) - \delta(t). \quad (2.69)$$

By virtue of (2.44),

$$\eta(t) - GMw(t) = -[NA, 0, I] \begin{bmatrix} \zeta \\ \delta \end{bmatrix}. \quad (2.70)$$

Since $\zeta(0) = [x^T(0), \hat{\theta}(0) - h^T(MS)^{-1}]^T$ and $\delta(0) = -NAx(0) - \eta(0) + GMw(0)$, following (2.65) and (2.67) we get that the solution $x(t) \equiv 0$, $\hat{\theta}(t) \equiv (MS)^{-T}h$, $\eta(t) \equiv GMw(t)$ is globally uniformly asymptotically stable and locally exponentially stable. Furthermore, according to Lemma 2.2, $\hat{\theta}^T(t)\xi(t) - \nu(t) \rightarrow 0$ exponentially as $t \rightarrow \infty$, namely, perfect estimation of the disturbance is achieved.

The reason why we are not claiming *global exponential* stability is that the quantities $\sup_{0 \leq \tau \leq t} |F(\tau)|$, κ_0 , γ_0 , while bounded, actually depend on the initial conditions $x(0)$, $\hat{\theta}(0)$, $\eta(0)$, as can be observed by tracing the derivation of these quantities throughout the paper and in the quoted sources. ■

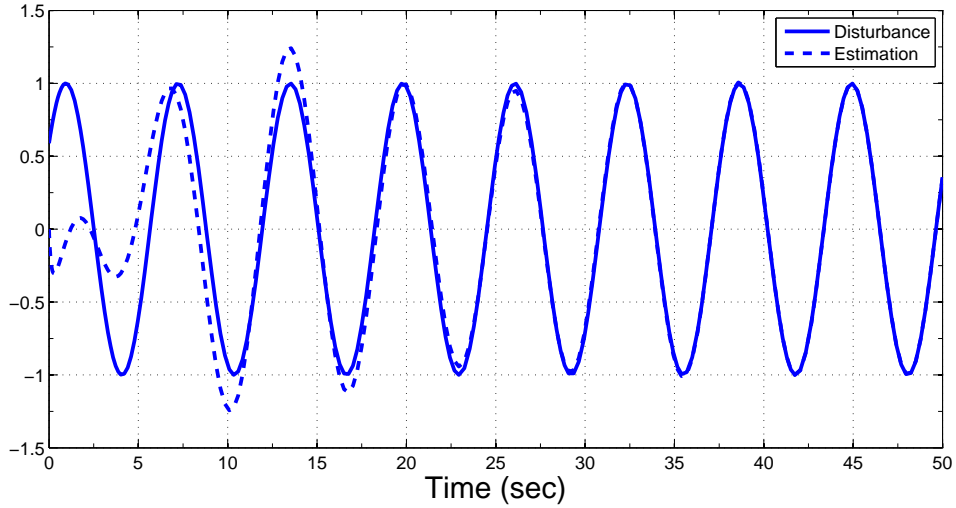


Figure 2.2: Disturbance estimation for the simulation example where the system parameters are known and the unknown disturbance is matched.

2.1.3 Simulation Results

We illustrate the performance of our controller with a second-order system with $A = \begin{bmatrix} 0 & 1 \\ 1 & 3 \end{bmatrix}$, $B = \begin{bmatrix} 0 \\ 1 \end{bmatrix}$, the unknown disturbance $\nu(t) = 3 \sin(t + \pi/5)$ and initial condition $x = \begin{bmatrix} 5 & 0 \end{bmatrix}^T$. The control gain K is chosen such that the eigenvalues of $(A^{-1} + A^{-1}BK)$ are -2 and -1 . For the update law, we choose $\gamma = 1$. Finally, the controllable pair (G, l) is chosen as $G = \begin{bmatrix} 0 & 1 \\ -1.95 & -2.8 \end{bmatrix}$, $B = \begin{bmatrix} 0 \\ 1 \end{bmatrix}$, and $N = \begin{bmatrix} 0 & 0 \\ 1 & 0 \end{bmatrix}$. From Figures 2.1 and 2.2 one can observe that $x(t)$ exponentially converges to zero and the unknown disturbance is perfectly estimated, as Theorem 2.1 predicts.

The placement of the poles of $(A^{-1} + A^{-1}BK)$ as well as the update gain γ affect the convergence of the states and the estimation. Increasing the absolute value of the real part of the poles provides high control gain. The update gain γ should be chosen proportionally high or low with respect to control gain to provide an optimum convergence rate.

2.2 Unmatched and Unknown Sinusoidal Disturbance

2.2.1 Problem Statement and Backstepping Adaptive Controller Design

In this section, we consider the single-input LTI system

$$\dot{x} = Ax + B(p + \nu) \quad (2.71)$$

$$\dot{p} = a^T x + b_p p + b_u u \quad (2.72)$$

with the state $x \in \mathbb{R}^n$ and $p \in \mathbb{R}$, input $u \in \mathbb{R}$, and sinusoidal disturbance $\nu \in \mathbb{R}$ given by

$$\nu(t) = \sum_{i=1}^q g_i \sin(\omega_i t + \phi_i), \quad (2.73)$$

where $i \neq j \Rightarrow \omega_i \neq \omega_j$, $\omega \in \mathbb{Q}$, $g_i, \phi_i \in \mathbb{R}$. The main difference between (2.1) and (2.71) is the unmatched sinusoidal disturbance. Since p has its own dynamics (2.72), the main input u and ν are not in the same equation. There is an integrator between them. Therefore, we use a backstepping procedure to design an adaptive controller.

We state now our adaptive controller with a disturbance observer. In Section 2.2.2 we analyze the stability properties of the closed-loop system.

The adaptive controller for the system (2.3), (2.4), (2.71), (2.72) is given by

$$\begin{aligned} u = & \frac{1}{(1 + KB)b_u} \left((\hat{\theta}^T l - (1 + KB)(b_p - a^T A^{-1} B)) p \right. \\ & - (\hat{\theta}^T N + (\hat{\theta}^T N + K)A + (1 + KB)a^T A^{-1} \\ & - (A^{-1} B)^T P) \dot{x} + (1 + KB)(a^T A^{-1} B) \hat{\theta}^T \xi \\ & - (KB + \hat{\theta}^T l) \hat{\beta}^T \xi - \hat{\theta}^T \eta - \hat{\theta}^T \dot{\eta} \\ & \left. - \left((KB + \hat{\theta}^T l)^2 + c \right) e \right), \end{aligned} \quad (2.74)$$

where $c > \frac{1}{2}$ and

$$e = p - \left(-K\dot{x} - \hat{\theta}^T \xi \right). \quad (2.75)$$

The update laws for $\hat{\theta}(t)$ and $\hat{\beta}(t)$ are given by

$$\dot{\hat{\theta}} = -\gamma_t \xi \left((A^{-1}B)^T P \dot{x} + (1 + KB)(a^T A^{-1}B)e \right), \quad (2.76)$$

$$\dot{\hat{\beta}} = \gamma_b \xi \left(KB + \hat{\theta}^T l \right) \quad (2.77)$$

with $\gamma_t, \gamma_b > 0$. The positive definite matrix P and the disturbance observer filters are given in (2.7)–(2.12). The error signal e represents the deviation of the the actual p from the desired value which is given in (2.5) as the control law for matched disturbance.

We first define the signals needed in the analysis and state a theorem describing our main stability result. Then we prove the theorem using a series of technical lemmas in Section 2.2.2.

Estimation errors of the unknown parameters are denoted by

$$\tilde{\theta}(t) = (MS)^{-T} h - \hat{\theta}(t), \quad (2.78)$$

$$\tilde{\beta}(t) = \frac{1}{1 - h^T (MS)^{-1} l} G^T (MS)^{-T} h - \hat{\beta}(t), \quad (2.79)$$

and $\delta(t)$ and $\tilde{\xi}(t)$ denotes the signals,

$$\delta(t) = MSw(t) - \xi(t), \quad (2.80)$$

$$\tilde{\xi}(t) = \xi(t) - \bar{\xi}(t), \quad (2.81)$$

where

$$\bar{\xi}(t) = \int_0^t e^{G(t-\tau)} l \dot{v}(\tau) d\tau. \quad (2.82)$$

Theorem 2.2 *Consider the closed-loop system consisting of the plant (2.71)–(2.72) forced by the unknown sinusoidal disturbance (2.4), the disturbance observer (2.8), (2.9) and the adaptive controller (2.74), (2.76), (2.77). Under Assumptions 2.1–2.7, the following holds:*

- (a) The equilibrium $x = 0, \delta = \tilde{\xi} = \tilde{\theta} = \tilde{\beta} = 0, e = 0$ is globally stable,
- (b) For all initial conditions $x(0) \in \mathbb{R}^n, \tilde{\xi}(0) \in \mathbb{R}^{2q}, \hat{\theta}(0) \in \mathbb{R}^{2q}, \hat{\beta}(0) \in \mathbb{R}^{2q}, e(0) \in \mathbb{R}$ and all $w(0) \in \mathbb{R}^{2q}$ such that Assumption 2.8 holds, the signals $x(t), e(t), \tilde{\theta}(t), \delta(t), \tilde{\xi}(t), \nu(t) - \hat{\theta}^T(t)\xi(t)$ converge to zero as $t \rightarrow \infty$.

2.2.2 Stability Proof

The following lemma establishes the properties of the observer for $\dot{\nu}$.

Lemma 2.4 *The inaccessible disturbance $\dot{\nu}$ can be represented in the form*

$$\dot{\nu} = \beta^T \xi + \beta^T \delta \quad (2.83)$$

where

$$\beta = \frac{1}{1 - \theta^T l} G^T \theta, \quad (2.84)$$

with $1 - \theta^T l > 0$. $\delta \in \mathbb{R}^q$ obeys the equation (2.20).

Proof Post-multiplying (2.12) by $(MS)^{-1}$ and using (2.15), we get $I - l\theta^T = GMS^{-1}M^{-1}$. Using Sylvester's determinant theorem [45], the fact that $\det M^{-1} = \frac{1}{\det M}$ and noting that G and S have $2q$ poles on left half plane and imaginary axis, respectively, we obtain $1 - \theta^T l > 0$. Differentiating (2.14) and using (2.21), we get

$$\dot{\nu} = \frac{1}{1 - \theta^T l} \theta^T G \dot{z}. \quad (2.85)$$

Using (2.14), (2.84), (2.22) and (2.85), we obtain (2.83). \blacksquare

Proof of Theorem 2.2: With the error variable (2.75), the closed-loop is written as

$$\dot{x} = A_{cl}x + \underline{B} \left(\tilde{\theta}^T \xi + \theta^T \delta + e \right), \quad (2.86)$$

$$\begin{aligned} \dot{e} = & \left((KB + \hat{\theta}^T l)^2 + c + \overline{B}^T P \underline{B} \right) e + (KB + \hat{\theta}^T l) \left(\tilde{\beta}^T \xi + \beta^T \delta \right) \\ & + \left(\overline{B}^T P \underline{B} - (1 + KB)a^T \overline{B} \right) \left(\tilde{\theta}^T \xi + \theta^T \delta \right) + \overline{B}^T P A_{cl} x, \end{aligned} \quad (2.87)$$

where A_{cl} and \underline{B} are given in (2.46) and (2.47), respectively and $\overline{B} = A^{-1}B$.

The stability of the equilibrium of the closed-loop system is established with the use of Lyapunov function

$$V = \frac{1}{2}x^T P x + \frac{1}{2}e^2 + \frac{1}{2}\tilde{\theta}^T \tilde{\theta} + \frac{1}{2}\tilde{\beta}^T \tilde{\beta} + \frac{\varepsilon_\delta}{2}\delta^T P_\delta \delta \quad (2.88)$$

where

$$G^T P_G + P_G G = -2I, \quad (2.89)$$

$$\varepsilon_\delta = \lambda_{\max}\{\theta \bar{B}^T P P \bar{B} \theta^T\} + ((1 + KB)a^T \bar{B})^2 \lambda_{\max}\{\theta \theta^T\} + \lambda_{\max}\{\beta \beta^T\}. \quad (2.90)$$

Taking time derivative of V , in view of (2.76), (2.77), (2.20), (2.86) and (2.87), we obtain

$$\begin{aligned} \dot{V} = & -\dot{x}^T \dot{x} + \left((KB + \hat{\theta}^T l)^2 + c \right) e^2 - (1 + KB)a^T \bar{B} \theta^T \delta e \delta^T \theta \bar{B}^T P \dot{x} \\ & + (KB + \hat{\theta}^T l) \beta^T \delta e - \varepsilon_\delta \delta^T \delta. \end{aligned} \quad (2.91)$$

Using Young's inequality for the cross terms, we get

$$\begin{aligned} \dot{V} \leq & -\dot{x}^T \dot{x} + \left((KB + \hat{\theta}^T l)^2 + c \right) e^2 + \frac{1}{2}e^2 + ((1 + KB)a^T \bar{B})^2 \delta^T \theta \theta^T \delta + \frac{1}{2}\dot{x}^T \dot{x} \\ & + \frac{1}{2}\delta^T \theta \bar{B}^T P P \bar{B} \theta^T \delta + \frac{1}{2}(KB + \hat{\theta}^T l)^2 e^2 + \frac{1}{2}\delta^T \beta \beta^T \delta - \varepsilon_\delta \delta^T \delta, \end{aligned} \quad (2.92)$$

$$\leq -\frac{1}{2}\dot{x}^T \dot{x} - \left(c - \frac{1}{2} \right) e^2 - \frac{1}{2}\varepsilon_\delta \delta^T \delta. \quad (2.93)$$

Using (2.93), we conclude

$$V(t) \leq V(0). \quad (2.94)$$

Defining

$$\Theta(t) = [x^T(t), e(t), \tilde{\theta}^T(t), \tilde{\beta}^T(t), \delta^T(t)]^T, \quad (2.95)$$

and using (2.88) and (2.94), we get

$$|\Theta(t)|^2 \leq M_1 |\Theta(0)|^2, \quad (2.96)$$

for some $M_1 > 0$. Taking derivative of (2.81) and using (2.82) and (2.25) we get

$$\dot{\tilde{\xi}}(t) = G \tilde{\xi}(t). \quad (2.97)$$

Since G is Hurwitz, using (2.97), we have

$$|\tilde{\xi}(t)| \leq M_2 e^{-\alpha_1 t} |\tilde{\xi}(0)|, \quad (2.98)$$

for some $M_2, \alpha_1 > 0$. By using (2.98), we write

$$|\tilde{\xi}(t)| \leq M_2 |\tilde{\xi}(0)| + M_3 |\Theta(0)|, \quad (2.99)$$

for some $M_3 > 0$. By using (2.96) and (2.99), we obtain

$$|\Xi(t)| \leq M_4 |\Xi(0)|, \quad (2.100)$$

where

$$\Xi(t) = \begin{bmatrix} \Theta(t) \\ \tilde{\xi}(t) \end{bmatrix}, \quad (2.101)$$

for some $M_4 > 0$. This proves part (a) of Theorem 2.2.

For all Ξ , the right-hand side of (2.86) and (2.87) are continuous in Ξ and t , which implies that the right-hand side of (2.93) is continuous in Ξ and t . Furthermore, the right-hand side of (2.93) is zero at $\Xi = 0$. By the LaSalle-Yoshizawa theorem, (2.93) ensures that \dot{x}, e and δ converge to zero as $t \rightarrow \infty$.

We represent the closed-loop of $(x, \tilde{\theta})$ system as a linear time-varying (LTV) system which is given by

$$\dot{\zeta} = E(t)\zeta + F(t)d, \quad (2.102)$$

where

$$E(t) = \begin{bmatrix} A_{cl} & \underline{B}\xi^T \\ \gamma_t \xi \overline{B}^T P A_{cl} & \gamma_t \xi \overline{B}^T P \underline{B}\xi^T \end{bmatrix} \quad (2.103)$$

$$F(t) = \begin{bmatrix} \underline{B}\theta^T & \underline{B} \\ \gamma_t \xi \overline{B}^T P \underline{B}\theta^T & \gamma_t \xi (\overline{B}^T P \underline{B} + (1 + KB)a^T \overline{B}) \end{bmatrix} \quad (2.104)$$

$$\zeta = \begin{bmatrix} x^T, & \tilde{\theta}^T \end{bmatrix}^T \quad (2.105)$$

$$d = \begin{bmatrix} \delta^T, & e \end{bmatrix}^T. \quad (2.106)$$

We first show that the equilibrium $\zeta = 0$ of the homogenous part of the LTV system (2.102) is exponentially stable. Towards that end, we choose the following Lyapunov function

$$V_c = \frac{1}{2} \zeta^T P_c \zeta, \quad (2.107)$$

where

$$P_c = \begin{bmatrix} P & 0 \\ 0 & \frac{1}{\gamma_t} I \end{bmatrix}. \quad (2.108)$$

Taking the derivative of V_c , we get

$$\dot{V}_c = \frac{1}{2} \zeta^T \begin{bmatrix} Q_1 & Q_2 \\ Q_2^T & Q_3 \end{bmatrix} \zeta, \quad (2.109)$$

where

$$\begin{aligned} Q_1 &= A_{cl}^T P + P A_{cl}, \\ Q_2 &= (A_{cl}^T P A_{cl}^{-1} + P) \underline{B} \xi^T, \\ Q_3 &= \xi \underline{B}^T (A_{cl}^{-T} P + P A_{cl}^{-1}) \underline{B} \xi^T. \end{aligned}$$

Substituting (2.7), (2.51)–(2.53) into (2.109), we get

$$\dot{V} = -\zeta^T \begin{bmatrix} A_{cl}^T A_{cl} & A_{cl}^T \underline{B} \xi^T \\ \xi \underline{B}^T A_{cl} & \xi \underline{B}^T \underline{B} \xi^T \end{bmatrix} \zeta. \quad (2.110)$$

where $C(t)$ is given in (2.55) we get

$$\begin{aligned} \dot{V} &= \frac{1}{2} \zeta^T (E^T(t) P_c + P_c E(t)) \zeta \\ &= -\zeta^T C(t) C(t)^T \zeta. \end{aligned} \quad (2.111)$$

Therefore, it follows that P_c , as defined in (2.108), satisfies the following inequality $E^T(t) P_c + P_c E(t) + \alpha C^T(t) C(t) \leq 0$ for some $\alpha > 0$.

The equilibrium $\zeta = 0$ of the homogenous part of (2.102) is exponentially stable if $(C(t), E(t))$ is a uniformly completely observable (UCO) pair [26]. For a bounded $H(t)$, the pairs $(C(t), E(t))$ and $(C(t), E(t) + H(t)C(t)^T)$ have the

same UCO property [26]. Choosing $H(t) = \begin{bmatrix} -I \\ -\xi \underline{B}^T P \end{bmatrix}$, we write the system corresponding to the pair $(C, E + HC^T)$ as given in (2.59). The state transition matrix of (2.59) is $\Phi = I$. Therefore, $(C, E + HC^T)$ is a UCO pair if there exist positive constants α_2, α_3, ρ such that the observability Gramian satisfies (2.61) for all $t_0 \geq 0$. Since ξ is bounded, recalling (2.55), the upper bound of (2.61) is satisfied. We now prove the lower bound in (2.61). Calculating the integral in (2.61),

$$\begin{aligned} X &= \int_{t_0}^{t_0+\rho} C(t)C^T(t) dt \\ &= \begin{bmatrix} A_{cl}^T A_{cl} \rho & A_{cl}^T \underline{B} \int_{t_0}^{t_0+\rho} \xi^T dt \\ \int_{t_0}^{t_0+\rho} \xi dt \underline{B}^T A_{cl} & \int_{t_0}^{t_0+\rho} \xi \underline{B}^T \underline{B} \xi^T dt \end{bmatrix}. \end{aligned} \quad (2.112)$$

Let S_h be the Schur complement of $A_{cl}^T A_{cl} \rho$ in X , where

$$\begin{aligned} S_h &= \int_{t_0}^{t_0+\rho} \xi \underline{B}^T \underline{B} \xi^T dt - \frac{1}{\rho} \int_{t_0}^{t_0+\rho} \xi dt \underline{B}^T A_{cl} A_{cl}^{-1} A_{cl}^{-T} A_{cl}^T \underline{B} \int_{t_0}^{t_0+\rho} \xi^T dt \\ &= \underline{B}^T \underline{B} \left(\int_{t_0}^{t_0+\rho} \xi \xi^T dt - \frac{1}{\rho} \int_{t_0}^{t_0+\rho} \xi dt \int_{t_0}^{t_0+\rho} \xi^T dt \right). \end{aligned} \quad (2.113)$$

Since $A_{cl}^T A_{cl} \rho$ is positive definite, X is positive definite if and only if S_h is positive definite. Since $\underline{B}^T \underline{B}$ is a positive scalar, according to Lemma 2.3 there exists a positive ρ such that for all $t_0 > 0$, $S_h > 0$. Hence, $(C, E + HC^T)$ is UCO, which implies that (C, E) is UCO. Therefore, the state transition matrix $\Phi(t, t_0)$ corresponding to $E(t)$ in (2.102) satisfies

$$\|\Phi(t, t_0)\| \leq \kappa_0 e^{-\gamma_0(t-t_0)} \quad (2.114)$$

for some positive constants κ_0, γ_0 . From (2.106), $d(t)$ is bounded and, from (2.104), $F(t)$ is bounded. Recalling that it has already been established that $d(t)$ goes to zero, from (2.102) and (2.114) it follows that ζ is bounded and $\zeta = [x^T, \tilde{\theta}^T]^T \rightarrow 0$ as $t \rightarrow \infty$. By using (2.97) and the fact that G is Hurwitz, we conclude that $\tilde{\xi}(t)$ converges to zero as $t \rightarrow \infty$. Furthermore, thanks to Lemma 2.2, $\hat{\theta}^T(t)\xi(t) - \nu(t) \rightarrow 0$ as $t \rightarrow \infty$. This proves part (b) of Theorem 2.2. \blacksquare

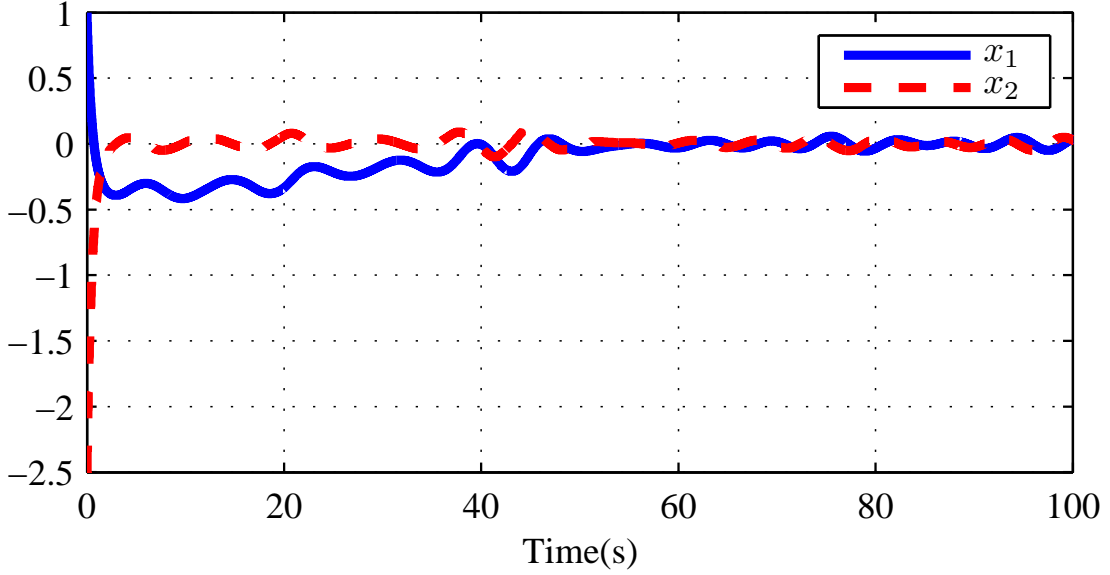


Figure 2.3: Closed loop system's response for the simulation example where the system parameters are known and the unknown disturbance is unmatched.

2.2.3 Simulation Results

We illustrate the performance of our controller with a third-order system with $A = \begin{bmatrix} 0 & 1 \\ 1 & 3 \end{bmatrix}$, $B = \begin{bmatrix} 0 \\ 1 \end{bmatrix}$, $a^T = \begin{bmatrix} 1 & 2 \end{bmatrix}$, $b_u = b_p = 1$, the unknown disturbance $\nu(t) = 1.2 \sin(0.8t + \pi/4) - 0.5 \sin(t + \pi/2)$ and initial conditions $x(0) = \begin{bmatrix} 1 & -2.5 \end{bmatrix}^T$, $p(0) = 0.5$. The control gain K is chosen such that the eigenvalues of A_{cl} are $-3, -4$ and $c = 0.8$. For the update law, we choose $\gamma_t = \gamma_b = 2$. Finally,

the controllable pair (G, l) is chosen as $G = \begin{bmatrix} 0 & 1 & 0 & 0 \\ 0 & 0 & 1 & 0 \\ 0 & 0 & 0 & 1 \\ -4.37 & -12.12 & -12.60 & -5.80 \end{bmatrix}$,

$l = \begin{bmatrix} 0 \\ 0 \\ 0 \\ 1 \end{bmatrix}$ and $N = \begin{bmatrix} 0 & 0 \\ 0 & 0 \\ 0 & 0 \\ 0 & 1 \end{bmatrix}$. From Figures 2.3 and 2.4, one can observe that $x(t)$

converges to zero and the unknown disturbance is perfectly estimated, as Theorem

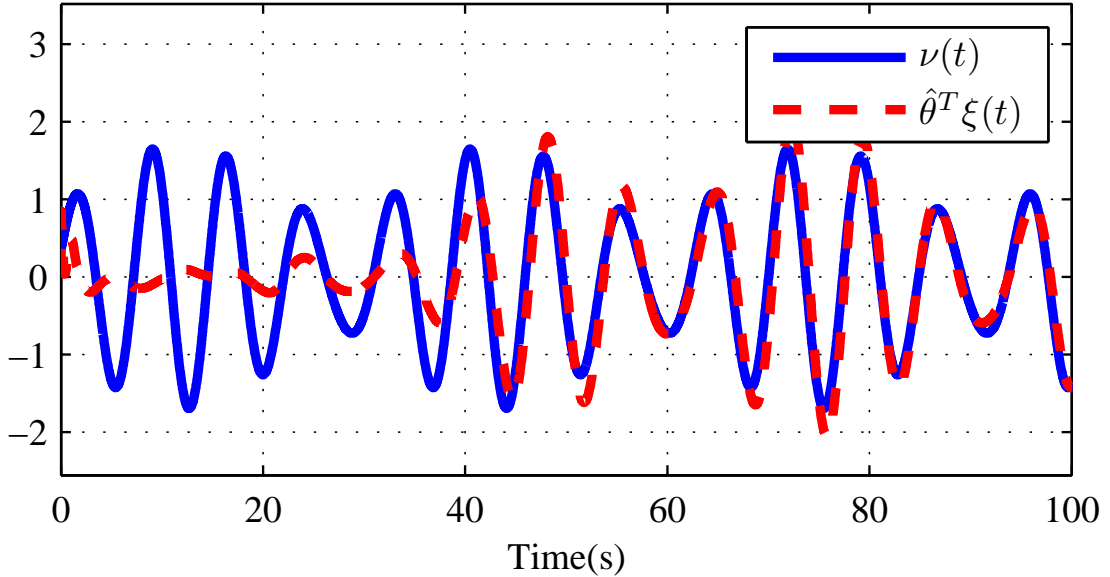


Figure 2.4: Disturbance estimation for the simulation example where the system parameters are known and the unknown disturbance is unmatched.

2.2 predicts.

2.3 Summary

In the present work we design an adaptive controller by state derivative feedback to cancel matched and unmatched unknown sinusoidal disturbances forcing a linear time-invariant systems. In section 2.1, we consider matched unknown disturbance and prove that the closed loop system's solution $x(t) \equiv 0$, $\hat{\theta}(t) \equiv (MS)^{-T}h$, $\eta(t) \equiv GMw(t)$ is globally uniformly asymptotically stable and locally exponentially stable. In section 2.2, we add input dynamic into the system and make the input and unknown disturbance unmatched. We prove that the equilibrium of the closed loop system is stable and the system states and disturbance estimation error converge to zero as $t \rightarrow \infty$. The effectiveness of our controllers is demonstrated with a numerical example.

This chapter is an adaptation of materials appearing in: H. I. Basturk and M. Krstic, "Adaptive cancelation of matched unknown sinusoidal disturbances for

LTI systems by state derivative feedback,” *ASME Journal of Dynamic Systems, Measurement, and Control*, vol. 153, paper 014501-2, 2013. and H. I. Basturk and M. Krstic, “Adaptive backstepping cancelation of *unmatched* unknown sinusoidal disturbances for LTI systems by state derivative feedback,” *ASME Dynamic Systems and Control Conference*, 2012.

The dissertation author is the primary investigator and author of this work.

Chapter 3

State Derivative Feedback for Adaptive Cancellation of Unmatched Disturbances in Unknown Strict-Feedback LTI Systems

We design an adaptive backstepping controller to cancel sinusoidal disturbances forcing an unknown linear time-invariant system in controllable canonical form which is augmented by a linear input subsystem with unknown system parameters by using only measurement of state-derivatives of the original subsystem and state of the input subsystem. Since the system parameters are unknown, it is not possible to use the same disturbance observer which is proposed in Chapter 2. To overcome this problem, we design a linearly parametrized conceptual observer that uses multiple filters and over-parametrization. Our design is based on four steps, 1) parametrization of the sinusoidal disturbance as the output of a known feedback system with an unknown output vector that depends on both unknown disturbance parameters and unknown plant parameters, 2) design of an adaptive disturbance observer for both disturbance and its derivative, 3) design

of an adaptive controller for virtual control input, and 4) design final adaptive controller by using backstepping procedure. We prove that the equilibrium of the closed-loop adaptive system is stable and state of the considered original subsystem goes to zero as $t \rightarrow \infty$ with perfect disturbance estimation. The effectiveness of the controller is illustrated with a simulation example of a third order system.

This chapter is organized as follows: We state the problem in Section 3.1. In Section 3.2 we propose an adaptive controller for the case where the system parameters are unknown and the disturbance is unmatched disturbance by using a backstepping procedure. The stability of the proof and a numerical example are given in Section 3.3 and Section 3.4, respectively. Section 3.5 summarizes the results.

3.1 Problem Statement

We consider the single-input LTI system

$$\dot{x} = A_0 x + B(\bar{\gamma}_1^T x + \nu + \bar{b}_p p), \quad (3.1)$$

$$\dot{p} = \bar{\gamma}_2^T x + \bar{b}_1 p + \bar{b}_2 u, \quad (3.2)$$

where

$$A_0 = \begin{bmatrix} 0_{n-1} & I_{n-1} \\ 0 & 0_{n-1}^T \end{bmatrix} \quad (3.3)$$

$$B = \begin{bmatrix} 0_{n-1} \\ 1 \end{bmatrix} \quad (3.4)$$

$$\bar{\gamma}_1 = [a_{11}, a_{12}, a_{13}, \dots, a_{1n}]^T, \quad (3.5)$$

$$\bar{\gamma}_2 = [a_{21}, a_{22}, a_{23}, \dots, a_{2n}]^T, \quad (3.6)$$

with $0_{n-1} = [0, \dots, 0]^T \in \mathbb{R}^{n-1}$, the state $x \in \mathbb{R}^n$, input $u \in \mathbb{R}$, and sinusoidal disturbance $\nu \in \mathbb{R}$ given by

$$\nu(t) = \sum_{i=1}^q g_i \sin(\omega_i t + \phi_i), \quad (3.7)$$

where $i \neq j \Rightarrow \omega_i \neq \omega_j$, $\omega_i \in \mathbb{Q}_+$, $g_i, \phi_i \in \mathbb{R}$. In this problem, the disturbance $\nu(t)$ and the control input $u(t)$ are not matched (*i.e.*, they are unmatched) because they do not appear in the same equation. The values of $\bar{b}_1, \bar{b}_2, \bar{b}_p, \bar{\gamma}_1$ and $\bar{\gamma}_2$ are unknown. The state $x(t)$ and the disturbance $\nu(t)$ are not measured but $\dot{x}(t)$ and $p(t)$ are measured.

The sinusoidal disturbance ν can be represented as the output of a linear exosystem,

$$\dot{w} = Sw \tag{3.8}$$

$$\nu = h^T w \tag{3.9}$$

where $w \in \mathbb{R}^{2q}$ and the choice of $S \in \mathbb{R}^{2q \times 2q}$ and $h \in \mathbb{R}^{2q}$ is not unique. Since $\nu(t)$ is unknown, S and h are also unknown.

We make the following assumptions regarding the plant (3.1)–(3.2) and the exosystem (3.8)–(3.9):

Assumption 3.1 *The sign of a_{11}, \bar{b}_p and \bar{b}_2 are known and $|\bar{b}_p| \geq \bar{\varsigma} > 0$ where $\bar{\varsigma}$ is known.*

Assumption 3.2 *The pair (h^T, S) is observable and the eigenvalues of S are imaginary, distinct and rational.*

Assumption 3.3 *q is known.*

Assumption 3.4 *$g_i \neq 0$ for all $i \in \{1, \dots, q\}$.*

3.2 Main Result–Design and Stability Statement

We design an adaptive controller which estimates and cancels the unmatched unknown sinusoidal disturbance $\nu(t)$ in system (3.1)–(3.2) by using the measurement of $\dot{x}(t)$ and $p(t)$ for the case where the system parameters are unknown. The design procedure contains four important parts: parametrization of the sinusoidal disturbance, design of an adaptive disturbance observer for both disturbance and its derivative, design of an adaptive controller for virtual control input $p(t)$

by representing the system in reciprocal state space (RSS) form which depends on switching the state vector with its derivative [32] and design of final adaptive controller for input $u(t)$ by using backstepping procedure.

3.2.1 Disturbance Observer

The following lemma enables us to represent the unknown sinusoidal disturbance as the output of a linear system whose input is the disturbance itself, whose state and input matrices are known, and whose output matrix is unknown.

Lemma 3.1 *Let $G \in \mathbb{R}^{2q \times 2q}$ be a Hurwitz matrix with distinct eigenvalues and let (G, l) be a controllable pair. Then, ν can be represented as the output of the model*

$$\dot{z} = Gz + l\nu, \quad (3.10)$$

$$\nu = \theta_{sd}^T \dot{z}, \quad (3.11)$$

$$\theta_{sd}^T = h^T (MS)^{-1}, \quad (3.12)$$

where M is the unique and invertible solution of the Sylvester equation

$$MS - GM = lh^T. \quad (3.13)$$

Proof This result and its proof are inspired by [39]. To establish (3.10) from (3.8), consider $z = Mw$. Differentiating z , we obtain $\dot{z} = MSw$. Using (3.13), we have $\dot{z} = MSw = GMw + lh^T w$. Substituting (3.9) and $z = Mw$ into $\dot{z} = MSw = GMw + lh^T w$ yields (3.10). Substituting $w = (MS)^{-1} \dot{z}$ into (3.9), we obtain (3.11) and (3.12). ■

The previous lemma enables us to write the unknown external disturbance ν as the product of an unknown constant θ_{sd} and the vector \dot{z} . However, \dot{z} is not accessible, since the signal ν can not be measured. To overcome this problem, we design a linearly parametrized conceptual observer that uses multiple filters and over-parametrization.

The following lemma establishes the properties of the observer.

Lemma 3.2 *The inaccessible disturbance ν and $\dot{\nu}$ can be represented in the form*

$$\nu = \theta_{\text{sd}}^T (\eta_0 + N\dot{x}) + \sum_{i=1}^n a_{1i} \theta_{\text{sd}}^T \eta_i + \bar{b}_p \theta_{\text{sd}}^T (\eta_p - lp) + \theta_{\text{sd}}^T \delta, \quad (3.14)$$

$$\begin{aligned} \dot{\nu} = & \frac{1}{1 - \theta_{\text{sd}}^T l} \left(\theta_{\text{sd}}^T G (\eta_0 + N\dot{x}) + \sum_{i=1}^n a_{1i} \theta_{\text{sd}}^T G \eta_i \right. \\ & \left. + \bar{b}_p \theta_{\text{sd}}^T G (\eta_p - lp) + \theta_{\text{sd}}^T G \delta \right), \end{aligned} \quad (3.15)$$

where $1 - \theta_{\text{sd}}^T l > 0$. The observer filters are given by

$$\dot{\eta}_i = G\eta_i - l\dot{x}_i, \quad 1 \leq i \leq n, \quad (3.16)$$

$$\dot{\eta}_0 = G(\eta_0 + N\dot{x}), \quad (3.17)$$

$$\dot{\eta}_p = G(\eta_p - lp), \quad (3.18)$$

with $N \in \mathbb{R}^{2q \times n}$ which is given by $N = \frac{1}{B^T B} l B^T$, where the given N is one of the many solutions of the equation $NB = l$ and the estimation error $\delta \in R^q$ obeys the equation

$$\dot{\delta} = G\delta. \quad (3.19)$$

Proof Post-multiplying (3.13) by $(MS)^{-1}$ and using (3.12), we get $I - l\theta_{\text{sd}}^T = GMS^{-1}M^{-1}$. Using Sylvester's determinant theorem [45], the fact that $\det M^{-1} = \frac{1}{\det M}$ and noting that G and S have $2q$ poles on left half plane and imaginary axis, respectively, we obtain $1 - \theta_{\text{sd}}^T l > 0$.

Defining estimation error, we get

$$\delta = \dot{z} - \left(\eta_0 + N\dot{x} + \sum_{i=1}^n a_{1i} \eta_i + \bar{b}_p (\eta_p - lp) \right). \quad (3.20)$$

Differentiating δ with respect to time and in view of (3.1), (3.16)–(3.18) and (3.10) and using (3.20), (3.10), the fact that $B(\bar{\gamma}_1^T x + \nu) = \dot{x} - Bp - A_0 x$ and by noting that $NA_0 x = 0$ and $NB = l$, we get (3.19). Using (3.11) and (3.20), we obtain (3.14). Differentiating (3.10), and (3.11) and substituting $\ddot{z}(t)$, we get $\dot{\nu} = \frac{1}{1 - \theta_{\text{sd}}^T l} \theta_{\text{sd}}^T G \dot{z}$ and using (3.20) we obtain (3.15). \blacksquare

The representations (3.14), (3.15) established with Lemmas 3.1 and 3.2, allows us to represent a time-varying unknown sinusoidal disturbance $\nu(t)$ and its

derivative $\dot{\nu}(t)$ as a constant unknown vector multiplied by a known regressor, plus an unknown exponentially decaying disturbance. Thus, we convert the problem from cancelation of an unknown sinusoidal disturbance with unknown system parameters to an adaptive control problem.

3.2.2 Reciprocal State-Space Representation

Reciprocal state space representation is a beneficial platform for state derivative feedback control design. Substituting (3.14) into (3.1) and representing the system in RSS form, we obtain

$$x = A_0^T \dot{x} + \overline{B} \frac{1}{\varrho} \left(b_p \dot{x}_n - \gamma_1 \dot{x} - \theta_t^T \eta_t - \beta_{1p}^T \eta_p - \theta_1^T \delta - p \right) \quad (3.21)$$

where

$$\varrho = \frac{a_{11}}{\overline{b}_p (1 - \theta_{sd}^T l)} \quad (3.22)$$

$$b_p = \frac{1}{\overline{b}_p} \quad (3.23)$$

$$\gamma_1 = \frac{1}{\overline{b}_p (1 - \theta_{sd}^T l)} A_0 \overline{\gamma}_1 \quad (3.24)$$

$$\theta_1 = \frac{1}{\overline{b}_p (1 - \theta_{sd}^T l)} \theta_{sd} \quad (3.25)$$

$$\beta_{1p} = \frac{1}{(1 - \theta_{sd}^T l)} \theta_{sd} \quad (3.26)$$

$$\theta_t = [\theta_1^T, a_{11} \theta_1^T, \dots, a_{1n} \theta_1^T]^T, \quad (3.27)$$

with $\eta_t = [\eta_0^T, \eta_1^T, \dots, \eta_n^T]^T$. Substituting (3.21) into (3.2), we get

$$\dot{p} = \gamma_p^T \varphi - \theta_2^T \delta + \frac{1}{b_2} u, \quad (3.28)$$

where

$$\varphi = [\dot{x}^T, p, \eta_t^T, \eta_p^T]^T, \quad (3.29)$$

$$\gamma_p = \left[\gamma_2, \bar{b}_1 - \frac{a_{21}}{\varrho}, -\theta_2^T, -a_{11}\theta_2^T, \dots, -a_{1n}\theta_2^T, -\bar{b}_p\theta_2^T \right], \quad (3.30)$$

$$b_2 = \frac{1}{\bar{b}_2}, \quad (3.31)$$

$$\theta_2 = \frac{a_{21}}{a_{11}}\theta_{sd}, \quad (3.32)$$

$$\gamma_2 = \left[-\frac{a_{21}a_{12}}{a_{11}} + a_{22}, -\frac{a_{21}a_{13}}{a_{11}} + a_{23}, -\frac{a_{21}a_{14}}{a_{11}} + a_{24}, \dots, -\frac{a_{21}a_{1n}}{a_{11}} + a_{2n}, \frac{a_{21}}{a_{11}}(1 - \theta_{sd}^T l) \right]^T. \quad (3.33)$$

In order to handle unmatched uncertainty, we apply a backstepping design [22]. Firstly, we design a control law for virtual input $p(t)$. Then an error term is defined to represent the difference between actual $p(t)$ and its desired value. The error term is given by

$$e(t) = p - \left(-(R\hat{\gamma}_1)^T \dot{x} + \hat{b}_p \dot{x}_n - \hat{\varrho} K \dot{x} - \hat{\theta}_t^T \eta_t - \hat{\beta}_{1p}^T \eta_p \right), \quad (3.34)$$

where $R = \text{diag}\{I_{(n-1) \times (n-1)}, 0\}$ and the control gain $K \in R^{1 \times n}$ is chosen so that $(A_0^T + \bar{B}K)$ is Hurwitz with the positive definite matrix P which is a solution of the matrix equation

$$(A_0^T + \bar{B}K)^T P + P(A_0^T + \bar{B}K) = -4I. \quad (3.35)$$

Since the controllability matrix of the pair (A_0^T, \bar{B}) , $Co = [\bar{B} \ A_0^T \bar{B} \ \dots \ (A_0^T)^{n-1} \bar{B}] = I_{n \times n}$, it is possible to find a control gain K so that $(A_0^T + \bar{B}K)$ is Hurwitz and solve (3.35) for a positive definite matrix P . Besides, the details of pole placement by direct state-derivative feedback and controllability features of reciprocal state space form are given in [48]. Finally, we convert (x, p) system to (x, e) system and design an adaptive controller for input $u(t)$.

In the next section, we give the main result and the stability statement.

3.2.3 Main Controller and Stability Statement

The adaptive controller for system (3.1), (3.2), (3.8), (3.9) is given by

$$u = \frac{\hat{b}_2}{1 - \hat{b}_p(\hat{b}_p - \hat{\rho}k_n)} \bar{u}, \quad (3.36)$$

where k_n is the n^{th} element of the control gain K ,

$$\begin{aligned} \bar{u} = & \hat{\gamma}_3^T (\hat{b}_p - \hat{\rho}k_n) \varphi - \hat{\gamma}_p^T \varphi + \hat{b}_p \dot{x}_n - (\hat{\gamma}_1^T + \hat{\rho}K) A_0 \dot{x} \\ & - \left(\hat{\gamma}_1^T R + \hat{\rho}K - \hat{\rho} \bar{B}^T P \right) \dot{x} - \hat{\theta}_t^T \eta_t - \hat{\theta}_t^T \dot{\eta}_t \\ & - \hat{\beta}_{1p}^T \eta_p - \hat{\beta}_{1p}^T \dot{\eta}_p - \left((\hat{b}_p - \hat{\rho}k_n)^2 + c \right) e, \end{aligned} \quad (3.37)$$

with $c > 0$. We use projection operator to avoid singularity in (3.36). The update laws are given by

$$\dot{\hat{\gamma}}_1 = -\kappa_{\gamma_1} \text{sgn}(\bar{b}_p a_{11}) \dot{x} \bar{B}^T P \dot{x}, \quad \kappa_{\gamma_1} > 0, \quad (3.38)$$

$$\dot{\hat{\gamma}}_p = \kappa_{\gamma_p} \varphi e, \quad \kappa_{\gamma_p} > 0, \quad (3.39)$$

$$\dot{\hat{\gamma}}_3 = -\kappa_{\gamma_3} \varphi (\hat{b}_p - \hat{\rho}k_n) e, \quad \kappa_{\gamma_3} > 0, \quad (3.40)$$

$$\dot{\hat{b}}_2 = -\kappa_{b_2} \text{sgn}(\bar{b}_2) \bar{u} e, \quad \kappa_{b_2} > 0, \quad (3.41)$$

$$\dot{\hat{\theta}}_t = -\kappa_{\theta_1} \text{sgn}(\bar{b}_p a_{11}) \eta_t \bar{B}^T P \dot{x}, \quad \kappa_{\theta_1} > 0, \quad (3.42)$$

$$\dot{\hat{\beta}}_{1p} = -\kappa_{\beta_{1p}} \text{sgn}(\bar{b}_p a_{11}) \eta_p \bar{B}^T P \dot{x}, \quad \kappa_{\beta_{1p}} > 0, \quad (3.43)$$

$$\dot{\hat{\rho}} = -\kappa_{\bar{\rho}} e \bar{B}^T P \dot{x}, \quad \kappa_{\bar{\rho}} > 0, \quad (3.44)$$

$$\dot{\hat{b}}_p = \begin{cases} \tau_{\bar{b}_p}, & \hat{b}_p \text{sgn}(\bar{b}_p) > \bar{\varsigma} \text{ or } \tau_{\bar{b}_p} \text{sgn}(\bar{b}_p) \geq 0 \\ 0, & \hat{b}_p \text{sgn}(\bar{b}_p) \leq \bar{\varsigma} \text{ and } \tau_{\bar{b}_p} \text{sgn}(\bar{b}_p) < 0 \end{cases}, \quad (3.45)$$

$$\begin{bmatrix} \dot{\hat{b}}_p \\ \dot{\hat{\rho}} \end{bmatrix} = \begin{cases} \tau_{b_p, \rho}, & \text{sgn}(\bar{b}_p)(\hat{b}_p - \hat{\rho}k_n) > \frac{1}{\xi} \\ & \text{or } \mathcal{P}^T \tau_{b_p, \rho} \leq 0 \\ \left(I - \Gamma \frac{\mathcal{P} \mathcal{P}^T}{\mathcal{P}^T \Gamma \mathcal{P}} \right) \tau_{b_p, \rho}, & \text{sgn}(\bar{b}_p)(\hat{b}_p - \hat{\rho}k_n) \leq \frac{1}{\xi} \\ & \text{and } \mathcal{P}^T \tau_{b_p, \rho} > 0, \end{cases} \quad (3.46)$$

where

$$\tau_{\bar{b}_p} = -\kappa_{\bar{b}_p} \operatorname{sgn}(\bar{b}_2) \left(\hat{b}_p - \hat{\varrho} k_n \right) u e, \quad \kappa_{\bar{b}_p} > 0, \quad (3.47)$$

$$\tau_{\bar{b}_p, \varrho} = \kappa_{\bar{b}_p, \varrho} \begin{bmatrix} \operatorname{sgn}(\varrho) \dot{x}_n \bar{B}^T P \dot{x} \\ -\operatorname{sgn}(\varrho) K \dot{x} \bar{B}^T P \dot{x} \end{bmatrix}, \quad \kappa_{\bar{b}_p, \varrho} > 0, \quad (3.48)$$

$$P = \begin{bmatrix} -\operatorname{sgn}(\bar{b}_p) & k_n \operatorname{sgn}(\bar{b}_p) \end{bmatrix}^T, \quad (3.49)$$

Γ belongs to the set of all positive definite symmetric 2×2 matrices and the positive matrix P is given in (3.35).

Going forward, the symbol $\tilde{\cdot}$ denotes estimation error between actual value of a plant parameter and its estimate. For combinations of plant parameters, estimation errors are denoted by

$$\tilde{\varrho}(t) = \frac{(1 - \theta_{\text{sd}}^T l) \bar{b}_p}{a_{11}} - \hat{\varrho}(t), \quad (3.50)$$

$$\tilde{\gamma}_3(t) = \left[\tilde{\gamma}_1^T + \bar{b}_p \gamma_2^T + \frac{1}{(1 - \theta_{\text{sd}}^T l)} (\theta_{\text{sd}}^T G N), \theta_3^T, a_{11} \theta_3^T, \dots, a_{1n} \theta_3^T, \bar{b}_p \theta_3^T \right]^T - \hat{\gamma}_3(t), \quad (3.51)$$

with $\theta_3(t) = \left(\frac{1}{(1 - \theta_{\text{sd}}^T l)} G^T - \frac{\bar{b}_p a_{21}}{a_{11}} I_{2q} \right) \theta_{\text{sd}}$ and $\tilde{\eta}_0(t)$ denotes the signal,

$$\tilde{\eta}_p(t) = \bar{b}_p \eta_p(t) + \eta_0 - \bar{\eta}_p(t), \quad (3.52)$$

where $\bar{\eta}_p(t) = \int_0^t e^{G(t-\tau)} G l \nu(\tau) d\tau$. Finally, defining

$$\Theta_1(t) = [x^T(t), \tilde{\gamma}_1^T(t), \tilde{\gamma}_p^T(t), \tilde{\gamma}_3^T(t), \tilde{b}_2(t), \eta_t^T(t), \delta^T(t), \tilde{\theta}_t^T(t), \tilde{\beta}_{1p}^T, \tilde{\varrho}(t)]^T, \quad (3.53)$$

we can now state our Theorem.

Theorem 3.1 *Consider the closed-loop system consisting of the plant (3.1), (3.2) forced by the unknown sinusoidal disturbance (3.8), the disturbance observer (3.16), (3.17), (3.18) and the adaptive controller (3.36), (3.38)–(3.46). Under Assumptions 3.1–3.3, the following holds:*

(a) *The equilibrium $\Theta_1 = 0, \tilde{\eta}_p = 0, \tilde{\varrho} = \tilde{b}_p = \tilde{b}_p = e = 0$ is stable,*

(b) For all initial conditions $\text{sgn}(\bar{b}_p)\hat{b}_p(0) > \bar{\varsigma}$, $(\hat{b}_p(0) - \hat{\rho}(0)k_n)\text{sgn}(\bar{b}_p) > \frac{1}{\bar{\varsigma}}$, $\hat{\rho}(0)$, $p(0) \in \mathbb{R}$, $\Theta_1(0) \in \mathbb{R}^{(4+6q)n+16q+4}$, $\eta_p(0) \in \mathbb{R}^{2q}$ and all $w(0) \in \mathbb{R}^{2q}$ such that Assumption 3.4 holds, the signals $e(t)$, $x(t)$, η_0 , $\eta_i(t)$, $\tilde{\beta}_{1p}(t)$, $\frac{\nu(t)}{b_p} - \hat{\beta}_{1p}^T(t)\eta_p(t)$, $\delta(t)$, $\tilde{\eta}_p(t)$ converge to zero as $t \rightarrow \infty$.

3.3 Stability Proof

The following lemma is used in the proof of the part b of Theorem 3.1.

Lemma 3.3 *Let $x_1(t) \in \mathbb{R}$ be a bounded signal and $\dot{x}_1(t) \in \mathbb{R}$ be square integrable, $\int_0^\infty \dot{x}_1^2 dt \leq M_1$, for some $M_1 > 0$. Then there exists $\rho > 0$ such that for all $t_0 \geq 0$, the following holds*

$$Q_p(\rho, t_0) = \int_{t_0}^{t_0+\rho} \bar{\xi}(t)\bar{\xi}^T(t) dt - \frac{1}{\rho} \int_{t_0}^{t_0+\rho} \bar{\xi}(t) dt \int_{t_0}^{t_0+\rho} \bar{\xi}^T(t) dt > 0, \quad (3.54)$$

where

$$\bar{\xi} = \eta_p + \frac{1}{b_p} \tilde{\xi}(t), \quad (3.55)$$

with

$$\tilde{\xi}(t) = \left(\eta_0 + \sum_{i=1}^n a_{1i} \eta_i + l \bar{b}_p (1 - \theta_{sd}^T l) \gamma_1^T \dot{x} + \delta \right). \quad (3.56)$$

Proof Using (3.10), (3.12), (3.20), (3.24) and by noting that $N = lB^T$ and $\dot{x}_n - \bar{b}_p p = \bar{\gamma}_1^T x + \nu$, we obtain $\eta_p = \frac{1}{b_p} Gz - l \frac{a_{11}}{b_p} x_1 - \frac{1}{b_p} \tilde{\xi}$. Substituting η_p into (3.55), we get

$$\bar{\xi} = \xi - l \frac{a_{11}}{b_p} x_1, \quad (3.57)$$

where $\xi = \frac{1}{b_p} Gz$. Since G has distinct eigenvalues and is Hurwitz, it is diagonalizable. Using a Jordan decomposition of the matrix G , we can write $G = L\Lambda L^{-1}$. By solving (3.10) for $z(t)$ as given in Lemma 2.3, we obtain

$$\xi(\tau) = L (e^{\Lambda\tau} C_c + \Psi(\tau)), \quad (3.58)$$

where $C_c = L^{-1}\xi(0) - \Psi(0)$, $\bar{l} = L^{-1}Gl\frac{1}{\bar{b}_p}$ and $\Psi \in R^{2q}$ is a vector whose j^{th} row is

$$\sum_{i=1}^q \frac{\bar{l}_j g_i}{\lambda_j^2 + \omega_i^2} \left(\lambda_j \sin(\omega_i \tau + \phi_i) - \omega_i \cos(\omega_i \tau + \phi_i) \right). \quad (3.59)$$

Since ν is a sufficiently rich signal order of $2q$ and (G, l) is a controllable pair, G is full rank and $\bar{b}_p \neq 0$, ξ is persistently exciting [18]. Therefore, there exist positive ρ^* and α_0 such that for all $\rho > \rho^*$ and $t_0 \geq 0$ the following holds

$$\int_{t_0}^{t_0+\rho} \xi(t) \xi^T(t) dt \geq \rho \alpha_0 I. \quad (3.60)$$

Under Assumption 3.2, the frequencies of ν can be represented as

$$\omega_i = \frac{\text{num}(\omega_i)}{\text{den}(\omega_i)}, \quad \text{num}(\omega_i), \text{den}(\omega_i) \in \mathbb{Z}^+, \quad i = 1 \dots q.$$

Then ρ that is given by

$$\rho = \vartheta \text{lcm}(\text{num}(\omega_1), \dots, \text{num}(\omega_q)) \times \text{lcm}(\text{den}(\omega_1), \dots, \text{den}(\omega_q)) 2\pi > \rho^*, \quad (3.61)$$

where lcm is the abbreviation of the least common multiple, satisfies (3.60) if $\vartheta \in \mathbb{Z}^+$ is chosen sufficiently large for given ρ^* and $\omega_1, \dots, \omega_q$. Since $\Psi(t)$ defined by (3.59) has a period ρ and incorporates only zero-mean functions, it follows that

$$\int_{t_0}^{t_0+\rho} \Psi(t) dt = 0. \quad (3.62)$$

Substituting (3.57), (3.58)–(3.62) into (3.54) and using integration by parts, we obtain

$$Q_p(\rho, t_0) \geq L\Pi L^T, \quad (3.63)$$

where

$$\begin{aligned} \Pi = & \rho \bar{\alpha}_0 I - \frac{1}{\rho} \left(\Gamma(\rho) \Gamma^T(\rho) + \Gamma(\rho) \tilde{l}^T \int_{t_0}^{t_0+\rho} x_1(t) dt + \tilde{l} \Gamma^T(\rho) \int_{t_0}^{t_0+\rho} x_1(t) dt \right) \\ & - \tilde{\Psi}^T(t_0, \rho) - \tilde{\Psi}(t_0, \rho) + \tilde{l} \tilde{l}^T \int_{t_0}^{t_0+\rho} x_1^2(t) dt - \frac{1}{\rho} \tilde{l} \tilde{l}^T \left(\int_{t_0}^{t_0+\rho} x_1(t) dt \right)^2, \end{aligned} \quad (3.64)$$

with $\bar{\alpha}_0 = \alpha_0 / \lambda_{\max}\{LL^T\}$, $\tilde{l} = \frac{a_{11}}{b_p} L^{-1} l$,

$$\Gamma^T(\rho) = \left[c_1 e^{\lambda_1 t_0} (e^{\lambda_1 \rho} - 1) \quad \dots \quad c_{2q} e^{\lambda_{2q} t_0} (e^{\lambda_{2q} \rho} - 1) \right], \quad (3.65)$$

$$\begin{aligned} \tilde{\Psi}^T(t_0, \rho) &= (\Lambda^{-1} e^{\Lambda(t_0+\rho)} C_c + \bar{\Psi}(t_0 + \rho)) x_1(t_0 + \rho) - (\Lambda^{-1} e^{\Lambda t_0} C_c + \bar{\Psi}(t_0)) x_1(t_0) \\ &\quad - \int_{t_0}^{t_0+\rho} (\Lambda^{-1} e^{\Lambda t} C_c + \bar{\Psi}(t)) \dot{x}_1(t) dt \end{aligned} \quad (3.66)$$

where $\bar{\Psi}(t) \in R^{2q}$ is the vector whose j^{th} row is

$$\sum_{i=1}^q -\frac{\bar{l}_j g_i}{\lambda_j^2 + \omega_i^2} \left(\frac{\lambda_j}{\omega_i} \cos(\omega_i t + \phi_i) + \sin(\omega_i t + \phi_i) \right), \quad (3.67)$$

and c_i denotes the i^{th} row of the vector C_c / λ_i .

Since L is full rank, Q_p satisfies the inequality (3.54) if $\mu^T \Pi \mu > 0$ for all nonzero $\mu \in R^{2q}$. Using (3.64), the Cauchy-Schwarz inequality and by noting that $\lambda_i < 0$, $|e^{\lambda_i \rho} - 1| \leq 1$, $x_1(t)$ is bounded and $\int_0^\infty \dot{x}_1^2 dt \leq M_1$, we have

$$\begin{aligned} \mu^T \Pi \mu &\geq \sqrt{\rho} \left((\sqrt{\rho} \bar{\alpha}_0 - \frac{1}{\rho^{3/2}} \bar{C}_c) (\mu_1^2 + \dots + \mu_{2q}^2) - 2|\tilde{l}^T \mu| \right) \\ &\quad \times \sqrt{M_1 \sup_{t_0 \leq t < \infty} \bar{\mu}^2(t)} - |\tilde{l}^T \mu| \bar{\Gamma} \end{aligned} \quad (3.68)$$

where

$$\begin{aligned} \bar{\Gamma} &= \sup_{t_0 \leq t < \infty} |x_1(t)| (|\mu_1 c_1| e^{\lambda_1 t_0} + \dots + |\mu_{2q} c_{2q}| e^{\lambda_{2q} t_0}) \\ &\quad + 2 \left(|\bar{\mu}(t_0) x_1(t_0)| + \sup_{t_0 \leq t < \infty} |\bar{\mu}(t) x_1(t)| \right), \end{aligned} \quad (3.69)$$

with $\bar{\mu}(t) = \mu^T (\Lambda^{-1} e^{\Lambda t} C_c + \bar{\Psi}(t))$ and $\bar{C}_c = c_1^2 e^{2\lambda_1 t_0} + \dots + c_{2q}^2 e^{2\lambda_{2q} t_0}$.

Since $\sqrt{\rho} \bar{\alpha}_0 (\mu_1^2 + \dots + \mu_{2q}^2) - 2|\tilde{l}^T \mu| \sqrt{M_1 \sup_{t_0 \leq t < \infty} \bar{\mu}^2(t)}$ is positive and in-

creasing for $\rho > 4 \frac{|\tilde{l}^T \mu|^2 M_1 \sup_{t_0 \leq t < \infty} \bar{\mu}^2(t)}{\bar{\alpha}_0^2 (\mu_1^2 + \dots + \mu_{2q}^2)^2}$ and $\frac{1}{\rho^{3/2}} (\mu_1^2 + \dots + \mu_{2q}^2) \bar{C}_c$ is monotonically decreasing with respect to ρ and $\bar{\Gamma}$ is constant for all fixed t_0 , one can find a ρ using (3.61) such that for all $t_0 \geq 0$, (3.54) holds. \blacksquare

Proof of Theorem 3.1: The stability of the equilibrium of the closed-loop system is established with the use of Lyapunov function

$$\begin{aligned}
V = & \frac{1}{2}x^T Px + \frac{1}{2|\varrho|} \left(\frac{1}{\kappa_{b_p, \varrho}} (\varrho^2 + \tilde{b}_p^2) + \frac{1}{\kappa_{\gamma_1}} \tilde{\gamma}_1^T \tilde{\gamma}_1 + \frac{1}{\kappa_{\theta_t}} \tilde{\theta}_t^T \tilde{\theta}_t + \frac{1}{\kappa_{\beta_{1p}}} \tilde{\beta}_{1p}^T \tilde{\beta}_{1p} \right) \\
& + \frac{1}{2}e^2 + \frac{1}{\kappa_{2\gamma_p}} \tilde{\gamma}_p^T \tilde{\gamma}_p + \frac{1}{\kappa_{\bar{\varrho}}} \tilde{\varrho}^2 + \frac{1}{\kappa_{\gamma_3}} \tilde{\gamma}_3^T \tilde{\gamma}_3 + \frac{1}{2|b_2|} \left(\frac{\tilde{b}_2^2}{\kappa_{b_2}} + \frac{\tilde{b}_p^2}{\kappa_{\bar{b}_p}} \right) \\
& + \frac{1}{2\varepsilon_\eta} \left(\eta_0^T P_G \eta_0 + \sum_{i=1}^n \eta_i^T P_G \eta_i \right) + \frac{\varepsilon_\delta}{2} \delta^T P_G \delta, \tag{3.70}
\end{aligned}$$

where the positive definite matrix P_G which is a solution of the matrix equation $G^T P_G + P_G G = -2I$ and

$$\begin{aligned}
\varepsilon_\delta = & \frac{1}{\varrho^2} \lambda_{\max} \{ \theta_1 \bar{B}^T P P \bar{B} \theta_1^T \} + \frac{a_{21}^2}{a_{11}^2} \lambda_{\max} \{ \theta_{sd} \theta_{sd}^T \} \\
& + \lambda_{\max} \{ \theta_3 \theta_3^T \}, \tag{3.71}
\end{aligned}$$

$$\varepsilon_\eta = l^T P_G P_G l. \tag{3.72}$$

Taking the time derivative of V and using the property of the projection operator, $-\tilde{b}_p \dot{\hat{b}}_p \leq -\tilde{b}_p \tau_{\tilde{b}_p}$, $\text{sgn}(b_2) \hat{b}_p \geq \bar{\varsigma} > 0$ and $-\tilde{b}_p, \tilde{\varrho} [\dot{\hat{b}}_p, \dot{\hat{\varrho}}]^T \leq -[\tilde{b}_p, \tilde{\varrho}] \tau_{b_p, \varrho}$, $\text{sgn}(\bar{b}_p) (\hat{b}_p - \hat{\varrho} k_n) \geq \frac{1}{\bar{\varsigma}} > 0$ [22, Appendix E] and Young's inequality for the cross terms, we obtain

$$\dot{V} \leq -\frac{1}{2} \dot{x}^T \dot{x} - ce^2 - \frac{1}{2\varepsilon_\eta} \sum_{i=0}^n \eta_i^T \eta_i - \frac{\varepsilon_\delta}{2} \delta^T \delta. \tag{3.73}$$

Using (3.73), we conclude

$$V(t) \leq V(0). \tag{3.74}$$

Defining

$$\Theta(t) = [\Theta_1^T(t), \tilde{b}_p(t), \tilde{b}_p(t), \tilde{\varrho}(t), e(t)]^T, \tag{3.75}$$

and using (3.70) and (3.74), we get

$$|\Theta(t)|^2 \leq M_2 |\Theta(0)|^2, \tag{3.76}$$

for some $M_2 > 0$. Taking the derivative of (3.52) and using (3.17) and the fact that $\dot{x}_n - \bar{b}_p p = \bar{\gamma}_1^T x + \nu$, we get

$$\dot{\tilde{\eta}}_p(t) = G\tilde{\eta}_p + Gt\bar{\gamma}_1^T x. \quad (3.77)$$

Since G is Hurwitz, using (3.77), we have

$$|\tilde{\eta}_p(t)| \leq M_3 e^{-\alpha_1 t} |\tilde{\eta}_p(0)| + M_4 \sup_{\tau \in [0, t]} |x(\tau)| \quad (3.78)$$

for some $M_3, M_4, \alpha_1 > 0$. By using (3.76) and (3.78), we obtain

$$|\tilde{\eta}_p(t)| \leq M_3 |\tilde{\eta}_p(0)| + M_4 \sqrt{M_2} |\Theta(0)|. \quad (3.79)$$

By using (3.76) and (3.79), we obtain

$$\left| \left[\Theta^T(t), \tilde{\eta}_p^T(t) \right]^T \right| \leq M_5 \left| \left[\Theta^T(t), \tilde{\eta}_p^T(t) \right]^T \right|, \quad (3.80)$$

for some $M_5 > 0$. This proves part (a) of Theorem 3.1.

We write the closed-loop system in the following form

$$\dot{x} = \tilde{A}^{-1} x + \tilde{A}^{-1} \bar{B} \frac{1}{\varrho} \left(\tilde{\theta}_t^T \eta_t + \frac{1}{\bar{b}_p} \tilde{\beta}_{1p}^T (\tilde{\eta}_p - \eta_0 + \bar{\eta}_p) + e + \theta_1^T \delta \right), \quad (3.81)$$

where $\tilde{A} = A_0^T + \bar{B} \left(\frac{1}{\varrho} (\tilde{\gamma}_1^T + \tilde{b}_p B^T + K \hat{\varrho}) \right)$. From (3.3), (3.4), (3.24) and by noting that $\bar{B} = \left[1, 0_{n-1} \right]^T$, we get

$$\det(\tilde{A}) = (-1)^{n+1} \left(\frac{1}{\varrho} \left(\frac{1}{\bar{b}_p} - (\hat{b}_p - \hat{\varrho} k_n) \right) \right). \quad (3.82)$$

From (3.82) it follows that, for all Ξ such that $\text{sgn}(\bar{b}_p)(\hat{b}_p - \hat{\varrho} k_n) \geq \frac{1}{\xi} > 0$, the right-hand side of (3.81) is continuous in Ξ and t , which implies that the right-hand side of (3.73) is continuous in Ξ and t . Furthermore, the right-hand side of (3.73) is zero at $\Xi = 0$. By the LaSalle-Yoshizawa theorem, (3.73) ensures that $\dot{x}, e, \eta_0, \dots, \eta_n$ and δ converge to zero as $t \rightarrow \infty$.

By adding $\pm \frac{\kappa_{\beta_{1p}} \text{sgn}(\varrho)}{\bar{b}_p} \tilde{\xi}(t) \bar{B}^T P \dot{x}$ and $\pm \frac{1}{\bar{b}_p \varrho} \bar{B} \tilde{\beta}_{1p}^T \tilde{\xi}(t)$ to (3.43) and (3.81) respectively, we represent the close-loop of $(x, \tilde{\beta}_{1p})$ system as a linear-time varying (LTV) system which is given by

$$\dot{\zeta} = E(t)\zeta + F(t)d, \quad (3.83)$$

where

$$E(t) = \begin{bmatrix} A_{cl} & \frac{1}{\varrho} \underline{B} \bar{\xi}^{-T} \\ \kappa_{\beta_{1p}} \text{sgn}(\varrho) \bar{\xi} \bar{B}^T P A_{cl} & \frac{\kappa_{\beta_{1p}}}{|\varrho|} \bar{\xi} \bar{B}^T P \underline{B} \bar{\xi}^{-T} \end{bmatrix} \quad (3.84)$$

$$F(t) = \begin{bmatrix} f_1 & f_2 & f_3 & \frac{1}{\varrho} \underline{B} \\ f_0 f_1 & f_0 f_2 & f_0 f_3 & \frac{\kappa_{\theta_1}}{|\varrho|} \bar{\xi} \bar{B}^T P \underline{B} \end{bmatrix} \quad (3.85)$$

$$d = \left[\dot{x}^T, \eta_t^T, \delta^T, e \right]^T \quad (3.86)$$

$$\zeta = \left[x^T, \tilde{\beta}_{1p}^T \right]^T \quad (3.87)$$

with $f_0 \in \mathbb{R}^{2q \times n}$, $f_1 \in \mathbb{R}^{n \times n}$, $f_2 \in \mathbb{R}^{n \times 2q(n+1)}$, $f_3 \in \mathbb{R}^{n \times 2q}$ are given by

$$f_0 = \frac{\kappa_{\beta_{1p}}}{\text{sgn}(\varrho)} \bar{\xi} \bar{B}^T P \quad (3.88)$$

$$f_1 = \frac{1}{\varrho} \underline{B} (\tilde{\varrho} K + \tilde{\gamma}_1^T + \tilde{b}_p B^T - \frac{1}{\tilde{b}_p} \tilde{\beta}_{1p}^T l \bar{b}_p (1 - \bar{\theta}_1^T l) \gamma_1^T), \quad (3.89)$$

$$f_2 = \frac{1}{\varrho} \underline{B} \left(\tilde{\theta}_t^T - \frac{1}{\tilde{b}_p} \left[\tilde{\beta}_{1p}^T, a_{11} \tilde{\beta}_{1p}^T, \dots, a_{1n} \tilde{\beta}_{1p}^T \right] \right), \quad (3.90)$$

$$f_3 = \frac{1}{\varrho} \underline{B} (\theta_1^T - \frac{1}{\tilde{b}_p} \tilde{\beta}_{1p}^T), \quad (3.91)$$

with $A_{cl} = (A_0^T + \bar{B}K)^{-1}$ and $\underline{B} = A_{cl} \bar{B}$.

We first show that the equilibrium $\zeta = 0$ of the homogenous part of the LTV system (3.83) is exponentially stable. Towards that end, we choose the following Lyapunov function

$$V_c = \frac{1}{2} \zeta^T P_c \zeta, \quad (3.92)$$

where

$$P_c = \text{diag} \left\{ P, \frac{1}{|\varrho| \kappa_{\beta_{1p}}} I_{2q \times 2q} \right\}. \quad (3.93)$$

Taking the derivative of V_c and using (3.35), we get

$$\dot{V}_c = -2\zeta^T C(t) C^T(t) \zeta, \quad (3.94)$$

where

$$C^T(t) = \begin{bmatrix} A_{cl} & \frac{1}{\varrho} \underline{B} \bar{\xi}^{-T} \end{bmatrix}. \quad (3.95)$$

Therefore, it follows that P_c , satisfies the following inequality

$$E^T(t)P_c + P_cE(t) + \alpha C^T(t)C(t) \leq 0, \quad (3.96)$$

for some $\alpha > 0$. The equilibrium $\zeta = 0$ of the homogenous part of (3.83) is exponentially stable if $(C(t), E(t))$ is a uniformly completely observable (UCO) pair [26]. For a bounded $H(t)$, the pairs $(C(t), E(t))$ and $(C(t), E(t) + H(t)C(t)^T)$ have the same UCO property [26]. Choosing $H(t) = \begin{bmatrix} -I, & -\kappa_{\beta_{1p}} \text{sgn}(\varrho) P \overline{B} \overline{\xi}^T \end{bmatrix}^T$, we write the system corresponding to the pair $(C, E + HC^T)$ as

$$\dot{Y} = 0 \quad (3.97)$$

$$y = C^T(t)Y. \quad (3.98)$$

The state transition matrix of (3.97) is $\Phi = I$. Therefore, $(C, E + HC^T)$ is a UCO pair if there exist positive constants α_2, α_3, ρ such that the observability Gramian satisfies

$$\alpha_2 I \geq \int_{t_0}^{t_0+\rho} C(t)C^T(t) dt \geq \alpha_3 I, \quad (3.99)$$

for all $t_0 \geq 0$. Since $\overline{\xi}$ is bounded, recalling (3.95), the upper bound of (3.99) is satisfied. We now prove the lower bound in (3.99). Calculating the integral in (3.99), we get

$$X = \begin{bmatrix} A_{\text{cl}}^T A_{\text{cl}} \rho & \frac{1}{\varrho} A_{\text{cl}}^T \underline{B} \int_{t_0}^{t_0+\rho} \overline{\xi}^T dt \\ \frac{1}{\varrho} \int_{t_0}^{t_0+\rho} \overline{\xi} dt \underline{B}^T A_{\text{cl}} & \frac{1}{\varrho^2} \int_{t_0}^{t_0+\rho} \overline{\xi} \underline{B}^T \underline{B} \overline{\xi}^T dt \end{bmatrix}. \quad (3.100)$$

Let S_h be the Schur complement of $A_{\text{cl}}^T A_{\text{cl}} \rho$ in X , where

$$S_h = \frac{\underline{B}^T \underline{B}}{\varrho^2} \left(\int_{t_0}^{t_0+\rho} \overline{\xi} \overline{\xi}^T dt - \frac{1}{\rho} \int_{t_0}^{t_0+\rho} \overline{\xi} dt \int_{t_0}^{t_0+\rho} \overline{\xi}^T dt \right). \quad (3.101)$$

Using (3.73) and (3.74) and calculating the integral, we obtain

$$\int_0^\infty \dot{x}_1^2(t) dt \leq 2(V(0) - V(\infty)) \leq M_1 \quad (3.102)$$

for some $M_1 > 0$. Since $A_{\text{cl}}^T A_{\text{cl}} \rho$ is positive definite, X is positive definite if and only if S_h is positive definite. Since $\frac{\underline{B}^T \underline{B}}{\varrho^2}$ is a positive scalar, using boundedness

of $\Xi(t)$ and (3.102), according to Lemma 3.3 there exists a positive ρ such that for all $t_0 \geq 0$, $S_h > 0$. Hence, $(C, E + HC^T)$ is UCO, which implies that (C, E) is UCO. Therefore, the state transition matrix $\Phi(t, t_0)$ corresponding to $E(t)$ in (3.83) satisfies $\|\Phi(t, t_0)\| \leq \kappa_0 e^{-\gamma_0(t-t_0)}$, for some positive constants κ_0, γ_0 . From the boundedness of $\Xi(t)$ and $\bar{\eta}_p$, it follows from (3.81) that $\dot{x}(t)$ is bounded. From (3.86), $d(t)$ is bounded and, from (3.85), $F(t)$ is bounded. Recalling that it has already been established that $d(t)$ goes to zero, from (3.83) and the property of $\Phi(t, t_0)$, it follows that ζ is bounded and $\zeta = [x^T, \tilde{\beta}_{1p}^T]^T \rightarrow 0$ as $t \rightarrow \infty$. By using (3.77) and the fact that G is Hurwitz and $x(t)$ converges to zero, we conclude that $\tilde{\eta}_p(t)$ converges to zero as $t \rightarrow \infty$. Furthermore, using (3.12), (3.14), (3.26), (3.34) and by noting that $d(t) \rightarrow 0$, $\hat{\beta}_{1p}(t) \rightarrow \frac{1}{1-\theta_{sd}^T} \theta_{sd}$ we obtain $\left(\theta_{sd}^T + \frac{\theta_{sd}^T l}{1-\theta_{sd}^T} \theta_{sd}^T\right) \eta_p(t) \rightarrow \frac{1}{b_p} \nu(t)$. Recalling $\hat{\beta}_{1p}(t) \rightarrow \frac{1}{1-\theta_{sd}^T} \theta_{sd}$ and $\theta_{sd}^T l$ is scalar, we obtain $\hat{\beta}_{1p}^T \eta_p(t) \rightarrow \frac{1}{b_p} \nu(t)$. This proves part (b) of Theorem 3.1. \blacksquare

3.4 Simulation Results

We illustrate the performance of our controller with a third-order system with $\bar{\gamma}_1^T = \begin{bmatrix} 1 & 3 \end{bmatrix}$, $\bar{\gamma}_2^T = \begin{bmatrix} 1 & 2 \end{bmatrix}$, $\bar{b}_p = \bar{b}_1 = 2$, $\bar{b}_2 = 1$, the unknown disturbance $\nu(t) = 1.2 \sin(0.8t + \pi/4) - 0.5 \sin(t + \pi/2)$ and initial conditions $x(0) = \begin{bmatrix} 2 & -2.5 \end{bmatrix}^T$, $p(0) = 0.5$. The control gain K is chosen such that the eigenvalues of A_{cl} are $-0.5, -0.25$ and $c = 10$. We set all update gains to 1 except $\kappa_{\gamma_1} = 3$. Finally, the controllable pair (G, l) is chosen as $l = \begin{bmatrix} 0 & 0 & 0 & 1 \end{bmatrix}^T$, $G = \begin{bmatrix} 0_3 & I_3 \\ 0 & 0_3^T \end{bmatrix} + l \begin{bmatrix} -4.37 & -12.12 & -12.60 & -5.80 \end{bmatrix}$. From Figures 3.1 and 3.2, one can observe that $x(t)$ and $\frac{1}{b_p} \nu(t) - \hat{\beta}_{1p}^T \eta_p(t)$ converge to zero as Theorem 3.1 predicts.

3.5 Summary

In the present work we design an adaptive backstepping controller by using state derivative of the system and state of the input subsystem to cancel unmatched unknown sinusoidal disturbances forcing an LTI system with unknown parameters.

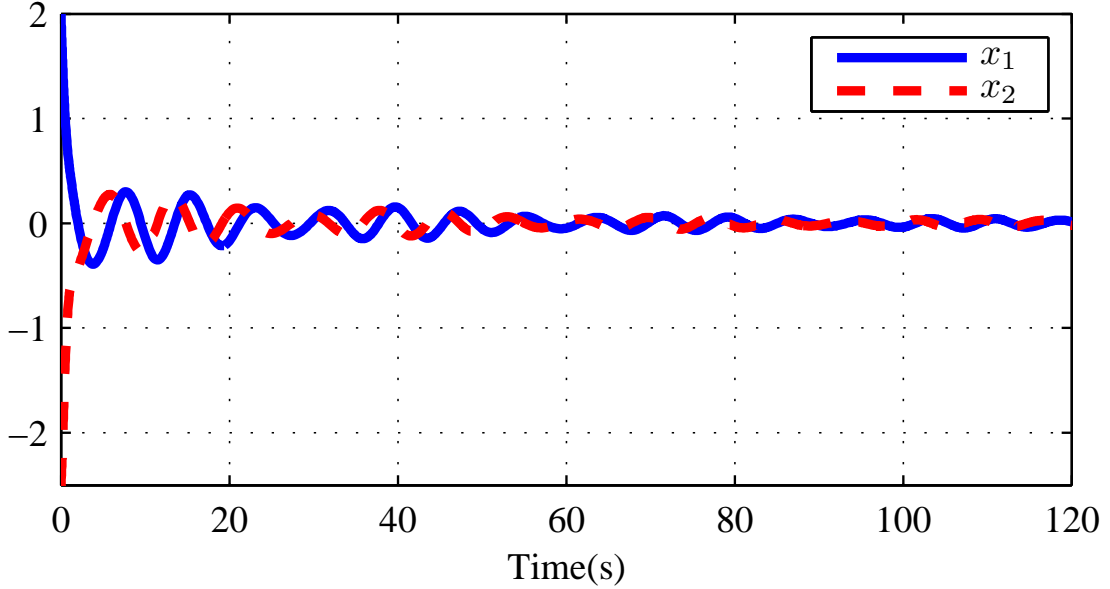


Figure 3.1: Closed loop system’s response for the simulation example where the system parameters are unknown and the unknown disturbance is unmatched.

We prove that the equilibrium of the closed loop system is stable and the state of the considered error system (x, e) goes to zero as $t \rightarrow \infty$ with perfect disturbance estimation. The effectiveness of our controller is demonstrated with a numerical example.

This chapter is an adaptation of material appearing in: H. I. Basturk and M. Krstic, “Adaptive backstepping cancelation of *unmatched* unknown sinusoidal disturbances for *unknown* LTI systems by state derivative feedback,” *IEEE Conference on Decision and Control*, 2012.

The dissertation author is the primary investigator and author of this work.

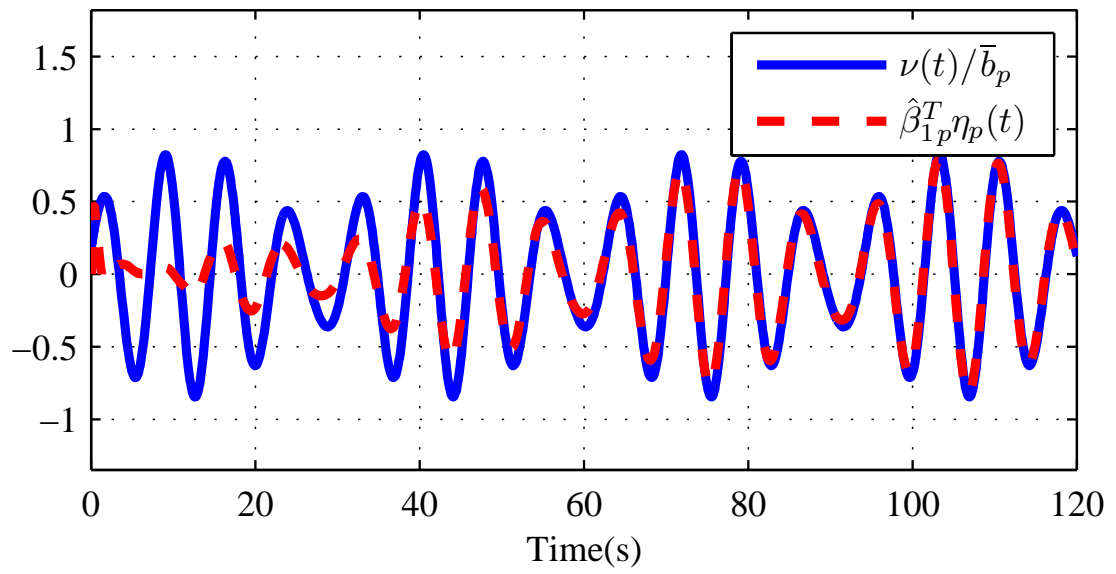


Figure 3.2: Disturbance estimation for the simulation example where the system parameters are unknown and the unknown disturbance is unmatched.

Chapter 4

Adaptive Wave Cancellation by Acceleration Feedback for Ramp-Connected Air Cushion-Actuated Surface Effect Ships

We solve here the problem of cargo transfer in high sea states over a ramp from a large, medium-speed, roll-on/roll-off (LMSR) vessel to a smaller connector vessel of a surface effect ship (SES) type. We design an air cushion actuated controller to estimate and cancel the wave disturbance and stabilize the heave of the SES via heave acceleration feedback with actuation of the louver area for the case where the hydrodynamic and other parameters of the SES are not known a priori and the pressure dynamics of the air-cushion contains nonlinearly parameterized unknown terms to provide a safer environment for cargo transfer. We demonstrate the effect of our control design in simulations in a time-domain seakeeping code, named AEGIR.

This chapter is organized as follows: We introduce the mathematical model of the heave and air cushion dynamics of an SES in Section 4.1. Design of the

controller and stability proof of the closed loop system are given in Section 4.2. In Section 4.3, we present the parameters of the ships and simulation platform. The results are discussed in Section 4.4.

4.1 Mathematical Model of System Dynamics

4.1.1 SES Heave Model

Following [37], we consider the linear model of the heave dynamics (decoupled from pitch) for control design purpose. The model is given by

$$(m + A_{33})\ddot{\zeta}_3(t) + B_{33}\dot{\zeta}_3(t) + C_{33}\zeta_3(t) - A_c P_c = F_3^e(t), \quad (4.1)$$

where ζ_3 represents the heave, P_c is the air cushion pressure. A_c is area of the air cushion and m is the mass of the ship. Hydrodynamic (added-mass), radiation damping coefficients and hydrostatic (restoring) term for heave are represented as A_{33} , B_{33} , C_{33} respectively. F_3^e is hydrodynamic excitation force. For single frequency wave, it is given by

$$F_3^e(t) = K_3^e \sin(\omega_e t + \phi), \quad (4.2)$$

with

$$K_3^e = 2ge^{kd} \frac{\sin \frac{kL}{2}}{\frac{kL}{2}} (C_{33} - \omega\omega_e A_{33} + \phi), \quad (4.3)$$

where d and L are the draft and length of the side hulls. g, ω, ϕ, k are the amplitude, frequency, phase and number of the wave respectively. ω_e is the encounter frequency which is represented by $\omega_e = \omega - kU \cos(\chi)$ where U and χ are the craft speed and heading angle, respectively. In the adaptive control design, the draft of the side hulls, d , is assumed to be constant.

4.1.2 Pressure dynamics for single chamber air-cushion

Assuming the uniform pressure distribution in the air cushion, the global continuity equation for mass flow into and out of the cushion can be written as

$$q_{in}(t) - q_{out}(t) = \frac{d}{dt} (\rho_c(t) V_c(t)) \quad (4.4)$$

where $q_{in}(t)$ is the air flow into the air cushion from the lift fan system, $q_{out}(t)$ is the air flow out of the air cushion due to the louver system, $V_c(t)$ is the cushion volume, $\rho_c(t)$ is the density of the air at the pressure $P_c(t)$.

Assuming the basic thermodynamic variation in the air cushion is adiabatic, we represent pressure-density relationship as

$$\rho_c(t) = \frac{\rho_{c0}}{P_{c0}^{1/\gamma}} (P_c(t))^{1/\gamma}, \quad (4.5)$$

where γ is the ratio of specific heat of air, and ρ_{c0} is the density of the air at the equilibrium pressure P_{c0} . Differentiating (4.5) with respect to time t , we reach the expression for the time derivative of air density as

$$\dot{\rho}_c(t) = \frac{\rho_{c0}}{\gamma P_{c0}^{1/\gamma}} (P_c(t))^{1/\gamma-1} \dot{P}_c(t). \quad (4.6)$$

The volume of the air cushion is given by

$$V_c(t) = A_c(h_0 + \zeta_3(t)) - V_0(t), \quad (4.7)$$

where h_0 is the air cushion height at equilibrium and $V_0(t)$ is the wave volume pumping disturbance. For single frequency wave, it is given by

$$V_0(t) = K_0 \sin(\omega_e(t) + \phi), \quad (4.8)$$

where

$$K_0 = A_c g \frac{\sin(\frac{kL}{2})}{\frac{kL}{2}}, \quad (4.9)$$

for regular head sea waves in [2], [25].

Assuming no dynamic response, the fan characteristic curve can be represented by

$$q_{in}(t) = \rho_c(t) \left(Q_0 + \frac{\partial Q}{\partial P} \Big|_{P_{c0}} (P_c(t) - P_{c0}) \right), \quad (4.10)$$

where Q_0 is the equilibrium air flow rate of fan when $P_c(t) = P_{c0}$ and $\frac{\partial Q}{\partial P} \Big|_{P_{c0}}$ is the corresponding linear fan slope about the ship equilibrium operating point Q_0 and P_{c0} [2]. The air flow out of the air cushion by louver system is given by

$$q_{out} = \rho_c(t) c_n \sqrt{\frac{2(P_c(t) - P_a)}{\rho_{c0}}} A_l, \quad (4.11)$$

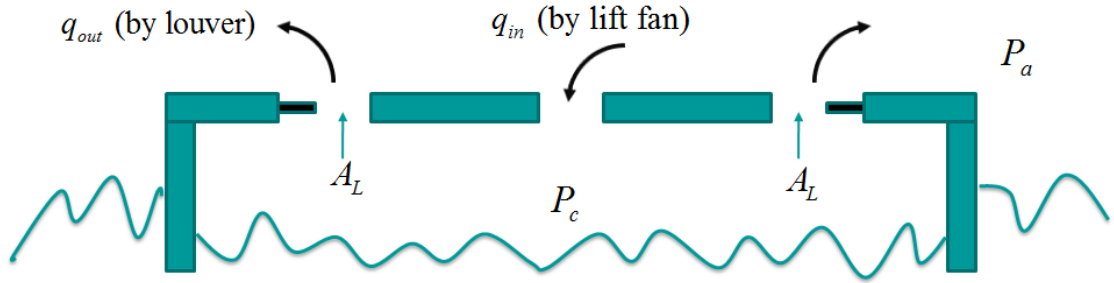


Figure 4.1: Illustration of the chamber of the air cushion of a surface effect ship. The symbol A_L denotes louver area which is used as the control input.

where P_a is the atmospheric pressure, c_n is the orifice coefficient varying between 0.61 and 1 and A_l is the leakage area of the louver system [2].

Using (4.4)–(4.11), we get

$$\dot{P}_c(t) = \frac{\bar{P}_c(t)}{V_c(t)}, \quad (4.12)$$

where

$$\bar{P}_c = \gamma P_c \left(Q_0 + \frac{\partial Q}{\partial P} \Big|_{P_{c0}} (P_c(t) - P_{c0}) - A_c \dot{\zeta}_3(t) + \dot{V}_0(t) - c_n \sqrt{\frac{2(P_c(t) - P_a)}{\rho_{c0}}} A_l \right). \quad (4.13)$$

The louver area, A_l , is considered as the control input of the system. The chamber of the air cushion is illustrated in Figure 4.1. It is hard to design an adaptive controller for the given pressure model, since it contains nonlinearly parameterized unknown term $V_c(t)$. However we achieve to handle this significant challenge, without linearizing the model, by using the physical property of the volume, $V_c(t)$ which is always positive, $V_c(t) > 0$.

4.2 Control Design for Heave

In this section, we design an adaptive backstepping controller by using the measurement of heave rate and acceleration of the ship and air-cushion pressure for the case where the system parameters are not known. The objective of the controller is to stabilize the heave of the craft in the presence of sea wave disturbances

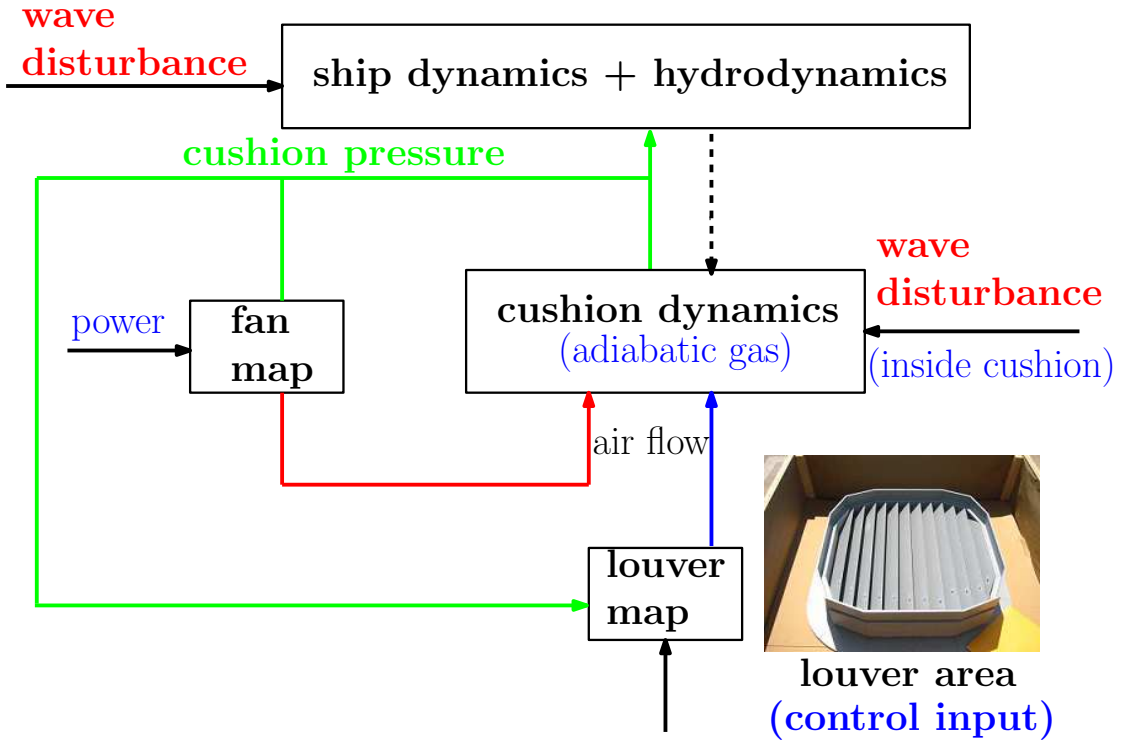


Figure 4.2: The structure of the control problem. The overall system consists of two dynamics, wave disturbances, fan and louver maps.

by the actuation of louver area. The structure of the control problem is given in Figure 4.2.

The decoupled heave dynamics can be represented in the state-space form as follows

$$\dot{x} = A_0 x + B (\bar{a}_1 x_1 + \bar{a}_2 x_2 + \bar{F}_3^e + \bar{b}_p P_c), \quad (4.14)$$

where

$$A_0 = \begin{bmatrix} 0 & 1 \\ 0 & 0 \end{bmatrix}, \quad (4.15)$$

$$B = \begin{bmatrix} 0 & 1 \end{bmatrix}^T, \quad (4.16)$$

$$x = \begin{bmatrix} \zeta_3, & \dot{\zeta}_3 \end{bmatrix}^T, \quad (4.17)$$

$$\bar{a}_1 = -\frac{C_{33}}{m + A_{33}} \quad (4.18)$$

$$\bar{a}_2 = -\frac{B_{33}}{m + A_{33}} \quad (4.19)$$

$$\bar{F}_3^e = \frac{F_3^e}{m + A_{33}} \quad (4.20)$$

$$\bar{b}_p = \frac{A_c}{m + A_{33}}. \quad (4.21)$$

4.2.1 Disturbance Representation

The sinusoidal disturbances (4.8) and (4.20) can be represented as the output of a linear exosystem,

$$\dot{w} = Sw \quad (4.22)$$

$$\bar{F}_3^e = h^T w, \quad (4.23)$$

$$V_0 = K_0 \frac{m + A_{33}}{K_3^e} h^T w, \quad (4.24)$$

where $w \in \mathbb{R}^2$ and the choice of $S \in \mathbb{R}^{2 \times 2}$ and $h \in \mathbb{R}^2$ is not unique. However, the pairs (S, h) is assumed to be observable. Since \bar{F}_3^e and V_0 are unknown, h and S are also unknown.

Using Lemma 3.1 and Lemma 3.2, the inaccessible disturbances \bar{F}_3^e, V_0 and their time derivatives $\dot{\bar{F}}_3^e, \dot{V}_0$ can be represented in the form

$$\bar{F}_3^e = \bar{\theta}_e^T (\eta_0 + N\dot{x}) + \sum_{i=1}^2 \bar{a}_i \bar{\theta}_e^T \eta_i + \bar{b}_p \bar{\theta}_e^T (\eta_p - lP_c) + \bar{\theta}_e^T \delta, \quad (4.25)$$

$$V_0 = \bar{\theta}_0^T (\eta_0 + N\dot{x}) + \sum_{i=1}^2 \bar{a}_i \bar{\theta}_0^T \eta_i + \bar{b}_p \bar{\theta}_0^T (\eta_p - lP_c) + \bar{\theta}_0^T \delta, \quad (4.26)$$

$$\dot{\bar{F}}_3^e = \frac{1}{1 - \bar{\theta}_e^T l} \left(\bar{\theta}_e^T G (\eta_0 + N\dot{x}) + \sum_{i=1}^2 \bar{a}_i \bar{\theta}_e^T G \eta_i + \bar{b}_p \bar{\theta}_e^T G (\eta_p - lP_c) + \bar{\theta}_e^T G \delta \right), \quad (4.27)$$

$$\dot{V}_0 = \frac{1}{1 - \bar{\theta}_e^T l} \left(\bar{\theta}_0^T G (\eta_0 + N\dot{x}) + \sum_{i=1}^2 \bar{a}_i \bar{\theta}_0^T G \eta_i + \bar{b}_p \bar{\theta}_0^T G (\eta_p - lP_c) + \bar{\theta}_0^T G \delta \right), \quad (4.28)$$

where

$$\dot{\eta}_i = G\eta_i - l\dot{x}_i, \quad \text{for } i = 1, 2, \quad (4.29)$$

$$\dot{\eta}_0 = G(\eta_0 + N\dot{x}), \quad (4.30)$$

$$\dot{\eta}_p = G(\eta_p - lP_c). \quad (4.31)$$

N is a 2×2 matrix which is given by $N = \frac{1}{B^T B} l B^T$. The given N is one of the many solutions of the equation $NB = l$. $\delta \in R^2$ obeys the equation

$$\dot{\delta} = G\delta. \quad (4.32)$$

4.2.2 Reciprocal State Space Representation

The reciprocal state space (RSS) representation depends on switching the state vector with its derivative [32]. Thus, one can design a controller by utilizing the state derivatives instead of states. Substituting the developed representation of \overline{F}_3^e , (4.25), into (4.14), we get

$$x = A_0^T \dot{x} + \overline{B} \frac{1}{\varrho} \left(b_p \dot{x}_2 - a_2 \dot{x}_1 - \theta_e^T \eta_0 - \sum_{i=1}^2 \beta_{1i}^T \eta_i - \beta_{1p}^T \eta_p - P_c - \theta_e^T \delta \right) \quad (4.33)$$

where

$$\overline{B} = \begin{bmatrix} 1 & 0 \end{bmatrix}^T, \quad (4.34)$$

$$\varrho = \frac{\overline{a}_1}{\overline{b}_p (1 - \overline{\theta}_e^T l)}, \quad (4.35)$$

$$b_p = \frac{1}{\overline{b}_p}, \quad (4.36)$$

$$a_2 = \frac{\overline{a}_2}{\overline{b}_p (1 - \overline{\theta}_e^T l)}, \quad (4.37)$$

$$\theta_e = \frac{1}{\overline{b}_p (1 - \overline{\theta}_e^T l)} \overline{\theta}_e, \quad (4.38)$$

$$\beta_{1i} = \frac{\overline{a}_i}{\overline{b}_p (1 - \overline{\theta}_e^T l)} \overline{\theta}_e, \quad (4.39)$$

$$\beta_{1p} = \frac{1}{(1 - \overline{\theta}_e^T l)} \overline{\theta}_e. \quad (4.40)$$

Using (4.18), (4.21) and noting that $1 - \bar{\theta}_e^T l > 0$, area of the air-cushion A_c , hydrodynamic, A_{33} , and hydrostatic, C_{33} terms are positive, we obtain $\text{sgn}(\varrho) = -1$ and $\text{sgn}(\bar{b}_p) = 1$. For the adaptive control design, we assume that the high frequency gain $\bar{b}_p > \bar{\varsigma} > 0$. From a physical point of view, $\bar{\varsigma}$ can be determined with rough knowledge of the dimensions and the mass of the catamaran.

4.2.3 Adaptive Backstepping Control Design

The representations (4.25)–(4.28) established with Lemmas 3.1 and 3.2, allows us to represent the time-varying unknown sinusoidal disturbances and their derivative as a constant unknown vector multiplied by a known regressor, plus an unknown exponentially decaying disturbance. Thus, we convert the problem from cancelation of an unknown sinusoidal disturbance with unknown system parameters to an adaptive control problem. Since the system (4.33), (4.12) has unmatched parametric uncertainties, we apply adaptive backstepping method to design a control law.

In adaptive backstepping method, we first find the desired value of the air cushion pressure to stabilize the heave of the surface effect ship. Considering the air-cushion pressure, P_c , as the virtual controller, desired pressure value is given by

$$P_{\text{desired}} = -\hat{\varrho}K\dot{x} - \hat{a}_2\dot{x}_1 + \hat{b}_p\dot{x}_2 - \hat{\theta}_e^T\eta_0 - \sum_{i=1}^2 \hat{\beta}_{1i}^T\eta_i - \hat{\beta}_{1p}^T\eta_p, \quad (4.41)$$

where the control gain $K \in R^{1 \times 2} = \begin{bmatrix} k_1 & k_2 \end{bmatrix}$ is chosen so that $(A_0^T + \bar{B}K)$ is Hurwitz and the positive definite matrix R is a solution of the matrix equation

$$(A_0^T + \bar{B}K)^T R + R(A_0^T + \bar{B}K) = -4I. \quad (4.42)$$

The deviation of P_c from its desired value, P_{desired} is written as

$$e(t) = P_c(t) - P_{\text{desired}}(t). \quad (4.43)$$

Substituting (4.43) into (4.33) and taking the time derivative of $e(t)$, we convert

(x, P_c) system to (x, e) system,

$$x = (A_0^T + \bar{B}K) \dot{x} + \bar{B} \frac{1}{\varrho} (\tilde{b}_p \dot{x}_2 - \tilde{a}_2 \dot{x}_1 - \tilde{\varrho} K \dot{x} - \tilde{\theta}_e^T \eta_0 - \sum_{i=1}^2 \tilde{\beta}_{1i}^T \eta_i - \tilde{\beta}_{1p}^T \eta_p - e - \theta_e^T \delta), \quad (4.44)$$

$$\begin{aligned} \dot{e}(t) &= (\hat{\varrho} k_1 + \hat{a}_2) \dot{x}_1 + (\hat{\varrho} k_1 + \hat{a}_2 + \hat{\varrho} k_2 - \hat{b}_p) \dot{x}_2 + \hat{\theta}_e^T \eta_0 + \hat{\theta}_e^T \dot{\eta}_0 \\ &+ \sum_{i=1}^2 (\hat{\beta}_{1i}^T \eta_i + \hat{\beta}_{1i}^T \dot{\eta}_i) + \hat{\beta}_{1p}^T \eta_p + \hat{\beta}_{1p}^T \dot{\eta}_p - \Theta_e^T \Xi_e - (\hat{b}_p - \hat{\varrho} k_2) \frac{1}{1 - \bar{\theta}_e^T l} \bar{\theta}_e^T G \delta \\ &+ \left(1 - (\hat{b}_p - \hat{\varrho} k_2) \bar{b}_p\right) \frac{\bar{P}_c}{V_c} \end{aligned} \quad (4.45)$$

where

$$\Theta_e = \left[\bar{a}_1, \quad \bar{a}_2 + \frac{1}{1 - \bar{\theta}_e^T l} \bar{\theta}_e^T G l, \quad \frac{1}{1 - \bar{\theta}_e^T l} \bar{\theta}_e^T G, \quad \frac{\bar{a}_1}{1 - \bar{\theta}_e^T l} \bar{\theta}_e^T G, \quad \frac{\bar{a}_2}{1 - \bar{\theta}_e^T l} \bar{\theta}_e^T G, \quad \frac{\bar{b}_p}{1 - \bar{\theta}_e^T l} \bar{\theta}_e^T G \right]^T \quad (4.46)$$

$$\Xi_e = (\hat{b}_p - \hat{\varrho} k_2) \left[\dot{x}_1, \quad \dot{x}_2, \quad \eta_0^T, \quad \eta_1^T, \quad \eta_2^T, \quad (\eta_p - l P_c)^T \right]^T, \quad (4.47)$$

$$\tilde{b}_p = b_p - \hat{b}_p, \quad (4.48)$$

$$\tilde{a}_2 = a_2 - \hat{a}_2, \quad (4.49)$$

$$\tilde{\varrho} = \varrho - \hat{\varrho}, \quad (4.50)$$

$$\tilde{\theta}_e = \theta_e - \hat{\theta}_e, \quad (4.51)$$

$$\tilde{\beta}_{1i} = \beta_{1i} - \hat{\beta}_{1i}, \quad (4.52)$$

$$\tilde{\beta}_{1p} = \beta_{1p} - \hat{\beta}_{1p}. \quad (4.53)$$

The air-cushion pressure dynamics, (4.12), contains nonlinearly parameterized term, V_c , and unmeasured heave, $x_1 = \zeta_3$. We write x_1 in terms of heave rate, heave acceleration, air-cushion pressure, the derived representation of \bar{F}_3^e and substitute it into the model. Furthermore, we can use the volume of the air-cushion, V_c , in the Lyapunov analysis since it is positive and its derivative, \dot{V}_c , can be represented in terms of measured signals, constant unknown terms with known regressors and exponentially decaying term by using (4.27). We use $V_c e^2$ instead of usual choice, e^2 , in our Lyapunov function in order to achieve a linearly parameterized expression in the time derivative of Lyapunov function. This choice increases the unknown terms and causes the over parametrization.

We assume the measurements of the heave rate and acceleration of the ship to be available for feedback loop throughout the analysis. However, the data from integrated heave accelerometers need to be filtered or processed before using them for control. It is important to have unbiased heave acceleration to avoid drift in parameter estimations and estimate heave rate properly. Although the type of a method employed to eliminate bias depends on the features of the sensor, a high pass filter with appropriate parameters will typically suffice. Heave rate for feedback can be obtained by filtering unbiased heave acceleration with a bandpass filter (a low pass filter in conjunction with a high pass filter). Other sensing and filtering options are also possible to obtain heave rate and acceleration for specific applications.

Remark 4.1 The proposed controller is designed based on system dynamics (4.1), (4.12) with disturbance models (4.2), (4.8) by assuming that the measurements are accurate and precise. Although the simulation platform which we implement our controller, provides a reliable environment to test the robustness of the controller with respect to some unmodeled system and disturbance dynamics such as coupling with other modes, irregular waves and different heading angles, there are still various other effects (measurement noise, wind disturbance, ...) which are not considered in the design and simulation but may be encountered in a practice. These effects may cause drift in parameter estimations which may harm the stability of the equilibrium of the closed loop system. The destabilizing effects of bounded disturbances and of a class of dynamic uncertainties may be counteracted by using simple modifications that involve leakage, dead-zone, projection, and dynamic normalization as given in [26]. We do not add these modifications to our design and analysis. However one can select an appropriate modification for certain application conditions and implement it to the proposed controller.

The adaptive controller for surface effect ship is given by

$$A_l = \frac{\hat{b}_u}{\left(1 - \hat{b}_p \left(\hat{b}_p - \hat{q}k_2\right)\right) \sqrt{2(P_c(t) - P_a)}} u \quad (4.54)$$

with

$$u = -\hat{\varrho}\dot{x}^T R\bar{B} + \hat{\Theta}_{dV_c}^T \Xi_{dV_c} + \hat{\Theta}_{\dot{e}V_c} \Xi_{\dot{e}V_c} + \hat{\Theta}_{P_c} \Xi_{P_c} + \hat{\Theta}_{\hat{b}_p P_c} \Xi_{P_c} \left(\hat{b}_p - \hat{\varrho}k_2 \right) + \Xi_\delta + ce, \quad (4.55)$$

with $c > 2$ and the regressors

$$\Xi_{dV_c} = e \left[\dot{x}_1, (\eta_0 + N\dot{x})^T, \eta_1^T, \eta_2^T, (\eta_p - lP_c)^T \right]^T, \quad (4.56)$$

$$\begin{aligned} \Xi_{\dot{e}V_c} = & \left[\xi_{de}, \Xi_e^T, \xi_{de}\dot{x}_1, \Xi_e^T \dot{x}_1, \xi_{de}\dot{x}_2, \Xi_e^T \dot{x}_2, \xi_{de}\eta_0^T l_1, \Xi_e^T \eta_0^T l_1, \xi_{de}\eta_0^T l_2, \right. \\ & \Xi_e^T \eta_0^T l_2, \xi_{de}\eta_1^T l_1, \Xi_e^T \eta_1^T l_1, \xi_{de}\eta_1^T l_2, \Xi_e^T \eta_1^T l_2, \xi_{de}\eta_2^T l_1, \Xi_e^T \eta_2^T l_1, \\ & \left. \xi_{de}\eta_2^T l_2, \Xi_e^T \eta_2^T l_2, \xi_{de}\eta_p^T l_1, \Xi_e^T \eta_p^T l_1, \xi_{de}\eta_p^T l_2, \Xi_e^T \eta_p^T l_2, \xi_{de}P_c, \Xi_e^T P_c \right]^T, \end{aligned} \quad (4.57)$$

$$\Xi_{P_c} = P_c \left[1, P_c, \dot{x}_1, (\eta_0 + N\dot{x})^T, \eta_1^T, \eta_2^T, \eta_p^T \right]^T, \quad (4.58)$$

where $l_1 = \left[1, 0 \right]^T$, $l_2 = B$ and

$$\Xi_\delta = \frac{1}{2} \left(\hat{b}_p - \hat{\varrho}k_2 \right)^2 \left[3, \dot{x}_1^2, \dot{x}_2^2, \eta_0^T \eta_0, \eta_1^T \eta_1, \eta_2^T \eta_2, \eta_p^T \eta_p, P_c^2 \right]^T, \quad (4.59)$$

$$\begin{aligned} \xi_{de} = & \left(\hat{\varrho}k_1 + \hat{a}_2 \right) \dot{x}_1 + \left(\hat{\varrho}k_1 + \hat{a}_2 + \hat{\varrho}k_2 - \hat{b}_p \right) \dot{x}_2 + \dot{\hat{\theta}}_e^T \eta_0 + \hat{\theta}_e^T \dot{\eta}_0 + \sum_{i=1}^2 \left(\dot{\hat{\beta}}_{1i}^T \eta_i + \hat{\beta}_{1i}^T \dot{\eta}_i \right) \\ & + \dot{\hat{\beta}}_{1p}^T \eta_p + \hat{\beta}_{1p}^T \dot{\eta}_p. \end{aligned} \quad (4.60)$$

The update laws are given by

$$\dot{\hat{a}}_2 = -\kappa_{a_2} \text{sgn}(\varrho) \dot{x}_1 \bar{B}^T R \dot{x}, \quad \kappa_{a_2} > 0, \quad (4.61)$$

$$\dot{\hat{\theta}}_e = -\kappa_{\theta_e} \text{sgn}(\varrho) \eta_0 \bar{B}^T R \dot{x}, \quad \kappa_{\theta_e} > 0, \quad (4.62)$$

$$\dot{\hat{\beta}}_{1i} = -\kappa_{\beta_{1i}} \text{sgn}(\varrho) \eta_i \bar{B}^T R \dot{x}, \quad \kappa_{\beta_{1i}} > 0, \quad (4.63)$$

$$\dot{\hat{\beta}}_{1p} = -\kappa_{\beta_{1p}} \text{sgn}(\varrho) \eta_p \bar{B}^T R \dot{x}, \quad \kappa_{\beta_{1p}} > 0, \quad (4.64)$$

$$\dot{\hat{b}}_u = -\kappa_{b_u} u e, \quad \kappa_{b_u} > 0, \quad (4.65)$$

$$\dot{\hat{\varrho}} = -\kappa_{\bar{\varrho}} e \dot{x}^T R \bar{B}, \quad \kappa_{\bar{\varrho}} > 0, \quad (4.66)$$

$$\dot{\hat{\Theta}}_{dV_c} = \kappa_{\Theta_{dV_c}} \Xi_{dV_c} e, \quad \kappa_{\Theta_{dV_c}} > 0, \quad (4.67)$$

$$\dot{\hat{\Theta}}_{\dot{e}V_c} = \kappa_{\Theta_{\dot{e}V_c}} \Xi_{\dot{e}V_c} e, \quad \kappa_{\Theta_{\dot{e}V_c}} > 0, \quad (4.68)$$

$$\dot{\hat{\Theta}}_{P_c} = \kappa_{\Theta_{P_c}} \Xi_{P_c} e, \quad \kappa_{\Theta_{P_c}} > 0, \quad (4.69)$$

$$\dot{\hat{\Theta}}_{\bar{b}_p P_c} = \kappa_{\Theta_{\bar{b}_p P_c}} \Xi_{\bar{b}_p P_c} \left(\hat{b}_p - \hat{\varrho} k_2 \right) e, \quad \kappa_{\Theta_{\bar{b}_p P_c}} > 0, \quad (4.70)$$

$$\dot{\hat{b}}_p = \begin{cases} \tau_{\bar{b}_p}, & \hat{b}_p \text{sgn}(\bar{b}_p) > \bar{\tau} \text{ or } \tau_{\bar{b}_p} \text{sgn}(\bar{b}_p) \geq 0 \\ 0, & \hat{b}_p \text{sgn}(\bar{b}_p) \leq \bar{\tau} \text{ and } \tau_{\bar{b}_p} \text{sgn}(\bar{b}_p) < 0 \end{cases}, \quad (4.71)$$

$$\begin{bmatrix} \dot{\hat{b}}_p \\ \dot{\hat{\varrho}} \end{bmatrix} = \begin{cases} \tau_{b_p, \varrho}, & \text{sgn}(\bar{b}_p) (\hat{b}_p - \hat{\varrho} k_n) > \frac{1}{\xi} \\ & \text{or } \mathcal{P}^T \tau_{b_p, \varrho} \leq 0 \\ \left(I - \Gamma \frac{\mathcal{R} \mathcal{R}^T}{\mathcal{R}^T \Gamma \mathcal{R}} \right) \tau_{b_p, \varrho}, & \text{sgn}(\bar{b}_p) (\hat{b}_p - \hat{\varrho} k_n) \leq \frac{1}{\xi} \\ & \text{and } \mathcal{R}^T \tau_{b_p, \varrho} > 0, \end{cases} \quad (4.72)$$

where

$$\tau_{\bar{b}_p} = \kappa_{\bar{b}_p} \left(\hat{b}_p - \hat{\varrho} k_n \right) A_l \sqrt{2(P_c(t) - P_a)} e, \quad \kappa_{\bar{b}_p} > 0 \quad (4.73)$$

$$\tau_{b_p, \varrho} = \kappa_{b_p, \varrho} \begin{bmatrix} \text{sgn}(\varrho) \dot{x}_n \bar{B}^T R \dot{x} \\ -\text{sgn}(\varrho) K \dot{x} \bar{B}^T R \dot{x} \end{bmatrix}, \quad \kappa_{b_p, \varrho} > 0, \quad (4.74)$$

$$\mathcal{R} = \begin{bmatrix} -\text{sgn}(\bar{b}_p) & k_2 \text{sgn}(\bar{b}_p) \end{bmatrix}^T, \quad (4.75)$$

and Γ belongs to the set of all positive definite symmetric 2×2 matrices.

We first define the signals needed in the analysis and state a theorem describing our main stability result. Then we prove the theorem using a technical

lemmas in next section. Estimation errors of the unknown parameters are denoted by

$$\tilde{\varrho} = \frac{1}{\varrho} - \hat{\varrho}, \quad (4.76)$$

$$\tilde{b}_u = b_u - \hat{b}_u, \quad (4.77)$$

$$\tilde{b}_p = \bar{b}_p - \hat{b}_p, \quad (4.78)$$

$$\tilde{\Theta}_{dV_c} = \Theta_{dV_c} - \hat{\Theta}_{dV_c}, \quad (4.79)$$

$$\tilde{\Theta}_{\dot{e}V_c} = \Theta_{\dot{e}V_c} - \hat{\Theta}_{\dot{e}V_c}, \quad (4.80)$$

$$\tilde{\Theta}_{P_c} = \Theta_{P_c} - \hat{\Theta}_{P_c}, \quad (4.81)$$

$$\tilde{\Theta}_{\bar{b}_p P_c} = \Theta_{\bar{b}_p P_c} - \hat{\Theta}_{\bar{b}_p P_c}, \quad (4.82)$$

where

$$b_u = \frac{c_n}{\sqrt{\rho_{c0}}}, \quad (4.83)$$

$$\Theta_{dV_c} = \left[A_c \quad -\frac{1}{1-\bar{\theta}_e^T l} \bar{\theta}_0^T G \quad -\frac{\bar{a}_1}{1-\bar{\theta}_e^T l} \bar{\theta}_0^T G \quad -\frac{\bar{a}_2}{1-\bar{\theta}_e^T l} \bar{\theta}_0^T G \quad -\frac{\bar{b}_p}{1-\bar{\theta}_e^T l} \bar{\theta}_0^T G \right]^T, \quad (4.84)$$

$$\Theta_{P_c} = \gamma \left[Q_0 - \frac{\partial Q}{\partial P_c} P_{c0}, \quad \frac{\partial Q}{\partial P_c} - \frac{\bar{b}_p}{1-\bar{\theta}_e^T l} \bar{\theta}_0^T G l, \quad -A_c, \quad \frac{1}{1-\bar{\theta}_e^T l} \bar{\theta}_0^T G, \quad \frac{\bar{a}_1}{1-\bar{\theta}_e^T l} \bar{\theta}_0^T G, \right. \\ \left. \frac{\bar{a}_2}{1-\bar{\theta}_e^T l} \bar{\theta}_0^T G, \quad \frac{\bar{b}_p}{1-\bar{\theta}_e^T l} \bar{\theta}_0^T G \right]^T, \quad (4.85)$$

$$\Theta_{\dot{e}V_c} = \left[A_c h_0, \quad A_c h_0 \Theta_e^T, \quad -\bar{a}_1 \frac{A_c}{\bar{a}_2}, \quad -\bar{a}_1 \frac{A_c}{\bar{a}_2} \Theta_e^T, \quad (1 - \bar{\theta}_e^T l) \frac{A_c}{\bar{a}_1} - \theta_0^T l, \right. \\ \left((1 - \bar{\theta}_e^T l) \frac{A_c}{\bar{a}_1} - \theta_0^T l \right) \Theta_e^T, \quad \bar{\theta}_{e0}^T l_1, \quad \bar{\theta}_{e0}^T l_1 \Theta_e^T, \quad \bar{\theta}_{e0}^T l_2, \quad \bar{\theta}_{e0}^T l_2 \Theta_e^T, \\ -\bar{a}_1 \bar{\theta}_{e0}^T l_1, \quad -\bar{a}_1 \bar{\theta}_{e0}^T l_1 \Theta_e^T, \quad -\bar{a}_1 \bar{\theta}_{e0}^T l_2, \quad -\bar{a}_1 \bar{\theta}_{e0}^T l_2 \Theta_e^T, \\ -\bar{a}_2 \bar{\theta}_{e0}^T l_1, \quad -\bar{a}_2 \bar{\theta}_{e0}^T l_1 \Theta_e^T, \quad -\bar{a}_2 \bar{\theta}_{e0}^T l_2, \quad -\bar{a}_2 \bar{\theta}_{e0}^T l_2 \Theta_e^T, \\ -\bar{b}_p \bar{\theta}_{e0}^T l_1, \quad -\bar{b}_p \bar{\theta}_{e0}^T l_1 \Theta_e^T, \quad -\bar{b}_p \bar{\theta}_{e0}^T l_2, \quad -\bar{b}_p \bar{\theta}_{e0}^T l_2 \Theta_e^T, \\ \left. -\bar{b}_p \left(\frac{A_c}{\bar{a}_1} (1 - \bar{\theta}_e^T l) - \bar{\theta}_0^T l \right), \quad -\bar{b}_p \left(\frac{A_c}{\bar{a}_1} (1 - \bar{\theta}_e^T l) - \bar{\theta}_0^T l \right) \Theta_e^T \right]^T, \quad (4.86)$$

$$\Theta_{\bar{b}_p P_c} = \bar{b}_p \Theta_{P_c}, \quad (4.87)$$

with $\bar{\theta}_{e0} = -\left(\frac{A_c}{\bar{a}_1} \bar{\theta}_e + \bar{\theta}_0\right)$ and $\tilde{\eta}_p(t)$ denotes the signal,

$$\tilde{\eta}_p(t) = \bar{b}_p \eta_p(t) + \eta_0 - \bar{\eta}_p(t), \quad (4.88)$$

where

$$\bar{\eta}_p(t) = \int_0^t e^{G(t-\tau)} Gl\nu(\tau) d\tau. \quad (4.89)$$

Theorem 4.1 *Consider the closed-loop system consisting of the plant (4.1), (4.12) forced by the unknown sinusoidal wave disturbances (4.22), (4.23) the disturbance observer (4.29), (4.30), (4.31) and the adaptive controller (4.54), (4.61)–(4.72). Under the assumptions the following holds:*

- (a) *The equilibrium $\tilde{\Theta}_{V_c} = 0, \tilde{\Theta}_{dV_c} = 0, \tilde{\Theta}_{P_c} = \tilde{\Theta}_{\bar{b}_p P_c} = 0, x = 0, \eta_0 = \eta_1 = \eta_2 = \delta = \tilde{\theta}_e = \tilde{\beta}_{11} = \tilde{\beta}_{12} = \tilde{\beta}_{1p} = 0, \tilde{a}_2 = \tilde{\varrho} = \tilde{\rho} = \tilde{b}_u = \tilde{b}_p = \tilde{\bar{b}}_p = e = 0$ is stable.*
- (b) *For all initial conditions $\text{sgn}(\bar{b}_p)\hat{b}_p(0) > \bar{\tau}, (\hat{b}_p(0) - \hat{\varrho}(0)k_2)\text{sgn}(\bar{b}_p) > \frac{1}{\xi}, \hat{a}_1(0), \hat{\varrho}(0), \hat{b}_u(0), p(0), x(0) \in \mathbb{R}^2, \eta_1(0) \in \mathbb{R}^2, \eta_2(0) \in \mathbb{R}^2, \eta_0(0) \in \mathbb{R}^2, \eta_p(0) \in \mathbb{R}^2, \hat{\theta}_1 \in \mathbb{R}^2, \hat{\beta}_{11}(0) \in \mathbb{R}^2, \hat{\beta}_{12}(0) \in \mathbb{R}^2, \hat{\beta}_{1p}(0) \in \mathbb{R}^2, \hat{\Theta}_{dV_c}(0) \in \mathbb{R}^9, \hat{\Theta}_{eV_c}(0) \in \mathbb{R}^{132}, \hat{\Theta}_{P_c}(0), \hat{\Theta}_{\bar{b}_p P_c}(0) \in \mathbb{R}^{11}$ for which $V_c(t)$ is positive for all time, the signals $e(t), x(t), \eta_0, \eta_1(t), \eta_2(t), \tilde{\beta}_{1p}(t), \frac{\bar{F}_3^e}{\bar{b}_p} - \hat{\beta}_{1p}^T(t)\eta_p(t), \delta(t), \tilde{\eta}_p(t)$ are bounded and converge to zero as $t \rightarrow \infty$.*

4.2.4 Stability Proof

Proof of Theorem 4.1: The stability of the equilibrium of the closed-loop system is established with the use of Lyapunov function

$$\begin{aligned} V = & \frac{1}{2}x^T R x + \frac{1}{2}V_c e^2 + \frac{1}{2|\varrho|} \left(\frac{1}{\kappa_{b_p, \varrho}}(\tilde{\varrho}^2 + \tilde{b}_p^2) + \frac{1}{\kappa_{a_2}}\tilde{a}_2^2 + \frac{1}{\kappa_{\theta_e}}\tilde{\theta}_e^T \tilde{\theta}_e + \sum_{i=1}^2 \frac{1}{\kappa_{\beta_{1i}}} \tilde{\beta}_{1i}^T \tilde{\beta}_{1i} \right. \\ & \left. + \frac{1}{\kappa_{\beta_{1p}}} \tilde{\beta}_{1p}^T \tilde{\beta}_{1p} \right) + \frac{1}{2\kappa_{\bar{\varrho}}}\tilde{\varrho}^2 + \frac{1}{2b_u} \left(\frac{1}{\kappa_{b_u}}\tilde{b}_u^2 + \frac{1}{\kappa_{\bar{b}_p}}\tilde{\bar{b}}_p^2 \right) + \frac{1}{2\kappa_{\Theta_{dV_c}}}\tilde{\Theta}_{dV_c}^T \tilde{\Theta}_{dV_c} \\ & + \frac{1}{2\kappa_{\Theta_{eV_c}}}\tilde{\Theta}_{eV_c}^T \tilde{\Theta}_{eV_c} + \frac{1}{2\kappa_{\Theta_{P_c}}}\tilde{\Theta}_{P_c}^T \tilde{\Theta}_{P_c} + \frac{1}{2\kappa_{\Theta_{\bar{b}_p P_c}}}\tilde{\Theta}_{\bar{b}_p P_c}^T \tilde{\Theta}_{\bar{b}_p P_c} + \frac{\varepsilon\delta}{2}\delta^T R_G \delta \\ & + \frac{1}{2\varepsilon_\eta} \left(\eta_0^T R_G \eta_0 + \sum_{i=1}^n \eta_i^T R_G \eta_i \right) + \frac{\varepsilon\delta^2}{2} (\delta^T R_G \delta)^2, \end{aligned} \quad (4.90)$$

where the positive definite matrix R is a solution of the matrix equation

$$G^T R_G + R_G G = -2I, \quad (4.91)$$

with

$$\varepsilon_\delta = \frac{1}{\varrho^2} \lambda_{\max}\{\bar{\theta}_e \bar{B}^T R R \bar{B} \bar{\theta}_e^T\} + \frac{1}{(1 - \bar{\theta}_e^T l)^2} \times \lambda_{\max}\{G^T \bar{\theta}_0 \bar{\theta}_0^T G\}, \quad (4.92)$$

$$\begin{aligned} \varepsilon_{\delta^2} = & \frac{1}{\lambda_{\min}\{R_G\}} \left(\left((A_c h_0)^4 + \left(\frac{A_c \bar{a}_2}{\bar{a}_1} \right)^4 + (1 + \bar{b}_p^4) \left(A_c \frac{1 - \bar{\theta}_e^T l}{\bar{a}_1} - \bar{\theta}_0^T l \right)^4 \right. \right. \\ & \left. \left. + (1 + \bar{a}_1^4 + \bar{a}_2^4 + \bar{b}_p^4) \left(\left(\left(\frac{A_c \bar{\theta}_e + \bar{\theta}_0 \right)^T l_1 \right)^4 + \left(\left(\frac{A_c \bar{\theta}_e + \bar{\theta}_0 \right)^T l_2 \right)^4 \right) \right) \right) \\ & \times \frac{1}{(1 - \bar{\theta}_e^T l)^4} \lambda_{\max}^2\{G^T \bar{\theta}_e^T \bar{\theta}_e G\} + \left(1 + \frac{1}{(1 - \bar{\theta}_e^T l)^4} \right) \lambda_{\max}^2\{G^T \bar{\theta}_0^T \bar{\theta}_0 G\}, \quad (4.93) \end{aligned}$$

$$\varepsilon_\eta = \lambda_{\max}\{l^T R_G R_G\}. \quad (4.94)$$

Taking the time derivative of V and using the property of the projection operator, $-\tilde{b}_p \dot{\hat{b}}_p \leq -\tilde{b}_p \tau_{\tilde{b}_p}$, $\text{sgn}(b_2) \hat{b}_p \geq \bar{c} > 0$ and $-\tilde{b}_p \tilde{\varrho} [\dot{\hat{b}}_p, \dot{\hat{\varrho}}]^T \leq -[\tilde{b}_p, \tilde{\varrho}] \tau_{b_p, \varrho}$, $\text{sgn}(\bar{b}_p) (\hat{b}_p - \hat{\varrho} k_n) \geq \frac{1}{\bar{\gamma}} > 0$ [22, Appendix E] and Young's inequality for the cross terms, we obtain

$$\dot{V} \leq -\frac{1}{2} \dot{x}^T \dot{x} - (c - 2)e^2 - \frac{1}{2\varepsilon_\eta} \sum_{i=0}^2 \eta_i^T \eta_i - \frac{\varepsilon_\delta}{2} \delta^T \delta. \quad (4.95)$$

Using (4.95), we conclude

$$V(t) \leq V(0). \quad (4.96)$$

Defining

$$\begin{aligned} \bar{\Upsilon}(t) = & [x^T(t), e(t), \tilde{a}_2(t), \tilde{b}_p^T(t), \tilde{\varrho}^T(t), \tilde{\varrho}(t), \tilde{b}_u(t), \tilde{b}_3(t), \tilde{\theta}_e^T(t), \tilde{\beta}_{11}(t)^T, \tilde{\beta}_{12}(t)^T, \tilde{\beta}_{1p}(t)^T, \\ & \eta_0(t)^T, \eta_1^T(t), \eta_2^T(t), \delta^T(t), \tilde{\Theta}_{dV_c}^T(t), \tilde{\Theta}_{\dot{e}V_c}^T(t), \tilde{\Theta}_{p_c}^T(t), \tilde{\Theta}_{\tilde{b}_p V_c}^T(t)]^T, \quad (4.97) \end{aligned}$$

and using (4.90) and (4.96), we get

$$|\bar{\Upsilon}(t)|^2 \leq M_2 |\bar{\Upsilon}(0)|^2, \quad (4.98)$$

for some $M_2 > 0$. Taking the derivative of (4.88) and using (4.30), (4.89) and the fact that $\dot{x}_2 - \bar{b}_p P_c = \bar{a}_1 x_1 + \bar{a}_2 x_2 + \bar{F}_3^e$, we get

$$\dot{\tilde{\eta}}_p(t) = G \tilde{\eta}_p + Gl (\bar{a}_1 x_1 + \bar{a}_2 x_2). \quad (4.99)$$

Since G is Hurwitz, using (4.99), we have

$$|\tilde{\eta}_p(t)| \leq M_3 e^{-\alpha_1 t} |\tilde{\eta}_p(0)| + M_4 \sup_{\tau \in [0, t]} |x(\tau)| \quad (4.100)$$

for some $M_3, M_4, \alpha_1 > 0$. By using (4.98) and (4.100), we obtain

$$|\tilde{\eta}_p(t)| \leq M_3 |\tilde{\eta}_p(0)| + M_4 \sqrt{M_2} |\bar{\Upsilon}(0)|. \quad (4.101)$$

By using (4.98) and (4.101), we obtain

$$|\Upsilon(t)| \leq M_5 |\Upsilon(0)|, \quad (4.102)$$

where

$$\Upsilon(t) = \left[\bar{\Upsilon}^T(t), \tilde{\eta}_p^T(t) \right]^T, \quad (4.103)$$

for some $M_5 > 0$. This proves part (a) of Theorem 4.1.

We write the closed-loop system in the following form

$$\dot{x} = \tilde{A}^{-1} x + \tilde{A}^{-1} \bar{B} \frac{1}{\varrho} \left(\tilde{\theta}_e^T \eta_0 + \sum_{i=1}^n \tilde{\beta}_{1i}^T \eta_i + \frac{1}{\tilde{b}_p} \tilde{\beta}_{1p}^T (\tilde{\eta}_p - \eta_0 + \bar{\eta}_p) + e + \theta_e^T \delta \right), \quad (4.104)$$

where

$$\tilde{A} = A_0^T + \bar{B} \left(\frac{1}{\varrho} \left[\begin{array}{c} \tilde{a}_2 \\ 0 \end{array} \right]^T + \tilde{b}_p B^T + K \hat{\varrho} \right). \quad (4.105)$$

From (4.15), (4.16), (4.105) and by noting that $\bar{B} = \left[1, 0 \right]^T$, we get

$$\det(\tilde{A}) = - \left(\frac{1}{\varrho} \left(\frac{1}{\tilde{b}_p} - (\hat{b}_p - \hat{\varrho} k_2) \right) \right). \quad (4.106)$$

From (4.106) it follows that, for all Υ such that $\text{sgn}(\bar{b}_p)(\hat{b}_p - \hat{\varrho} k_2) \geq \frac{1}{\xi} > 0$ and $V_c(t) > 0$, the right-hand side of (4.104) is continuous in Υ and t , which implies that the right-hand side of (4.95) is continuous in Υ and t . Furthermore, the right-hand side of (4.95) is zero at $\Upsilon = 0$. By the LaSalle-Yoshizawa theorem, (4.95) ensures that $\dot{x}, e, \eta_0, \eta_1, \eta_2$ and δ converge to zero as $t \rightarrow \infty$.

By adding $\pm \frac{\kappa_{\beta_{1p}} \text{sgn}(\varrho)}{\tilde{b}_p} \tilde{\xi}(t) \bar{B}^T P \dot{x}$ and $\pm \frac{1}{\tilde{b}_p \varrho} \bar{B} \tilde{\beta}_{1p}^T \tilde{\xi}(t)$ to (4.64) and (4.104) respectively, we represent the close-loop of (x, β_{1p}) system as a linear-time varying (LTV) system which is given by

$$\dot{\zeta} = E(t)\zeta + F(t)d, \quad (4.107)$$

where

$$E(t) = \begin{bmatrix} A_{cl} & \frac{1}{\varrho} \underline{B} \bar{\xi}^T \\ \kappa_{\beta_{1p}} \text{sgn}(\varrho) \bar{\xi} \bar{B}^T P A_{cl} & \frac{\kappa_{\beta_{1p}}}{|\varrho|} \bar{\xi} \bar{B}^T P \underline{B} \bar{\xi}^T \end{bmatrix} \quad (4.108)$$

$$F(t) = \begin{bmatrix} f_{11} & f_{12} & f_{13} & f_{14} & f_{15} & \frac{1}{\varrho} \underline{B} \\ f_{21} & f f_{12} & f f_{13} & f f_{14} & f f_{15} & \frac{1}{\varrho} f \underline{B} \end{bmatrix} \quad (4.109)$$

$$d = \left[\dot{x}^T, \eta_0^T, \eta_1^T, \eta_2^T, \delta^T, e \right]^T \quad (4.110)$$

$$\zeta = \left[x^T, \tilde{\beta}_{1p}^T \right]^T \quad (4.111)$$

with $f = \frac{\kappa_{\beta_{1p}}}{\text{sgn}(\varrho)} \bar{\xi} \bar{B}^T P$ and $f_{21}, f_{11}, f_{12}, f_{13}, f_{14}, f_{15} \in \mathbb{R}^{2 \times 2}$ are given by

$$f_{11} = \frac{1}{\varrho} \underline{B} \left(\tilde{\varrho} K + \begin{bmatrix} \tilde{a}_2 & 0 \end{bmatrix} + \tilde{b}_p B^T - \frac{1}{\tilde{b}_p} \tilde{\beta}_{1p}^T \tilde{b}_p (1 - \bar{\theta}_1^T l) \begin{bmatrix} a_2 & 0 \end{bmatrix} \right), \quad (4.112)$$

$$f_{12} = \frac{1}{\varrho} \underline{B} (\tilde{\theta}_e^T - \frac{1}{\tilde{b}_p} \tilde{\beta}_{1p}^T), \quad (4.113)$$

$$f_{13} = \frac{1}{\varrho} \underline{B} (\tilde{\beta}_{11}^T - \frac{\tilde{a}_1}{\tilde{b}_p} \tilde{\beta}_{1p}^T), \quad (4.114)$$

$$f_{14} = \frac{1}{\varrho} \underline{B} (\tilde{\beta}_{12}^T - \frac{\tilde{a}_2}{\tilde{b}_p} \tilde{\beta}_{1p}^T), \quad (4.115)$$

$$f_{15} = \frac{1}{\varrho} \underline{B} (\theta_1^T - \frac{1}{\tilde{b}_p} \tilde{\beta}_{1p}^T), \quad (4.116)$$

$$f_{21} = f f_{11} - \frac{\kappa_{\beta_{1p}} \text{sgn}(\varrho)}{\tilde{b}_p} \tilde{\xi}(t) \bar{B}^T P, \quad (4.117)$$

with $A_{cl} = (A_0^T + \bar{B}K)^{-1}$ and $\underline{B} = A_{cl} \bar{B}$. We first show that the equilibrium $\zeta = 0$ of the homogenous part of the LTV system (4.107) is exponentially stable.

Towards that end, we choose the following Lyapunov function

$$V_{LTV} = \frac{1}{2} \zeta^T R_{LTV} \zeta, \quad (4.118)$$

where

$$R_{LTV} = \text{diag} \left\{ R, \frac{1}{|\varrho| \kappa_{\beta_{1p}}} I_{2 \times 2} \right\} \quad (4.119)$$

Taking the derivative of V_{LTV} and using (4.42), we get

$$\dot{V}_{LTV} = -2 \zeta^T C(t) C^T(t) \zeta, \quad (4.120)$$

where

$$C^T(t) = \begin{bmatrix} A_{cl} & \frac{1}{\varrho} \underline{B} \bar{\xi}^T \end{bmatrix}. \quad (4.121)$$

Therefore, it follows that R_{LTV} , as defined in (4.119), satisfies the following inequality

$$E^T(t)R_{LTV} + R_{LTV}E(t) + \alpha C^T(t)C(t) \leq 0 \quad (4.122)$$

for some $\alpha > 0$.

The equilibrium $\zeta = 0$ of the homogenous part of (4.107) is exponentially stable if $(C(t), E(t))$ is a uniformly completely observable (UCO) pair [26]. For a bounded $H(t)$, the pairs $(C(t), E(t))$ and $(C(t), E(t) + H(t)C(t)^T)$ have the same UCO property [26]. Choosing $H(t) = \begin{bmatrix} -I, & -\kappa_{\beta_{1p}} \text{sgn}(\varrho) R \underline{B} \bar{\xi}^T \end{bmatrix}^T$, we write the system corresponding to the pair $(C, E + HC^T)$ as

$$\dot{Y} = 0 \quad (4.123)$$

$$y = C^T(t)Y. \quad (4.124)$$

The state transition matrix of (4.123) is $\Phi = I$. Therefore, $(C, E + HC^T)$ is a UCO pair if there exist positive constants α_2, α_3, ρ such that the observability Gramian satisfies

$$\alpha_2 I \geq \int_{t_0}^{t_0+\rho} C(t)C^T(t) dt \geq \alpha_3 I, \quad (4.125)$$

for all $t_0 \geq 0$. Since $\bar{\xi}$ is bounded, recalling (4.121), the upper bound of (4.125) is satisfied. We now prove the lower bound in (4.125). Calculating the integral in (4.125), we get

$$X = \begin{bmatrix} A_{cl}^T A_{cl} \rho & \frac{1}{\varrho} A_{cl}^T \underline{B} \int_{t_0}^{t_0+\rho} \bar{\xi}^T dt \\ \frac{1}{\varrho} \int_{t_0}^{t_0+\rho} \bar{\xi} dt \underline{B}^T A_{cl} & \frac{1}{\varrho^2} \int_{t_0}^{t_0+\rho} \bar{\xi} \underline{B}^T \underline{B} \bar{\xi}^T dt \end{bmatrix}. \quad (4.126)$$

Let S_h be the Schur complement of $A_{cl}^T A_{cl} \rho$ in X , where

$$S_h = \frac{\underline{B}^T \underline{B}}{\varrho^2} \left(\int_{t_0}^{t_0+\rho} \bar{\xi} \bar{\xi}^T dt - \frac{1}{\rho} \int_{t_0}^{t_0+\rho} \bar{\xi} dt \int_{t_0}^{t_0+\rho} \bar{\xi}^T dt \right). \quad (4.127)$$

Using (4.95) and (4.96) and calculating the integral, we obtain

$$\int_0^\infty \dot{x}_1^2(t) dt \leq 2(V(0) - V(\infty)) \leq M_1 \quad (4.128)$$

for some $M_1 > 0$. Since $A_{cl}^T A_{cl} \rho$ is positive definite, X is positive definite if and only if S_h is positive definite. Since $\frac{B^T B}{\rho^2}$ is a positive scalar, using boundedness of $\Upsilon(t)$ and (4.128), according to Lemma 3.3 there exists a positive ρ such that for all $t_0 \geq 0$, $S_h > 0$. Hence, $(C, E + HC^T)$ is UCO, which implies that (C, E) is UCO. Therefore, the state transition matrix $\Phi(t, t_0)$ corresponding to $E(t)$ in (4.107) satisfies

$$\|\Phi(t, t_0)\| \leq \kappa_0 e^{-\gamma_0(t-t_0)} \quad (4.129)$$

for some positive constants κ_0, γ_0 . From the boundedness of $\Upsilon(t)$ and $\bar{\eta}_p(t)$, it follows from (4.104) that $\dot{x}(t)$ is bounded. From (4.110), $d(t)$ is bounded and, from (4.109), $F(t)$ is bounded. Recalling that it has already been established that $d(t)$ goes to zero, from (4.107) and (4.129) it follows that ζ is bounded and $\zeta = [x^T, \tilde{\beta}_{1p}^T]^T \rightarrow 0$ as $t \rightarrow \infty$. By using (4.99) and the fact that G is Hurwitz and $x(t)$ converges to zero, we conclude that $\tilde{\eta}_p(t)$ converges to zero as $t \rightarrow \infty$. Furthermore, using (4.25), (4.40), (4.43), (4.53) and by noting that $d(t) \rightarrow 0$, $\hat{\beta}_{1p}(t) \rightarrow \frac{1}{1-\bar{\theta}_e^T l} \bar{\theta}_e$, we obtain $\left(\bar{\theta}_e^T + \frac{\bar{\theta}_e^T l}{1-\bar{\theta}_e^T l} \bar{\theta}_e^T\right) \eta_p(t) \rightarrow \frac{1}{b_p} \bar{F}_3^e(t)$. Recalling $\hat{\beta}_{1p}(t) \rightarrow \frac{1}{1-\bar{\theta}_e^T l} \bar{\theta}_e$ and $\bar{\theta}_e^T l$ is scalar, we obtain $\hat{\beta}_{1p}^T \eta_p(t) \rightarrow \frac{1}{b_p} \bar{F}_3^e(t)$. This proves part (b) of Theorem 4.1. ■

4.3 Simulation

We use time-domain sea-keeping code AEGIR provided by Navatek/APS, to solve hydrodynamic forcing imparted to vessels [7]. The general inputs of AEGIR for the simulation are 3D CAD models and parameters of the vessels, connection type and configuration of the ships and finally wave model with heading angle. In the scenario, the cargo is transferred from Large, Medium-Speed Roll-on/Roll-off (LMSR) type cargo ship which is illustrated as a mono hull to a surface effect ship with two hulls, over a connected ramp. The Rhino CAD program is used to model hulls of the surface effect ship and LMSR. CAD models are given in Figure 4.3. Since the current software doesn't contain the air cushion model, we add it with the designed controller during simulation by using MATLAB interface code.

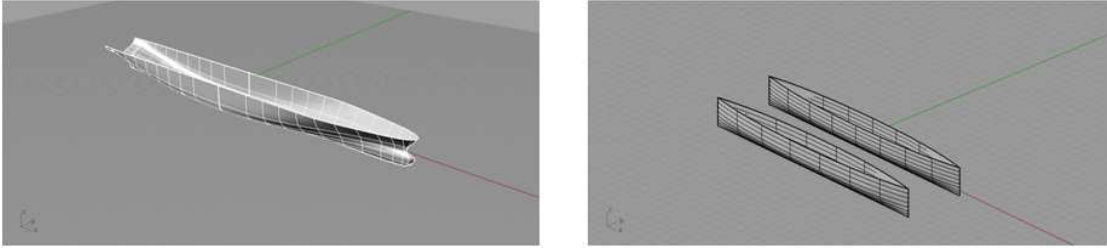


Figure 4.3: 3D Rhino model of hulls of large, medium-speed, roll-on/roll-off (LMSR) and surface effect ship (SES).



Figure 4.4: Top view of a bow to stern configuration. Bow of an SES is connected to stern of an LMSR by a ramp.

4.3.1 Configuration and Parameters

The vessel parameters are shown in Table 4.1. The ramp has two hinges that only allow pitch at each pivot point and is assumed to be massless and rigid. The length of the ramp is 90 ft. We assume the cargo transfer is performed in the bow to stern configuration as it is illustrated in Figure 4.4. We use a 1600 HP fan and approximately 15% of the deck area is considered as the louver in the simulations.

4.3.2 Sea States and Wave Modeling for Simulation

A sea state (SS) is used to represent the general condition of an ocean with respect to wind waves and swell at a certain location and moment. A sea state is characterized by statistics, including the wave height, period, and power spectrum. Table 4.2 gives observed relevant values for various sea states.

AEGIR uses a series of sine inputs provided by the user to represent a

Table 4.1: The vessel parameters of the surface effect ship (SES) and large, medium-speed, roll-on/roll-off (LMSR).

	LMSR	SES
Length(ft)	1190	250
Beam(ft)	220	70
Weight(tons)	81, 700	820
Roll Gyradius(ft)	40	15
Pitch Gyradius(ft)	200	50
Yaw Gyradius(ft)	200	50

typical wave pattern which requires heading angle for each sine wave and wave height, H_{wave} , which is given by,

$$H_{wave}(x, t) = \sum_{i=1}^N A_i \sin(\omega_i t + k_i(Ut - x) + \phi_i). \quad (4.130)$$

While many models exist to produce these sine waves, we use the Pierson-Moskowitz spectrum for fully developed wave conditions. The power for a given wave frequency is given by

$$S_p(\omega) = \frac{g^2 8.1 \times 10^{-3}}{\omega^5} \exp \left[-\beta_{wind} \left(\frac{\omega_0}{\omega} \right) \right], \quad (4.131)$$

in [27] where g is gravity, $\omega_0 = \frac{g}{U_{19.5}}$ with $U_{19.5}$ being the wind speed 19.5 meter above sea level and β_{wind} is function of the wind speed generating the waves. The peak frequency is the dominant frequency over a range of frequencies comprising the wave front. The peak frequency, ω_p , can be easily determined by setting the derivative of the spectrum with respect to the frequencies equal to zero. This approach gives us $\omega_p = \omega_0 \left(\frac{4\beta_{wind}}{5} \right)^{1/4}$. ω_0 is solved from ω_p specified by the profile used. The wind dependent value of β_{wind} can be calculated from its dependence on significant wave height, H_s . Since the problem specifies the fully developed wave characteristics, it allows us to use the given formula, $\beta_{wind} = \frac{3.11}{H_s^2 \omega_0}$, to calculate its value [27]. Lastly, the spectrum is broken down into a series of sine waves to calculate the corresponding amplitude for each frequency. This is done by relating the area under a portion of the power spectrum to an amplitude related to the frequency at that portion of the spectrum. For the simulation, we break

Table 4.2: Description of sea states from 2 to 4 in terms of important wave and wind values.

Wind Speed(Kts)	Sea State	Wave Height(ft)	Average Period(s)	Aver. Wave Length(ft)
10	2	2	3	26
15	3	4	4	52.5
19	4	7	5	92

the spectrum down into 100 components and representing the area between each frequency from 0 to 3 rad/sec, in steps of 0.03 with a single sine wave and using the rectangular method to solve for integral area gives

$$A_i = 2\sqrt{S_p(\omega_0 + 0.03i)} 0.03 \quad i = 1, \dots, 100. \quad (4.132)$$

Adding a random phase, ϕ_i , between 0 and 2π and using the average wavelength to calculate wave number completes the requirements for the wave decomposition into sine waves. The corresponding values are added to a table and imported into AEGIR. The wave output and further wave-wave interactions are all handled internally within AEGIR.

4.4 Results

We implement the developed adaptive controller to our simulation platform by using AEGIR/MATLAB interface. Since we use Lyapunov function in the design of the controller and stability proof of the closed loop system, the perfect estimation of the disturbance is achieved only in the closed loop system with actuator which is not saturated. In Figure 4.6, we give the simulation result of the wave disturbance in heave with its estimation multiplied by correct value of \bar{b}_p without restricting the louver area. One can observe that the controller achieves to estimate the wave disturbance perfectly in SS4 for the wave model which contains 100 distinct frequencies, although the controller is designed for only single frequency wave disturbance. This feature of the controller can be explained by using adaptive control theory and examining the simulation result.

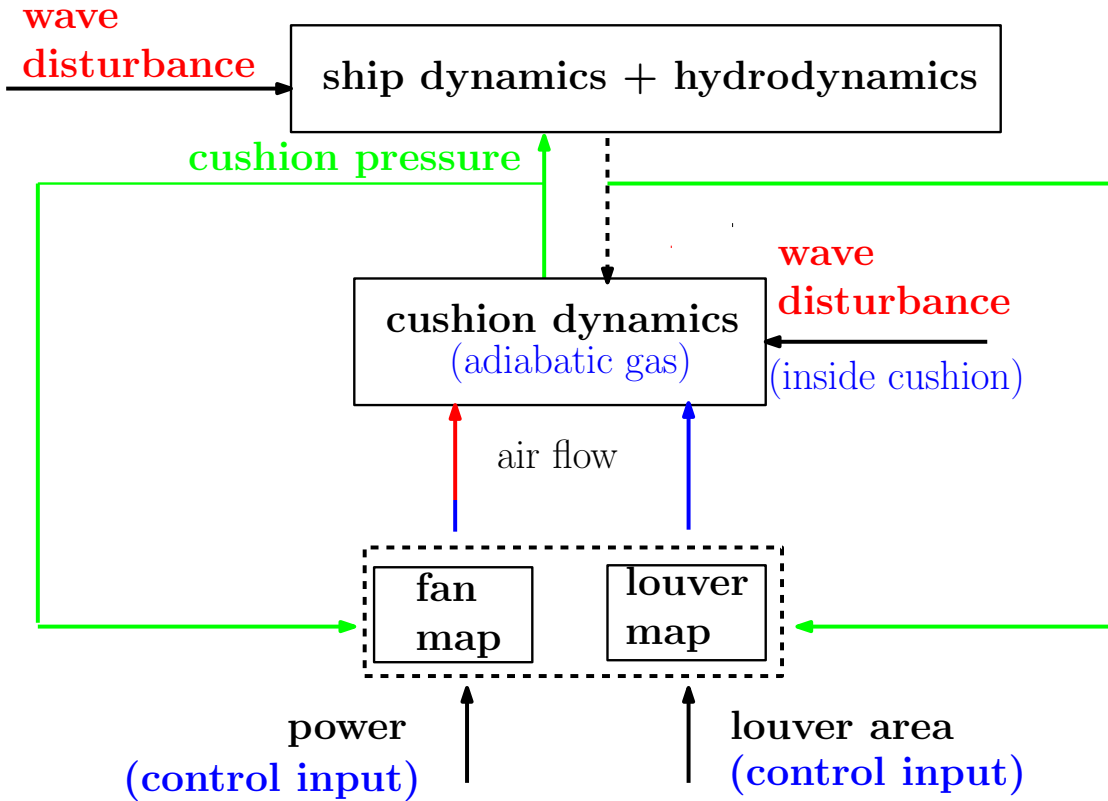


Figure 4.5: The structure of the control problem for simultaneous input actuation. The fan and louver system are used simultaneously to regulate air-flow rate.

Despite of 100 distinct frequencies in the wave model, the wave disturbance has a dominant frequency at around 0.18Hz due to the characteristics of SS4 as given in Table 4.2. On the other hand, because of the superposition of the sine waves, some fluctuations in the amplitude of the disturbance are observed. While the adaptation of β_{1p} is handling this variation, the output of the designed filter, η_p captures the slowly varying frequency in time. Thus, we achieve to estimate the disturbance almost perfectly by using 8th-order filter for the case where it contains 100 distinct frequencies, instead of using a 800th-order filter.

We run three simulations without control in SS4, SS3 and SS2 in head seas. In the fourth simulation, the controller is turned on after 300 seconds in SS4 and the louver area is saturated at 2500ft². The results of the simulations are given in Figures 4.7–4.9.

From Figures 4.7(a) and 4.7(c), one can observe that the controller achieves good reduction for smaller waves. However, there are limitations in damping larger positive waves due to the restricted louver area. Although the controller opens all the louvers and uses the maximum control effort for the case when a large wave hits, it is still not enough to reduce the pressure inside the air cushion and provide sufficient damping. Thus, large positive wave lifts SES with the pressure inside the air-cushion. Comparing the results of uncontrolled case in SS3 and SS2 given in Figures 4.7(b) and 4.7(d), the controller is able to reduce the effects of SS4 waves to those of a vessel in SS3 and SS2 waves. In other words, the control has the effect as if the sea has calmed from wave height of 7 ft to 2 ft. We present the relative vertical motion of the ramp edges connected to the SES and LMSR in Figure 4.9. As it is observed, the controller achieves significant reduction in ramp oscillation. We also test the controller for heading angle 200 degrees (bow seas) in SS4 and give the response of heave in Figure 4.10.

Heave of SES, excess pressure inside the air-cushion and the louver area between 662-680 seconds are given in Figure 4.8. Although the controller opens all available louver area at around 663 and 671 seconds when a high positive wave starts lifting the ship, it is not enough to damp all the effect of the wave disturbance in heave due to the limited louver area. In order to overcome this problem, we make a minor modification in the air-cushion model. We assume the revolution per minute (rpm) of the fan to be actuated by the controller and the fan to be able to turn in a reverse direction. The structure of the modified control problem is shown in Figure 4.5. Although it is hard to apply in a real model, it is important to see the improvement in the simulations. Since the rpm and the air-flow rate of the fan are directly proportional, we modify the pressure model (4.12) as follows

$$\dot{P}_c(t) = \frac{\gamma P_c}{V_c(t)} \left(-A_c \dot{\zeta}_3(t) + \dot{V}_0(t) - u \right), \quad (4.133)$$

with

$$u = -\alpha \left(Q_0 + \frac{\partial Q}{\partial P} \Big|_{P_{c0}} (P_c(t) - P_{c0}) \right) + c_n \sqrt{\frac{2(P_c(t) - P_a)}{\rho_{c0}}} A_l, \quad (4.134)$$

where α represents rpm coefficient. We assume $Q_0, \frac{\partial Q}{\partial P} \Big|_{P_{c0}}, c_n, \rho_{c0}$ to be known. We also modify the controller for the model (4.133) considering u as the input.

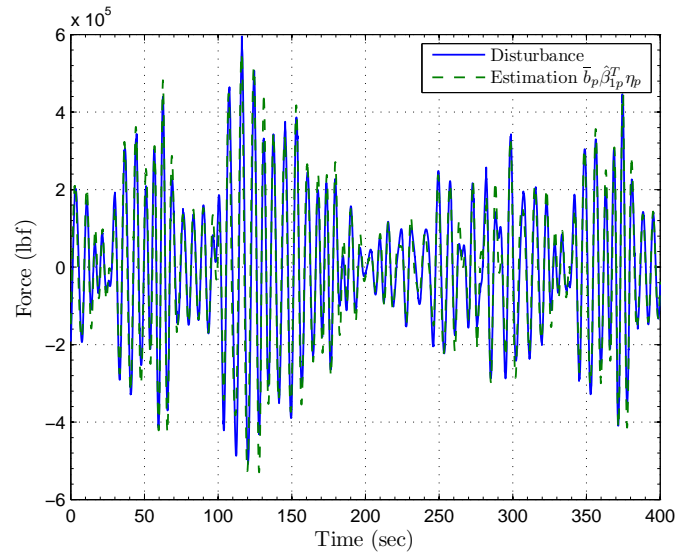
The rpm controller enters into an activity when the louver area A_l is saturated. We also implement an amplitude and rate saturation for rpm coefficient and run simulations. The comparison of the heave is given in Figure 4.11. The values of A_l and α are given in Figure 4.12. As it is observed from figures, including the fan into the control law improves the performance of the controller for the case where a high positive wave hit the catamaran and starts lifting the hulls.

4.5 Conclusion

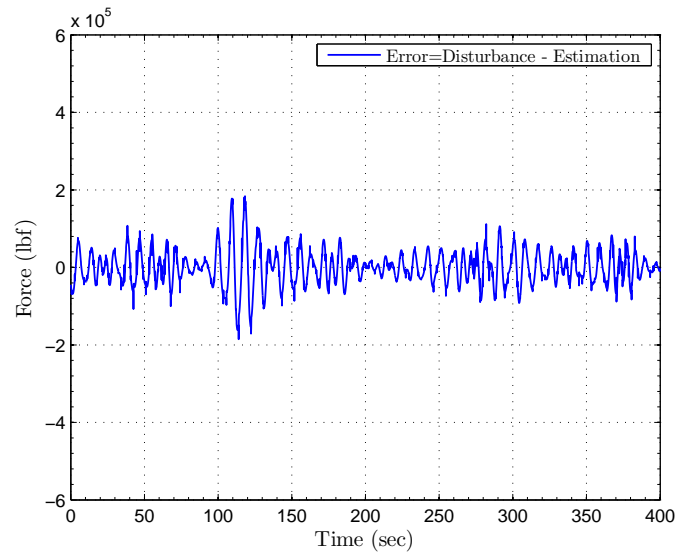
We design an air cushion actuated controller to estimate and cancel the wave disturbance and stabilize the heave of the SES and reduce the oscillation of the ramp which connects LMSR and SES each other to perform cargo transfer. We assume that heave rate, heave acceleration and the pressure itself are available for measurement and the all system parameters are uncertain. We use the louver area as the main actuator of the system to regulate the air-flow rate into the air-cushion. The developed controller achieves to significant reduction in smaller waves but there are limitations for larger positive waves due to the restricted louver area. We demonstrate the effect of our control design on the oscillation of ramp and heave of SES for the side by side configuration in simulations, using a time-domain seakeeping code, named AEGIR.

This chapter is an adaptation of material appearing in: H. I. Basturk and M. Krstic, "Adaptive wave cancelation by acceleration feedback for ramp-connected air-cushion actuated surface effect ships," *Automatica*, to appear.

The dissertation author is the primary investigator and author of this work.

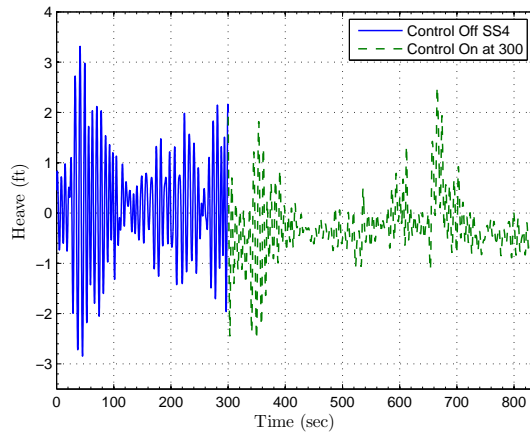


(a) The wave disturbance which effects SES in heave and its estimation in SS4.

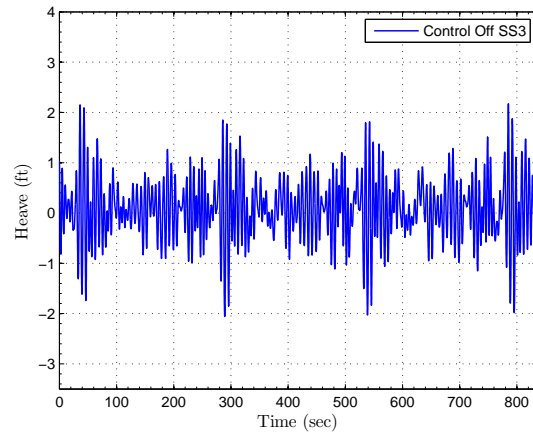


(b) Error between wave disturbance in heave and its estimation in SS4.

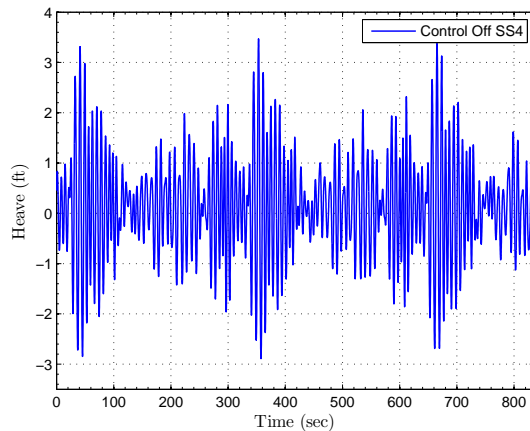
Figure 4.6: The wave disturbance estimation in heave in SS4. Figure 4.6(a) shows the wave disturbance and its estimation. Figure 4.6(b) presents the error between actual wave disturbance and its estimation



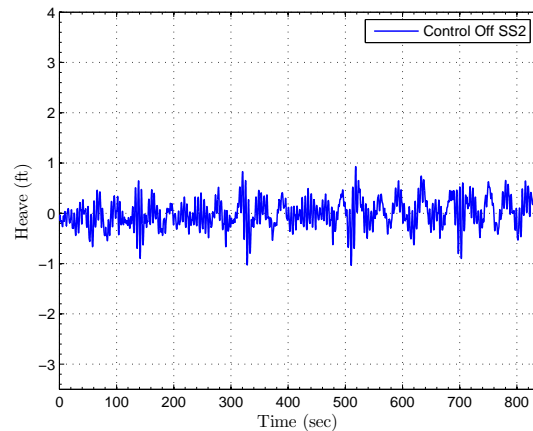
(a) Heave of SES in SS4, the controller is turned on at 300 seconds.



(b) Heave of SES in SS3 without control.



(c) Heave of SES in SS4 without control.



(d) Heave of SES in SS2 without control.

Figure 4.7: Heave of SES for different sea states with and without control in head seas. Figure 4.7(a) presents the heave of SES when the controller is turned on at 300 seconds.

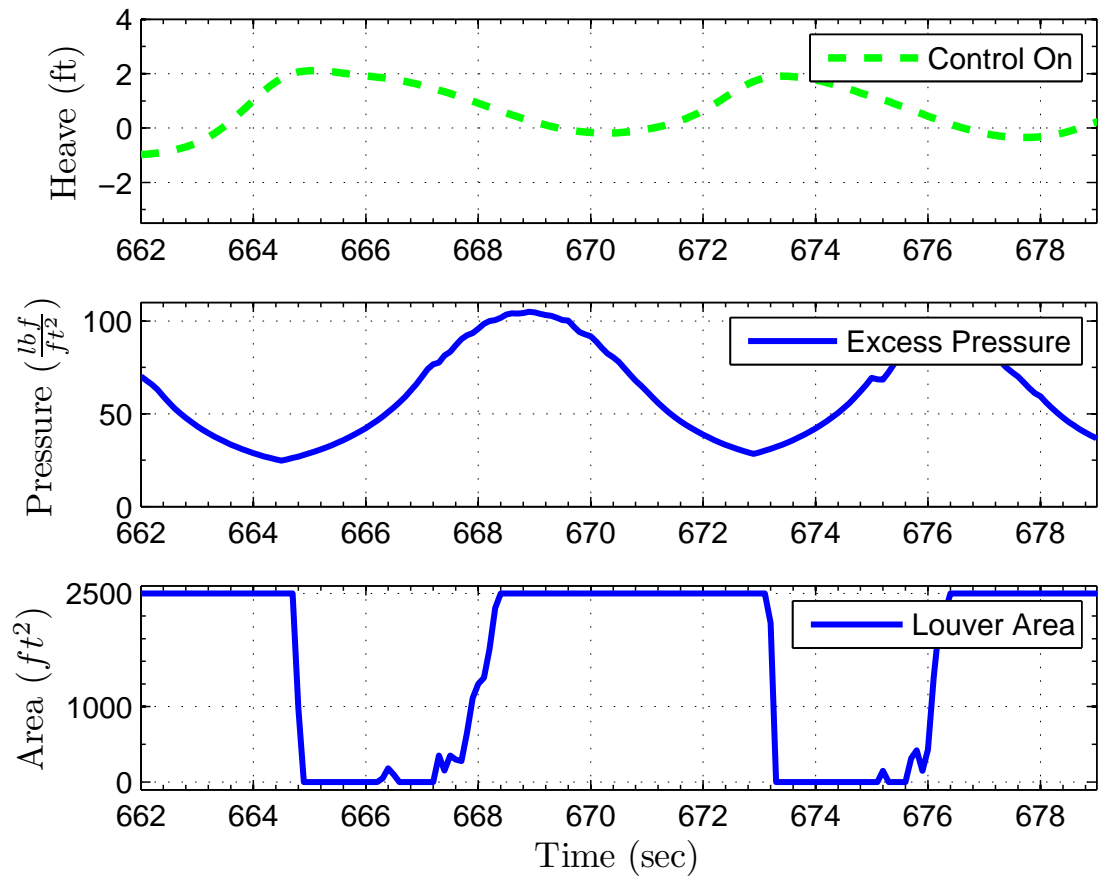


Figure 4.8: Heave, excess pressure inside the air-cushion and louver area of SES between 662 - 680 seconds.

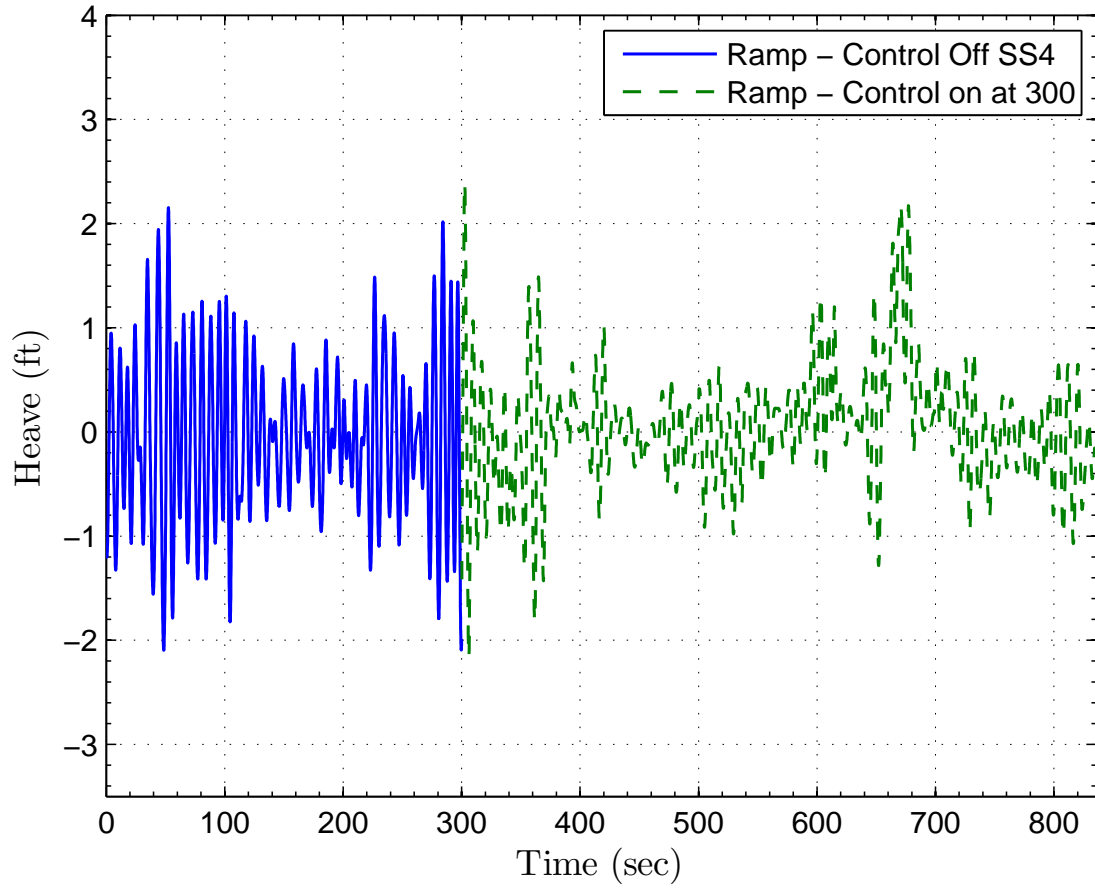


Figure 4.9: Relative vertical motion of the ramp edge at SES with respect to the edge at LMSR in SS4, the controller is turned on at 300 seconds.

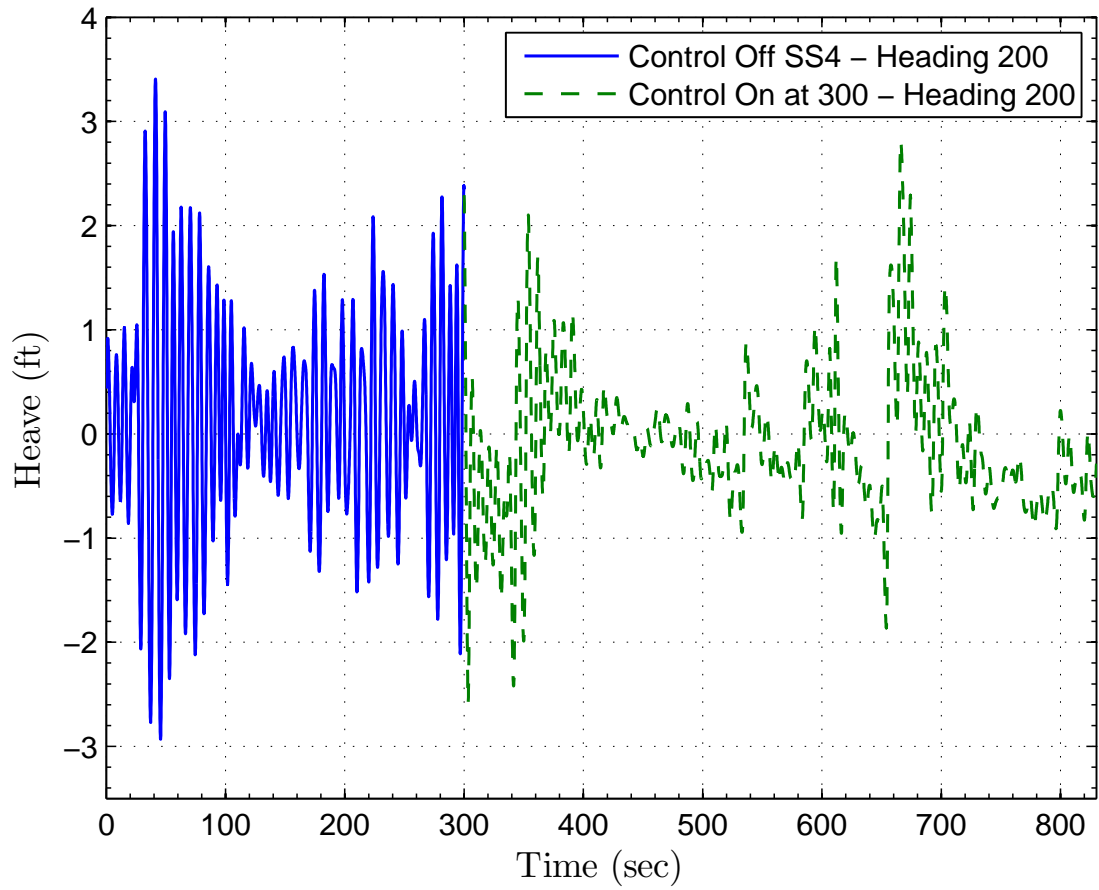


Figure 4.10: Heave of SES in SS4 for heading angle 200 degrees (bow seas), the controller is turned on at 300 seconds.

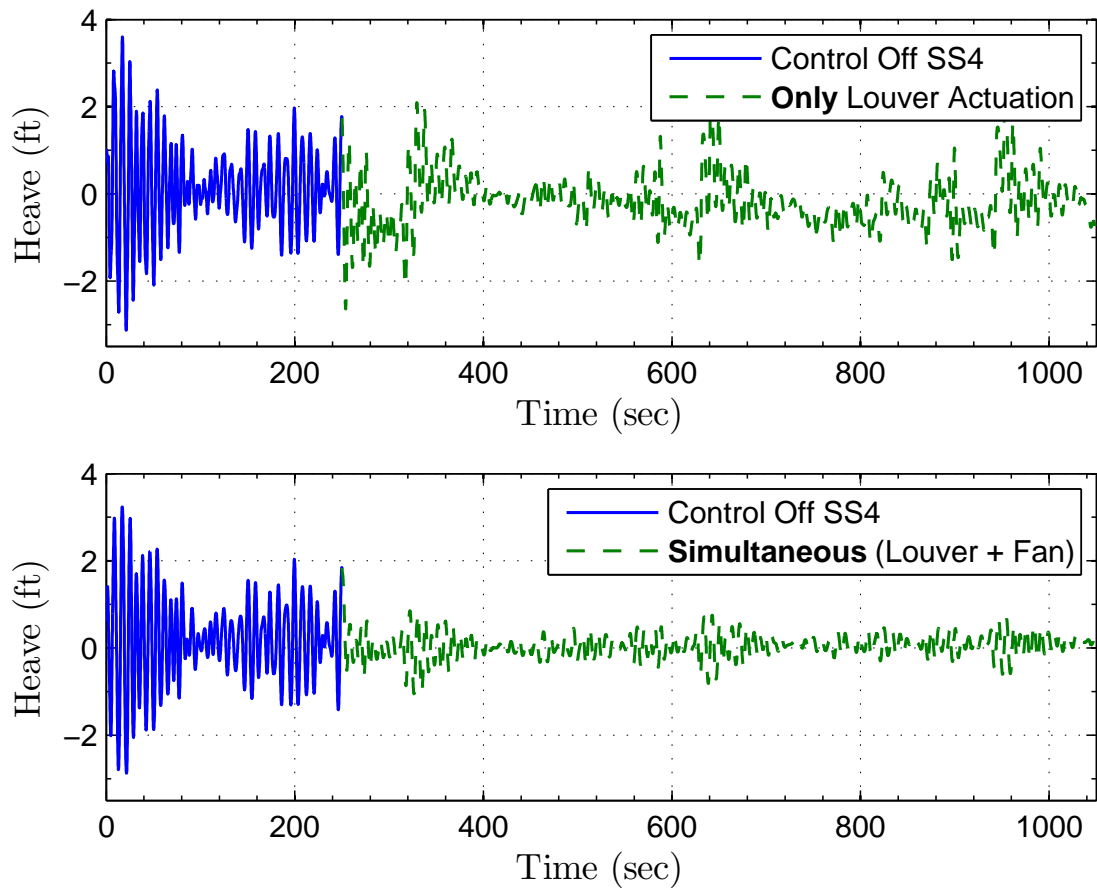


Figure 4.11: The comparison of heave of SES in SS4 between louver only control and fan+louver simultaneous control. The controller is turned on at 250 seconds.

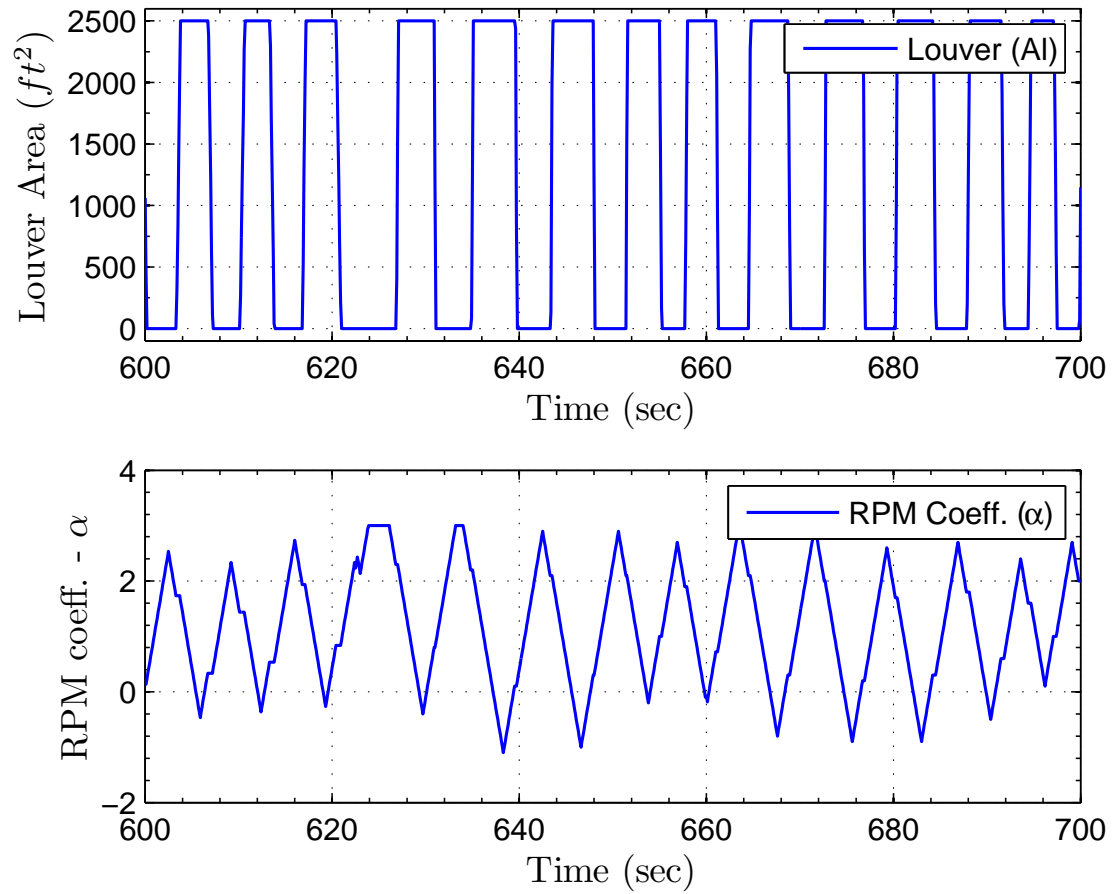


Figure 4.12: Louver area and rpm coefficient of SES between 600–700 seconds. Louver area and rpm coefficient are saturated at 0, 2500 ft^2 and $-3, 3$, respectively.

Chapter 5

Simultaneous Heave and Pitch Control of Two-Chamber Air-Cushion Surface Effect Ship

We consider here a two-chamber air-cushion SES. We design an air cushion actuated controller to regulate the heave and pitch of the SES simultaneously via acceleration feedback with actuation of the louver area for the case where the system parameters are not known. We also develop an tracking algorithm to keep the ramp stable during the cargo transfer in bow to stern configuration. The effect of our control design is demonstrated in the same simulations platform as the one presented in Chapter 4.

This chapter is organized as follows: We introduce the mathematical model of the pitch and two-chamber air cushion dynamics of an SES in Section 5.1. Design of the controller and stability properties of the closed loop system are given in Section 5.2. In Section 5.3, we present the design of the tracking algorithm. The simulation and results are given in Section 5.4.

5.1 Mathematical Model of System Dynamics

5.1.1 SES Pitch Model

Similar to Section 4.1.1, following [37], we consider the linear model of the pitch dynamics (decoupled from heave) for control design purpose. The model is given by

$$(I_{55} + A_{55}) \ddot{\zeta}_5(t) + B_{55} \dot{\zeta}_5(t) + C_{55} \zeta_5(t) - A_c P_d \frac{L}{2} = F_5^e(t), \quad (5.1)$$

where ζ_5 represents the pitch, P_d is the air cushion pressure difference between two chambers. A_c and L area area and length of the air cushion, respectively. I_{55} is the moment of inertia around y-axis. Hydrodynamic (added-mass), radiation damping coefficients and hydrostatic (restoring) term for heave are represented as A_{55} , B_{55} , C_{55} , respectively. F_5^e is hydrodynamic excitation force. For single frequency wave, it is given by

$$F_5^e(t) = K_5^e \cos(\omega_e t + \phi), \quad (5.2)$$

with

$$K_5^e = 2ge^{kd} \left(\left(\frac{1}{k} \cos \frac{kL}{2} - \frac{2}{k^2 L} \sin \frac{kL}{2} \right) (C_{33} - \omega \omega_e A_{33} + \phi) - U \omega \frac{\sin \frac{kL}{2}}{\frac{kL}{2}} A_{33} \right), \quad (5.3)$$

where d is the draft of the side hulls. g, ω, ϕ, k are the amplitude, frequency, phase and number of the wave respectively. ω_e is the encounter frequency which is represented by $\omega_e = \omega - kU \cos(\chi)$ where U and χ are the craft speed and heading angle, respectively. In our adaptive control design, the draft of the side hulls, d , is assumed to be constant.

5.1.2 Pressure dynamics for two chambers air-cushion

Considering a two-chamber air-cushion model shown in Figure 5.1, following the procedure given in Section 4.1.2 and assuming $\sin(\zeta_5) \cong \zeta_5$, $\cos(\zeta_5) \cong 1$, we obtain

$$\dot{P}_{ci}(t) = \frac{\overline{P}_{ci}(t)}{V_{ci}(t)}, \quad (5.4)$$

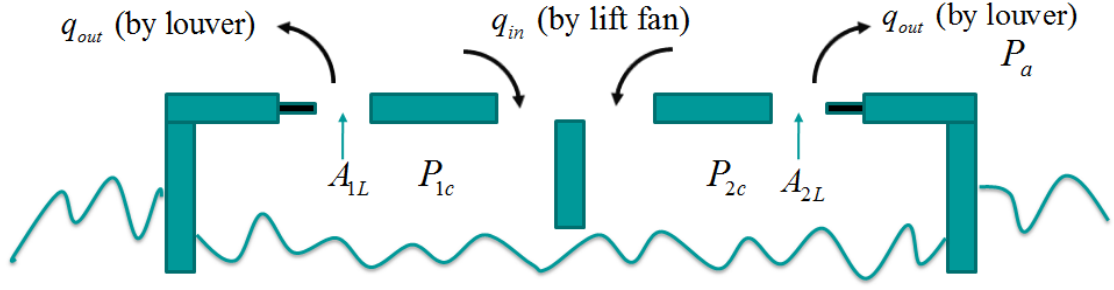


Figure 5.1: Illustration of a two-chamber air-cushion model. The symbol A_{1L} and A_{2L} denotes louver area which is used as the control input.

where

$$\bar{P}_{ci}(t) = \gamma \left(-\frac{A_c}{2} \dot{\zeta}_3 P_{ci} + \dot{V}_0 P_{ci} - (-1)^i \frac{A_c L}{8} \dot{\zeta}_5 P_{ci} - u_i \right), \quad (5.5)$$

$$V_{ci}(t) = \frac{A_c}{2} \left((h_0 + \zeta_3) + (-1)^i \frac{L}{4} \zeta_5 \right) - V_0. \quad (5.6)$$

with

$$u_i = -\alpha_i \left(Q_0 P_{ci} + \frac{\partial Q}{\partial P} \Big|_{P_{c0}} (P_{ci}(t) - P_{c0}) P_{ci} \right) + c_n \sqrt{\frac{2}{\rho_{c0}}} \sqrt{(P_{ci} - P_a) P_{ci}} A_{li} \quad (5.7)$$

where $i \in [1, 2]$ denotes the chamber number. We assume $Q_0, \frac{\partial Q}{\partial P} \Big|_{P_{c0}}, c_n, \rho_{c0}$ to be known.

It is possible to control heave and pitch simultaneously for two-chamber air cushion model. The pressure difference between two chambers causes moment with respect to y axis and it is used to control pitch. Similarly, the heave of the surface effect ship is controlled by total pressure. Although the pressure model (5.4) is used in simulations, we assume the volume of the chambers, $V_{c1}(t)$ and $V_{c2}(t)$ to be equal and constant to obtain the dynamics of pressure difference and total pressure for control design.

Assuming $V_{c1} \cong V_{c2} \cong V_t$, we get

$$\dot{P}_t(t) = \frac{2\gamma}{V_t} \left(-\frac{A_c}{2} \dot{\zeta}_3 P_t + \dot{V}_0 P_t - \frac{A_c L}{8} \dot{\zeta}_5 P_d - u_t \right), \quad (5.8)$$

$$\dot{P}_d(t) = \frac{2\gamma}{V_t} \left(-\frac{A_c}{2} \dot{\zeta}_3 P_d + \dot{V}_0 P_d - \frac{A_c L}{8} \dot{\zeta}_5 P_t - u_d \right), \quad (5.9)$$

where

$$P_t = P_{c1} + P_{c2}, \quad (5.10)$$

$$P_d = P_{c2} - P_{c1}, \quad (5.11)$$

$$u_t = u_1 + u_2, \quad (5.12)$$

$$u_d = u_2 - u_1. \quad (5.13)$$

5.2 Simultaneous Control Design for Heave and Pitch

We follow a similar but not exactly same procedure as given in Section 4.2 to design a controller in this section. The main difference is the assumption which is mentioned in the previous section, regarding the volume of the cushion chambers. Unlike the control design in Section 4.2, we assume the volume of the chambers to be equal and constant for control design. Firstly, we design a controller for pitch by considering u_d as our main actuator.

The decoupled pitch dynamics can be represented in the state-space form as follows

$$\dot{x}_p = A_0 x_p + B (\bar{a}_{p1} x_{p1} + \bar{a}_{p1} x_2 + \bar{F}_5^e + \bar{b}_d P_d), \quad (5.14)$$

where

$$x_p = \begin{bmatrix} \zeta_5 & \dot{\zeta}_5 \end{bmatrix}^T, \quad (5.15)$$

$$\bar{a}_{p1} = - \frac{C_{55}}{I_{55} + A_{55}} \quad (5.16)$$

$$\bar{a}_{p2} = - \frac{B_{55}}{I_{55} + A_{55}} \quad (5.17)$$

$$\bar{F}_5^e = \frac{F_5^e}{I_{55} + A_{55}} \quad (5.18)$$

$$\bar{b}_d = \frac{A_c L}{2(I_{55} + A_{55})}, \quad (5.19)$$

A_0 and B are given in (4.15) and (4.16), respectively. Using Lemmas 3.1 and 3.2, the inaccessible disturbances \bar{F}_5^e and its time derivatives $\dot{\bar{F}}_5^e$ can be represented in

the form

$$\bar{F}_5^e = \bar{\theta}_{pe}^T (\eta_{p0} + N\dot{x}_p) + \sum_{i=1}^2 \bar{a}_{pi} \bar{\theta}_{pe}^T \eta_{pi} + \bar{b}_d \bar{\theta}_{pe}^T (\eta_{pp} - lP_d) + \bar{\theta}_{pe}^T \delta_p, \quad (5.20)$$

$$\dot{\bar{F}}_5^e = \frac{1}{1 - \bar{\theta}_{pe}^T l} \left(\bar{\theta}_{pe}^T G (\eta_{p0} + N\dot{x}_p) + \sum_{i=1}^2 \bar{a}_{pi} \bar{\theta}_{pe}^T G \eta_{pi} + \bar{b}_d \bar{\theta}_{pe}^T G (\eta_{pp} - lP_d) + \bar{\theta}_{pe}^T G \delta_p \right), \quad (5.21)$$

where

$$\dot{\eta}_{pi} = G\eta_{pi} - l\dot{x}_{pi}, \quad \text{for } i = 1, 2, \quad (5.22)$$

$$\dot{\eta}_{p0} = G(\eta_{p0} + N\dot{x}_p), \quad (5.23)$$

$$\dot{\eta}_{pp} = G(\eta_{pp} - lP_d). \quad (5.24)$$

N is a 2×2 matrix which is given by $N = \frac{1}{B^T B} l B^T$. The given N is one of the many solutions of the equation $NB = l$. $\delta_p \in R^2$ obeys the equation

$$\dot{\delta}_p = G\delta_p. \quad (5.25)$$

Substituting (5.20) into (5.14) and representing the system in (RSS) form we get

$$\dot{x}_p = A_0^T \dot{x}_p + \bar{B} \frac{1}{\varrho_p} \left(b_d \dot{x}_{p2} - a_{p2} \dot{x}_{p1} - \theta_{pe}^T \eta_{p0} - \sum_{i=1}^2 \beta_{pi}^T \eta_{pi} - \beta_{pp}^T \eta_{pp} - P_d - \theta_{pe}^T \delta_p \right) \quad (5.26)$$

where

$$\varrho_p = \frac{\bar{a}_{p1}}{\bar{b}_d (1 - \bar{\theta}_{pe}^T l)}, \quad (5.27)$$

$$b_d = \frac{1}{\bar{b}_d}, \quad (5.28)$$

$$a_{p2} = \frac{\bar{a}_{p2}}{\bar{b}_d (1 - \bar{\theta}_{pe}^T l)}, \quad (5.29)$$

$$\theta_{pe} = \frac{1}{\bar{b}_d (1 - \bar{\theta}_{pe}^T l)} \bar{\theta}_{pe}, \quad (5.30)$$

$$\beta_{pi} = \frac{\bar{a}_{pi}}{\bar{b}_p (1 - \bar{\theta}_{pe}^T l)} \bar{\theta}_{pe}, \quad (5.31)$$

$$\beta_{pp} = \frac{1}{(1 - \bar{\theta}_e^T l)} \bar{\theta}_e. \quad (5.32)$$

Using (5.16), (5.19) and noting that $1 - \bar{\theta}_{pe}^T l > 0$, area of the air-cushion A_c , hydrodynamic, A_{55} , and hydrostatic, C_{55} terms are positive, we obtain $\text{sgn}(\varrho_p) = -1$ and $\text{sgn}(\bar{b}_d) = 1$. For the adaptive control design, we assume that the high frequency gain $\bar{b}_d > \bar{\varsigma}_p > 0$. From a physical point of view, $\bar{\varsigma}_p$ can be determined with rough knowledge of the dimensions and the inertia of the catamaran.

As given in Section 4.2.3, in adaptive backstepping method, we first define the desired value of the pressure difference between two chambers to stabilize the pitch of the surface effect ship. Considering P_d as the virtual controller, desired pressure difference value is given by

$$P_d \text{ desired} = -\hat{\varrho}_p K \dot{x}_p - \hat{a}_{p2} \dot{x}_{p1} + \hat{b}_d \dot{x}_{p2} - \hat{\theta}_{pe}^T \eta_{p0} - \sum_{i=1}^2 \hat{\beta}_{pi}^T \eta_{pi} - \hat{\beta}_{pp}^T \eta_{pp}, \quad (5.33)$$

where the control gain $K \in R^{1 \times 2} = \begin{bmatrix} k_1 & k_2 \end{bmatrix}$ is chosen so that $(A_0^T + \bar{B}K)$ is Hurwitz and the positive definite matrix R is a solution of the matrix equation

$$(A_0^T + \bar{B}K)^T R + R(A_0^T + \bar{B}K) = -4I. \quad (5.34)$$

The deviation of P_d from its desired value, $P_d \text{ desired}$ is written as

$$e_p(t) = P_d(t) - P_d \text{ desired}(t). \quad (5.35)$$

Substituting (5.35) into (5.26), taking the time derivative of $e_p(t)$, using (5.21) and assuming V_t to be constant, we convert (x_p, P_d) system to (x_p, e_p) system, as follows

$$x_p = (A_0^T + \bar{B}K) \dot{x}_p + \bar{B} \frac{1}{\varrho_p} \left(\tilde{b}_d \dot{x}_{p2} - \tilde{a}_{p2} \dot{x}_{p1} - \tilde{\varrho}_p K \dot{x}_p - \tilde{\theta}_{pe}^T \eta_{p0} - \sum_{i=1}^2 \tilde{\beta}_{pi}^T \eta_{pi} - \tilde{\beta}_{pp}^T \eta_{pp} - e_p - \theta_{pe}^T \delta_p \right), \quad (5.36)$$

$$\dot{e}_p(t) = \Pi_p^T \Phi_p + d^T d_p + \xi_{pe} - \Theta_{pe}^T \Xi_{pe} - \bar{\theta}_{pe}^T \delta_p - \left(1 - \left(\hat{b}_d - \hat{\varrho}_p k_2 \right) \bar{b}_d \right) \frac{u_d}{b_{ud}}, \quad (5.37)$$

where

$$\Pi_p = \frac{2\gamma}{V_t} \left[-\frac{A_c}{2}, \quad \frac{A_c L}{8} \right]^T, \quad (5.38)$$

$$\Phi_p = \left[\dot{x}_{h1} P_d, \quad \dot{x}_{p1} P_t \right]^T, \quad (5.39)$$

$$\bar{\theta}_{pe}^T = \frac{1}{1 - \bar{\theta}_{pe}^T l} \bar{\theta}_{pe}^T G l, \quad (5.40)$$

$$\Theta_{pe} = \left[\bar{a}_{p1}, \quad \bar{a}_{p2} + \bar{\theta}_{pe}^T, \quad \bar{\theta}_{pe}^T, \quad \bar{a}_{p1} \bar{\theta}_{pe}^T, \quad \bar{a}_{p2} \bar{\theta}_{pe}^T, \quad \bar{b}_p \bar{\theta}_{pe}^T \right]^T, \quad (5.41)$$

$$\Xi_{pe} = \left(\hat{b}_d - \hat{\varrho}_p k_2 \right) \left[\dot{x}_{p1}, \quad \dot{x}_{p2}, \quad \eta_{p0}^T, \quad \eta_{p1}^T, \quad \eta_{[2]}^T, \quad (\eta_{pp} - l P_d)^T \right]^T, \quad (5.42)$$

$$d = \left[\dot{V}_0, \quad \dot{V}_0 \bar{b}_d \right]^T, \quad (5.43)$$

$$d_p = \left[P_d, \quad - \left(\hat{b}_d - \hat{\varrho}_p k_2 \right) P_d \right]^T, \quad (5.44)$$

$$\begin{aligned} \xi_{pe} = & \left(\hat{\varrho}_p k_1 + \dot{\hat{a}}_{p2} \right) \dot{x}_{p1} + \left(\hat{\varrho}_p k_1 + \hat{a}_{p2} + \dot{\hat{q}}_p k_2 - \dot{\hat{b}}_d \right) \dot{x}_{p2} + \dot{\hat{\theta}}_{pe}^T \eta_{p0} + \hat{\theta}_{pe}^T \dot{\eta}_{p0} \\ & + \sum_{i=1}^2 \left(\dot{\hat{\beta}}_{pi}^T \eta_{pi} + \hat{\beta}_{pi}^T \dot{\eta}_{pi} \right) + \dot{\hat{\beta}}_{pp}^T \eta_{pp} + \hat{\beta}_{pp}^T \dot{\eta}_{pp}, \end{aligned} \quad (5.45)$$

$$b_{ud} = \frac{V_t}{2\gamma}, \quad (5.46)$$

with

$$x_h = \left[\zeta_3, \quad \dot{\zeta}_3 \right]. \quad (5.47)$$

The adaptive controller for u_d is given by

$$u_d = \frac{\hat{b}_{ud}}{\left(1 - \hat{b}_d \left(\hat{b}_d - \hat{\varrho}_p k_2 \right) \right)} \bar{u}_d, \quad (5.48)$$

with

$$\bar{u}_d = - \hat{\varrho}_p \dot{x}_p^T R \bar{B} - \hat{\Theta}_{pe}^T \Xi_{pe} + \xi_{pe} + \hat{\Pi}_p^T \Phi_p + \left(c_p + \kappa_{d_p} d_p^T d_p + \left(\hat{b}_d - \hat{\varrho}_p k_2 \right)^2 \right) e_p, \quad (5.49)$$

with $c_p > 2$.

The update laws are given by

$$\dot{\hat{a}}_{p2} = -\kappa_{a_{p2}} \text{sgn}(\varrho_p) \dot{x}_{p1} \bar{B}^T R \dot{x}_p, \quad \kappa_{a_{p2}} > 0, \quad (5.50)$$

$$\dot{\hat{\theta}}_{pe} = -\kappa_{\theta_{pe}} \text{sgn}(\varrho_p) \eta_{p0} \bar{B}^T R \dot{x}_p, \quad \kappa_{\theta_{pe}} > 0, \quad (5.51)$$

$$\dot{\hat{\beta}}_{pi} = -\kappa_{\beta_{pi}} \text{sgn}(\varrho_p) \eta_{pi} \bar{B}^T R \dot{x}_p, \quad \kappa_{\beta_{pi}} > 0, \quad (5.52)$$

$$\dot{\hat{\beta}}_{pp} = -\kappa_{\beta_{pp}} \text{sgn}(\varrho_p) \eta_{pp} \bar{B}^T R \dot{x}_p, \quad \kappa_{\beta_{pp}} > 0, \quad (5.53)$$

$$\dot{\hat{b}}_{ud} = -\kappa_{b_{ud}} \bar{u}_d e_p, \quad \kappa_{b_{ud}} > 0, \quad (5.54)$$

$$\dot{\hat{\varrho}}_p = -\kappa_{\bar{\varrho}_p} e_p \dot{x}_p^T R \bar{B}, \quad \kappa_{\bar{\varrho}_p} > 0, \quad (5.55)$$

$$\dot{\hat{\Theta}}_{pe} = \kappa_{\Theta_{pe}} \Xi_{pe} e_p, \quad \kappa_{\Theta_{pe}} > 0, \quad (5.56)$$

$$\dot{\hat{\Pi}}_p = \kappa_{\Pi_p} \Phi_p e_p, \quad \kappa_{\Phi_p} > 0, \quad (5.57)$$

$$\dot{\hat{b}}_d = \begin{cases} \tau_{\bar{b}_d}, & \hat{b}_d \text{sgn}(\bar{b}_d) > \bar{\varsigma}_p \text{ or } \tau_{\bar{b}_d} \text{sgn}(\bar{b}_d) \geq 0 \\ 0, & \hat{b}_d \text{sgn}(\bar{b}_d) \leq \bar{\varsigma}_p \text{ and } \tau_{\bar{b}_d} \text{sgn}(\bar{b}_d) < 0 \end{cases}, \quad (5.58)$$

$$\begin{bmatrix} \dot{\hat{b}}_d \\ \dot{\hat{\varrho}}_p \end{bmatrix} = \begin{cases} \tau_{b_d, \varrho_p}, & \text{sgn}(\bar{b}_d) (\hat{b}_d - \hat{\varrho}_p k_2) > \frac{1}{\bar{\varsigma}_p} \\ & \text{or } \mathcal{R}^T \tau_{b_d, \varrho_p} \leq 0 \\ \left(I - \Gamma \frac{\mathcal{R} \mathcal{R}^T}{\mathcal{R}^T \Gamma \mathcal{R}} \right) \tau_{b_d, \varrho_p}, & \text{sgn}(\bar{b}_d) (\hat{b}_d - \hat{\varrho}_p k_2) \leq \frac{1}{\bar{\varsigma}_p} \\ & \text{and } \mathcal{R}^T \tau_{b_d, \varrho_p} > 0, \end{cases} \quad (5.59)$$

where

$$\tau_{\bar{b}_d} = \kappa_{\bar{b}_d} (\hat{b}_d - \hat{\varrho}_p k_2) u_d e_p, \quad \kappa_{\bar{b}_d} > 0 \quad (5.60)$$

$$\tau_{b_d, \varrho_p} = \kappa_{b_d, \varrho_p} \begin{bmatrix} \text{sgn}(\varrho_p) \dot{x}_{p2} \bar{B}^T R \dot{x}_p \\ -\text{sgn}(\varrho_p) K \dot{x}_p \bar{B}^T R \dot{x}_p \end{bmatrix}, \quad \kappa_{b_d, \varrho_p} > 0, \quad (5.61)$$

$$\mathcal{R} = \begin{bmatrix} -\text{sgn}(\bar{b}_d) & k_2 \text{sgn}(\bar{b}_d) \end{bmatrix}^T, \quad (5.62)$$

and Γ belongs to the set of all positive definite symmetric 2×2 matrices. The stability of the equilibrium of the closed loop system is shown by considering the

following Lyapunov function,

$$\begin{aligned}
V = & \frac{1}{2} (x_p^T R x_p + e_p^2) + \frac{1}{2|\varrho_p|} \left(\frac{1}{\kappa_{a_{p2}}} \tilde{a}_{p2}^2 + \frac{1}{\kappa_{\theta_{pe}}} \tilde{\theta}_{pe}^T \tilde{\theta}_{pe} + \frac{1}{\kappa_{\beta_{pi}}} \sum_{i=1}^2 \tilde{\beta}_{pi}^T \tilde{\beta}_{pi} + \frac{1}{\kappa_{\beta_{pp}}} \tilde{\beta}_{pp}^T \tilde{\beta}_{pp} \right. \\
& \left. + \frac{1}{\kappa_{\varrho_p}} \tilde{\varrho}_p^2 + \frac{1}{\kappa_{b_d}} \tilde{b}_d^2 \right) + \frac{1}{\kappa_{\bar{b}_d}} \tilde{b}_d^2 + \frac{1}{\kappa_{\tilde{\varrho}_p}} \tilde{\varrho}_p^2 + \frac{1}{\kappa_{\Theta_{pe}}} \tilde{\Theta}_{pe}^T \tilde{\Theta}_{pe} + \frac{1}{\kappa_{\Pi_p}} \tilde{\Pi}_p^T \tilde{\Pi}_p \\
& + \frac{1}{2\varepsilon_\eta} \left(\eta_{p0}^T P_G \eta_{p0} + \sum_{i=1}^2 \eta_{pi}^T P_G \eta_{pi} \right) + \frac{\varepsilon_\delta}{2} \delta_p^T P_G \delta_p, \tag{5.63}
\end{aligned}$$

where

$$G^T P_G + P_G G = -2I, \tag{5.64}$$

$$\varepsilon_\delta = \frac{1}{\varrho^2} \lambda_{\max} \{ \theta_{pe} \bar{B}^T P P \bar{B} \theta_{pe}^T \} + \lambda_{\max} \{ \bar{\theta}_{pe} \bar{\theta}_{pe}^T \}, \tag{5.65}$$

$$\varepsilon_\eta = l^T P_G P_G l. \tag{5.66}$$

Taking the time derivative of V and using the following property of the projection operator, $-\tilde{b}_d \dot{\hat{b}}_d \leq -\tilde{b}_d \tau_{\bar{b}_d}$, $\text{sgn}(\bar{b}_d) \dot{\hat{b}}_d \geq \bar{\tau} > 0$ and $-\tilde{b}_d \tau_{\bar{b}_d} \leq -[\tilde{b}_d, \tilde{\varrho}_p] \tau_{\bar{b}_d, \varrho_p}$, $\text{sgn}(\bar{b}_d) (\hat{b}_d - \hat{\varrho}_p k_2) \geq \frac{1}{\xi} > 0$ [22, Appendix E] and Young's inequality for the cross terms, we obtain

$$\dot{V} \leq -\frac{1}{2} \dot{x}_p^T \dot{x}_p - c_p e_p^2 - \frac{1}{2\varepsilon_\eta} \sum_{i=0}^2 \eta_i^T \eta_i + \frac{d_p^T d_p}{4\kappa_{d_p}}. \tag{5.67}$$

Defining $\Xi_p = \left[\dot{x}_p^T, e_p, \eta_0^T, \eta_1^T, \eta_2^T \right]^T$, \dot{V} is negative whenever $|\Xi_p| > \frac{d_p^T d_p}{2\kappa_{d_p}}$. Since d_p is bounded, we conclude that \dot{V} is negative outside the compact residual set $\mathcal{R} = \left\{ \Xi_p : |\Xi_p| \leq \frac{\|d_p\|_\infty}{2\kappa_{d_p}} \right\}$. Recalling, the closed loop system (x, e_p) is continuous in all states, d_p and t , which implies that the right-hand side of (5.67) is continuous in all states, d_p and t . That guarantees global uniform boundedness of $x(t), e_p(t)$ and the parameter estimations.

Following the same procedure The adaptive controller for u_t is given by

$$u_t = \frac{\hat{b}_{ut}}{\left(1 - \hat{b}_t \left(\hat{b}_t - \hat{\varrho}_h k_2 \right) \right)} \bar{u}_t, \tag{5.68}$$

with

$$\bar{u}_t = -\hat{\varrho}_h \dot{x}_h^T R \bar{B} - \hat{\Theta}_{he}^T \Xi_{he} + \xi_{he} + \hat{\Pi}_h^T \Phi_h + \left(c_h + \kappa_{d_h} d_h^T d_h + \left(\hat{b}_t - \hat{\varrho}_h k_2 \right)^2 \right) e_h, \tag{5.69}$$

with $c_p > 2$.

The update laws are given by

$$\dot{\hat{a}}_{h2} = -\kappa_{a_{h2}} \text{sgn}(\varrho_h) \dot{x}_{h1} \overline{B}^T R \dot{x}_h, \quad \kappa_{a_{h2}} > 0, \quad (5.70)$$

$$\dot{\hat{\theta}}_{he} = -\kappa_{\theta_{he}} \text{sgn}(\varrho_h) \eta_{h0} \overline{B}^T R \dot{x}_h, \quad \kappa_{\theta_{he}} > 0, \quad (5.71)$$

$$\dot{\hat{\beta}}_{hi} = -\kappa_{\beta_{hi}} \text{sgn}(\varrho_h) \eta_{hi} \overline{B}^T R \dot{x}_h, \quad \kappa_{\beta_{hi}} > 0, \quad (5.72)$$

$$\dot{\hat{\beta}}_{hp} = -\kappa_{\beta_{hp}} \text{sgn}(\varrho_h) \eta_{hp} \overline{B}^T R \dot{x}_h, \quad \kappa_{\beta_{hp}} > 0, \quad (5.73)$$

$$\dot{\hat{b}}_{ut} = -\kappa_{b_{ut}} \overline{u}_d e_h, \quad \kappa_{b_{ut}} > 0, \quad (5.74)$$

$$\dot{\hat{\varrho}}_t = -\kappa_{\overline{\varrho}_h} e_h \dot{x}_h^T R \overline{B}, \quad \kappa_{\overline{\varrho}_h} > 0, \quad (5.75)$$

$$\dot{\hat{\Theta}}_{he} = \kappa_{\Theta_{he}} \Xi_{he} e_h, \quad \kappa_{\Theta_{he}} > 0, \quad (5.76)$$

$$\dot{\hat{\Pi}}_h = \kappa_{\Pi_h} \Phi_h e_h, \quad \kappa_{\Phi_h} > 0, \quad (5.77)$$

$$\dot{\hat{b}}_t = \begin{cases} \tau_{\overline{b}_t}, & \hat{b}_t \text{sgn}(\overline{b}_t) > \overline{\varsigma}_h \text{ or } \tau_{\overline{b}_t} \text{sgn}(\overline{b}_t) \geq 0 \\ 0, & \hat{b}_t \text{sgn}(\overline{b}_t) \leq \overline{\varsigma}_h \text{ and } \tau_{\overline{b}_t} \text{sgn}(\overline{b}_t) < 0 \end{cases}, \quad (5.78)$$

$$\begin{bmatrix} \dot{\hat{b}}_t \\ \dot{\hat{\varrho}}_h \end{bmatrix} = \begin{cases} \tau_{b_t, \varrho_h}, & \text{sgn}(\overline{b}_t) (\hat{b}_t - \hat{\varrho}_t k_2) > \frac{1}{\overline{\varsigma}_h} \\ & \text{or } \mathcal{R}^T \tau_{b_t, \varrho_h} \leq 0 \\ \left(I - \Gamma \frac{\mathcal{R} \mathcal{R}^T}{\mathcal{R}^T \Gamma \mathcal{R}} \right) \tau_{b_t, \varrho_h}, & \text{sgn}(\overline{b}_t) (\hat{b}_t - \hat{\varrho}_h k_2) \leq \frac{1}{\overline{\varsigma}_h} \\ & \text{and } \mathcal{R}^T \tau_{b_t, \varrho_h} > 0, \end{cases} \quad (5.79)$$

where

$$\tau_{\overline{b}_t} = \kappa_{\overline{b}_t} (\hat{b}_t - \hat{\varrho}_t k_2) u_t e_h, \quad \kappa_{\overline{b}_t} > 0 \quad (5.80)$$

$$\tau_{b_t, \varrho_h} = \kappa_{b_t, \varrho_h} \begin{bmatrix} \text{sgn}(\varrho_t) \dot{x}_{h2} \overline{B}^T R \dot{x}_h \\ -\text{sgn}(\varrho_h) K \dot{x}_h \overline{B}^T R \dot{x}_h \end{bmatrix}, \quad \kappa_{b_t, \varrho_h} > 0, \quad (5.81)$$

with

$$e_p = P_t - \left(-\hat{\varrho}_h K \dot{x}_h - \hat{a}_{h2} \dot{x}_{h1} + \hat{b}_t \dot{x}_{h2} - \hat{\theta}_{he}^T \eta_{h0} - \sum_{i=1}^2 \hat{\beta}_{hi}^T \eta_{hi} - \hat{\beta}_{hp}^T \eta_{hp} \right), \quad (5.82)$$

$$\Phi_p = \begin{bmatrix} \dot{x}_{h1} P_t, & \dot{x}_{p1} P_d \end{bmatrix}^T, \quad (5.83)$$

$$\Xi_{he} = \left(\hat{b}_t - \hat{\varrho}_h k_2 \right) \begin{bmatrix} \dot{x}_{h1}, & \dot{x}_{h2}, & \eta_{h0}^T, & \eta_{h1}^T, & \eta_{h2}^T, & (\eta_{hp} - l P_t)^T \end{bmatrix}^T, \quad (5.84)$$

$$d_h = \begin{bmatrix} P_t, & - \left(\hat{b}_t - \hat{\varrho}_h k_2 \right) P_t \end{bmatrix}^T, \quad (5.85)$$

$$\begin{aligned} \xi_{he} = & \left(\dot{\hat{\varrho}}_h k_1 + \dot{\hat{a}}_{h2} \right) \dot{x}_{h1} + \left(\hat{\varrho}_h k_1 + \hat{a}_{h2} + \dot{\hat{\varrho}}_h k_2 - \dot{\hat{b}}_t \right) \dot{x}_{h2} + \dot{\hat{\theta}}_{he}^T \eta_{h0} + \dot{\hat{\theta}}_{he}^T \eta_{h0} \\ & + \sum_{i=1}^2 \left(\dot{\hat{\beta}}_{hi}^T \eta_{hi} + \hat{\beta}_{hi}^T \dot{\eta}_{hi} \right) + \dot{\hat{\beta}}_{hp}^T \eta_{hp} + \hat{\beta}_{hp}^T \dot{\eta}_{hp}. \end{aligned} \quad (5.86)$$

The filters for wave disturbance observer in heave is given by

$$\dot{\eta}_{hi} = G \eta_{hi} - l \dot{x}_{hi}, \quad \text{for } i = 1, 2, \quad (5.87)$$

$$\dot{\eta}_{h0} = G (\eta_{h0} + N \dot{x}_h), \quad (5.88)$$

$$\dot{\eta}_{hp} = G (\eta_{hp} - l P_t). \quad (5.89)$$

Using (5.12) and (5.13), the control signals for the air flow rates of each chamber are given by

$$u_1 = \frac{u_t - u_d}{2}, \quad (5.90)$$

$$u_2 = \frac{u_t + u_d}{2}, \quad (5.91)$$

5.3 Adaptive Ramp Pitch Control in Bow to Stern Configuration

The side view of a bow to stern configuration is illustrated in Figure 5.2. We design an adaptive control algorithm to make the bow of T-Craft, **A**, track the stern of LMSR, **B**. Thus, the oscillation of the ramp is reduced. In this case, we assume the position, the velocity and the acceleration of T-Craft and LMSR to be measured. The reference heave and pitch which T-Craft needs to track, is given as $r_h = \zeta_{33}^{LMSR} - d_{\text{offset}}$ and $r_p = \frac{L_{LMSR}}{L_{T-Craft}} \zeta_{55}^{LMSR}$ where d_{offset} is the vertical

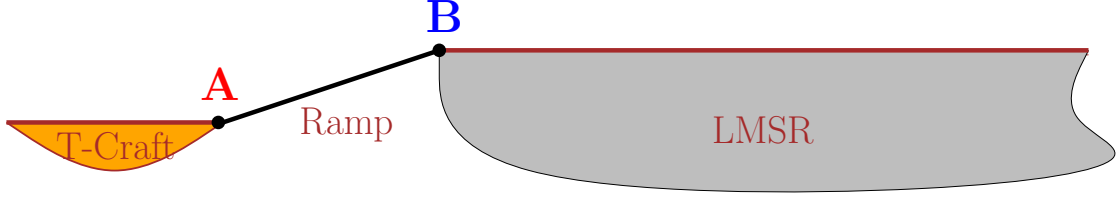


Figure 5.2: Side view of a bow to stern configuration. Bow of an SES, **A**, is connected to stern of an LMSR, **B**, by a ramp.

constant distance between T-Craft and LMSR in calm water, L represents length of the vehicles and $\zeta_{33}^{LMSR}, \zeta_{55}^{LMSR}$ are heave and pitch of LMSR, respectively.

We give the design procedure only for pitch mode since it is trivial to obtain a tracking algorithm by following the same procedure. Using the result given in [38], we represent \overline{F}_5^e as follows

$$\frac{1}{\overline{b}_d} \overline{F}_5^e = \Theta_{p-TC}^T \xi_{p-TC} + \theta_p^T \delta_{p-TC}, \quad (5.92)$$

where $\theta_p = h^T M^{-1}$ and

$$\Theta_{p-TC} = \left[\frac{1}{\overline{b}_d} \theta_p^T, \quad \frac{\overline{a}_{p1}}{\overline{b}_d} \theta_p^T, \quad \frac{\overline{a}_{p2}}{\overline{b}_d} \theta_p^T, \quad \theta_s^T \right]^T, \quad (5.93)$$

$$\xi_{p-TC} = \left[(\eta_{0p-TC} + N x_p)^T, \quad \eta_{1p-TC}^T, \quad \eta_{2p-TC}^T, \quad \eta_{Pp-TC}^T \right]^T, \quad (5.94)$$

with

$$\dot{\eta}_{ip-TC} = G \eta_{ip-TC} - l x_{pi}, \quad \text{for } i = 1, 2, \quad (5.95)$$

$$\dot{\eta}_{0p-TC} = G (\eta_{0p-TC} + N x_p), \quad (5.96)$$

$$\dot{\eta}_{up-TC} = G \eta_{up-TC} - l P_d, \quad (5.97)$$

and δ_{p-TC} obeys, $\dot{\delta}_{s-TLB} = G \delta_{p-TC}$. Defining an error signal between the pitch of T-Craft and the reference pitch as $z_p = \zeta_{55}^{T-Craft} - r_p$ and using (5.14), we obtain

$$\dot{z}_p = A_0 z_p + B \frac{1}{\overline{b}_d} (\overline{\gamma}^T x_p + \overline{F}_5^e + P_d - b_d \ddot{r}_p), \quad (5.98)$$

where $b_d = \frac{1}{\overline{b}_d}$, $\overline{\gamma} = \left[\frac{\overline{a}_{p1}}{\overline{b}_d}, \quad \frac{\overline{a}_{p2}}{\overline{b}_d} \right]^T$. Substituting (5.92) into (5.98), and using the backstepping design procedure, the adaptive controller for input $u_d(t)$ is given by

$$u_d = \hat{b}_{ud} \overline{u}_d, \quad (5.99)$$

where

$$\begin{aligned}
\bar{u}_d = & \hat{b}_d z_p^T P_s e_{sp} + \hat{\Pi}_p^T \Phi_p - \dot{\hat{b}}_d K_s z_p + \hat{\Theta}_{p-TC}^T \xi_{p-TC} + \dot{\hat{\gamma}}^T x_p - \hat{b}_d k_1 z_{p2} \\
& + \hat{\Theta}_{p-TC}^T \left[\dot{\eta}_{0p-TC}^T, \dot{\eta}_{1p-TC}^T, \dot{\eta}_{2p-TC}^T, \dot{\eta}_{Pp-TC}^T \right] + \hat{a}_{p1} x_{p2} \\
& - \left(\hat{b}_d k_2 - \hat{\theta}_s^T l - \hat{a}_{p2} \right) \hat{\Theta}^T \Xi_{\bar{\Theta}} + \hat{b}_d k_2 \ddot{r}_p - \dot{\hat{b}}_d \ddot{r}_p - \hat{b}_d \ddot{r}_p \\
& + \left(c_p + \left(\hat{b}_d k_2 - \hat{\theta}_s^T l - \hat{a}_{p2} \right)^2 \kappa_{\delta} + \kappa_{V_0} P_d^2 \right) e_{sp}. \tag{5.100}
\end{aligned}$$

and the update laws are given by

$$\dot{\hat{\Theta}}_{p-TC}(t) = \kappa_{\Theta} \text{sgn}(\bar{b}_d) \xi_{p-TC}(t) B^T P_s z_p(t), \quad \kappa_{\Theta} > 0, \tag{5.101}$$

$$\dot{\hat{\gamma}}(t) = \kappa_{\bar{\gamma}} \text{sgn}(\bar{b}_d) x_p(t) B^T P_s z_p(t), \quad \kappa_{\Theta} > 0, \tag{5.102}$$

$$\dot{\hat{b}}_d(t) = -\kappa_{b_d} \text{sgn}(\bar{b}_d) (K z_p + \ddot{r}_p) B^T P_s z_p(t), \quad \kappa_{b_d} > 0, \tag{5.103}$$

$$\dot{\hat{\Pi}}_p(t) = \kappa_{\Pi} \Phi_p(t) e_{sp}(t), \quad \kappa_{\Pi} > 0, \tag{5.104}$$

$$\dot{\hat{b}}_d(t) = \kappa_{\bar{b}_d} z_p^T P B e_{sp}(t), \quad \kappa_{\bar{b}_d} > 0, \tag{5.105}$$

$$\dot{\hat{\Theta}}(t) = -\kappa_{\bar{\Theta}} \Xi_{\bar{\Theta}} e_{sp}(t), \quad \kappa_{\Pi} > 0, \tag{5.106}$$

$$\dot{\hat{b}}_{ud}(t) = -\kappa_{b_{ud}} \bar{u}_d e_{sp}(t), \quad \kappa_{b_{ud}} > 0, \tag{5.107}$$

where

$$e_{sp} = P_d - \left(\hat{b}_d (K_s z_p + \ddot{r}_p) - \hat{\Theta}_{p-TC}^T \xi_{p-TC}(t) B^T P_s - \bar{\gamma}^T x_p \right), \tag{5.108}$$

$$\Xi_{\bar{\Theta}} = \left[x_p^T, \xi_{p-TC}^T, P_d \right]^T, \tag{5.109}$$

with the positive definite matrix P_s which is a solution of the matrix equation

$$(A_0 + BK_s)^T P_s + P_s (A_0 + K_s) = -2I. \tag{5.110}$$

Similarly, the adaptive controller for u_t is given by

$$u_t = \hat{b}_{ut} \bar{u}_t, \tag{5.111}$$

where

$$\begin{aligned}
\bar{u}_t = & \hat{b}_t z_t^T P_s e_{sh} + \hat{\Pi}_h^T \Phi_h - \dot{\hat{b}}_t K_s z_h + \dot{\hat{\Theta}}_{h-TC}^T \xi_{h-TC} + \dot{\hat{\gamma}}_h^T x_h - \dot{\hat{b}}_t k_1 z_{h2} \\
& + \hat{\Theta}_{h-TC}^T \left[\dot{\eta}_{0h-TC}^T, \dot{\eta}_{1h-TC}^T, \dot{\eta}_{2h-TC}^T, \dot{\eta}_{Ph-TC}^T \right] + \hat{a}_{h1} x_{h2} \\
& - \left(\hat{b}_t k_2 - \hat{\theta}_s^T l - \hat{a}_{h2} \right) \hat{\Theta}_h^T \Xi_{\bar{\Theta}_h} + \hat{b}_t k_2 \ddot{r}_h - \dot{\hat{b}}_t \ddot{r}_h - \hat{b}_t \ddot{r}_h \\
& + \left(c_h + \left(\hat{b}_t k_2 - \hat{\theta}_s^T l - \hat{a}_{h2} \right)^2 \kappa_\delta + \kappa_{V_0} P_t^2 \right) e_{sh}.
\end{aligned} \tag{5.112}$$

and the update laws are given by

$$\dot{\hat{\Theta}}_{h-TC}(t) = \kappa_\Theta \text{sgn}(\bar{b}_t) \xi_{h-TC}(t) B^T P_s z_h(t), \quad \kappa_\Theta > 0, \tag{5.113}$$

$$\dot{\hat{\gamma}}_h(t) = \kappa_{\bar{\gamma}_h} \text{sgn}(\bar{b}_t) x_h(t) B^T P_s z_h(t), \quad \kappa_\Theta > 0, \tag{5.114}$$

$$\dot{\hat{b}}_t(t) = -\kappa_{b_t} \text{sgn}(\bar{b}_t) (K z_h + \ddot{r}_h) B^T P_s z_h(t), \quad \kappa_{b_h} > 0, \tag{5.115}$$

$$\dot{\hat{\Pi}}_h(t) = \kappa_\Pi \Phi_h(t) e_{sh}(t), \quad \kappa_\Pi > 0, \tag{5.116}$$

$$\dot{\hat{b}}_t(t) = \kappa_{\bar{b}_t} z_h^T P B e_{sh}(t), \quad \kappa_{\bar{b}_t} > 0, \tag{5.117}$$

$$\dot{\hat{\Theta}}_h(t) = -\kappa_{\bar{\Theta}_h} \Xi_{\bar{\Theta}_h} e_{sh}(t), \quad \kappa_\Pi > 0, \tag{5.118}$$

$$\dot{\hat{b}}_{ut}(t) = -\kappa_{b_{ut}} \bar{u}_t e_{sh}(t), \quad \kappa_{b_{ut}} > 0, \tag{5.119}$$

where

$$e_{sh} = P_t - \left(\hat{b}_t (K_s z_h + \ddot{r}_h) - \dot{\hat{\Theta}}_{h-TC}^T \xi_{h-TC}(t) B^T P_s - \bar{\gamma}_h^T x_h \right), \tag{5.120}$$

$$\Xi_{\bar{\Theta}} = \left[x_h^T, \xi_{h-TC}^T, P_t \right]^T. \tag{5.121}$$

The air flow rates of each chamber are derived by using (5.90) and (5.91).

5.4 Results

We implement the two-chamber air-cushion model and designed controller into the same simulation platform as introduced in Section 4.3. The pitch and heave of SES are given in Figures 5.3 and 5.4. As it is observed, the controller achieves to stabilize the pitch and the heave simultaneously. The values of A_{l1} and α_1 are given in Figure 5.5.

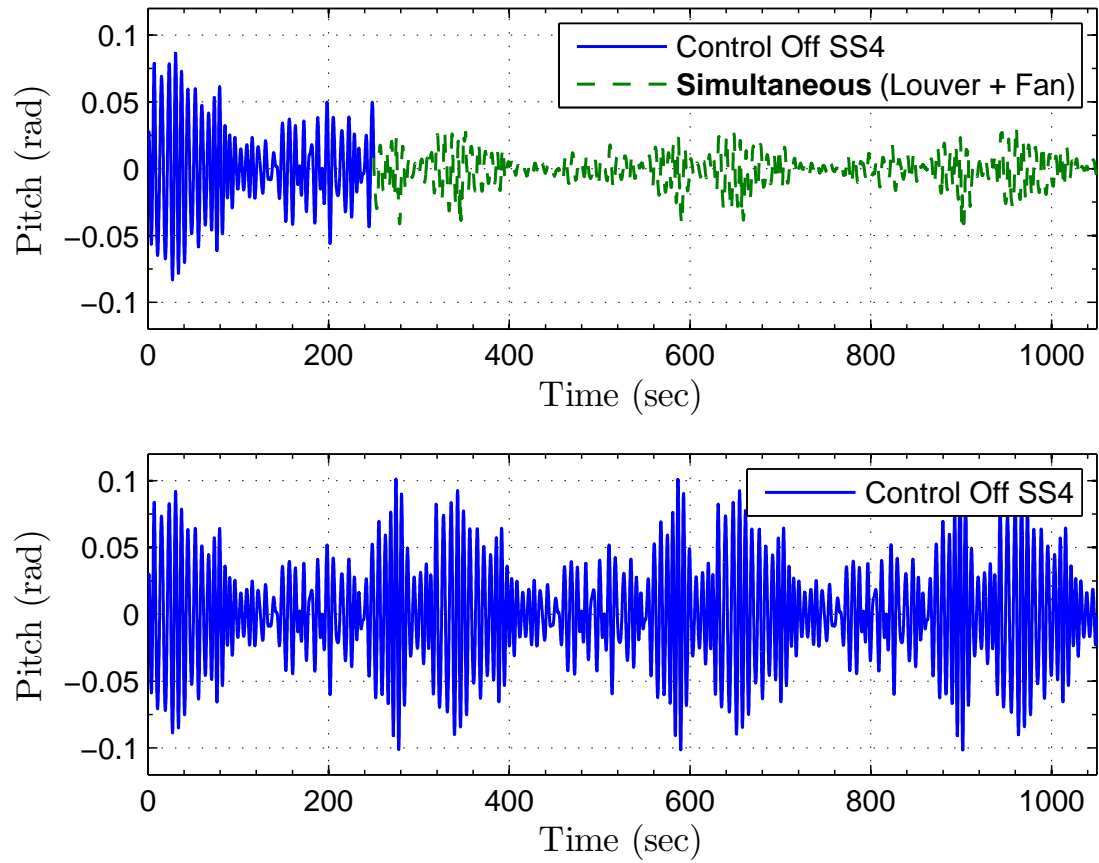


Figure 5.3: Pitch of SES in SS4 with and without controller. The controller is turned on at 250 seconds.

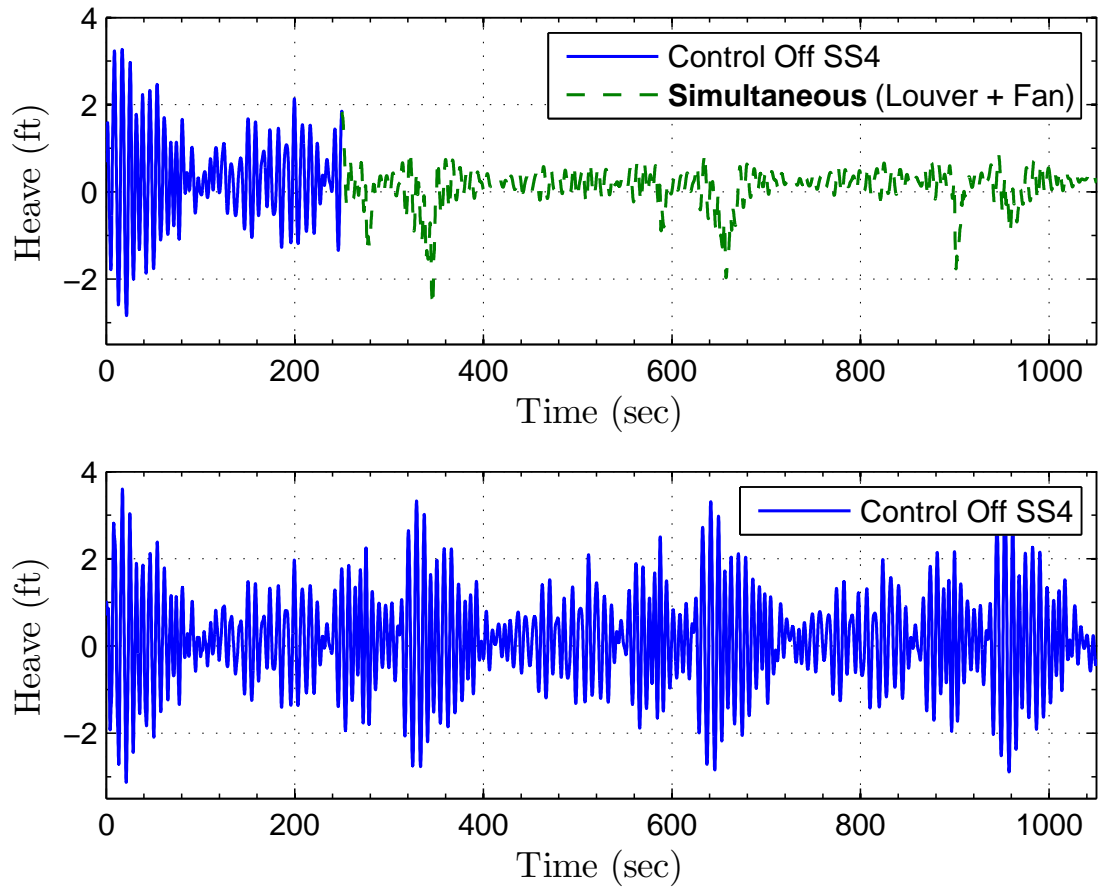


Figure 5.4: Heave of SES in SS4 with and without controller. The controller is turned on at 250 seconds.

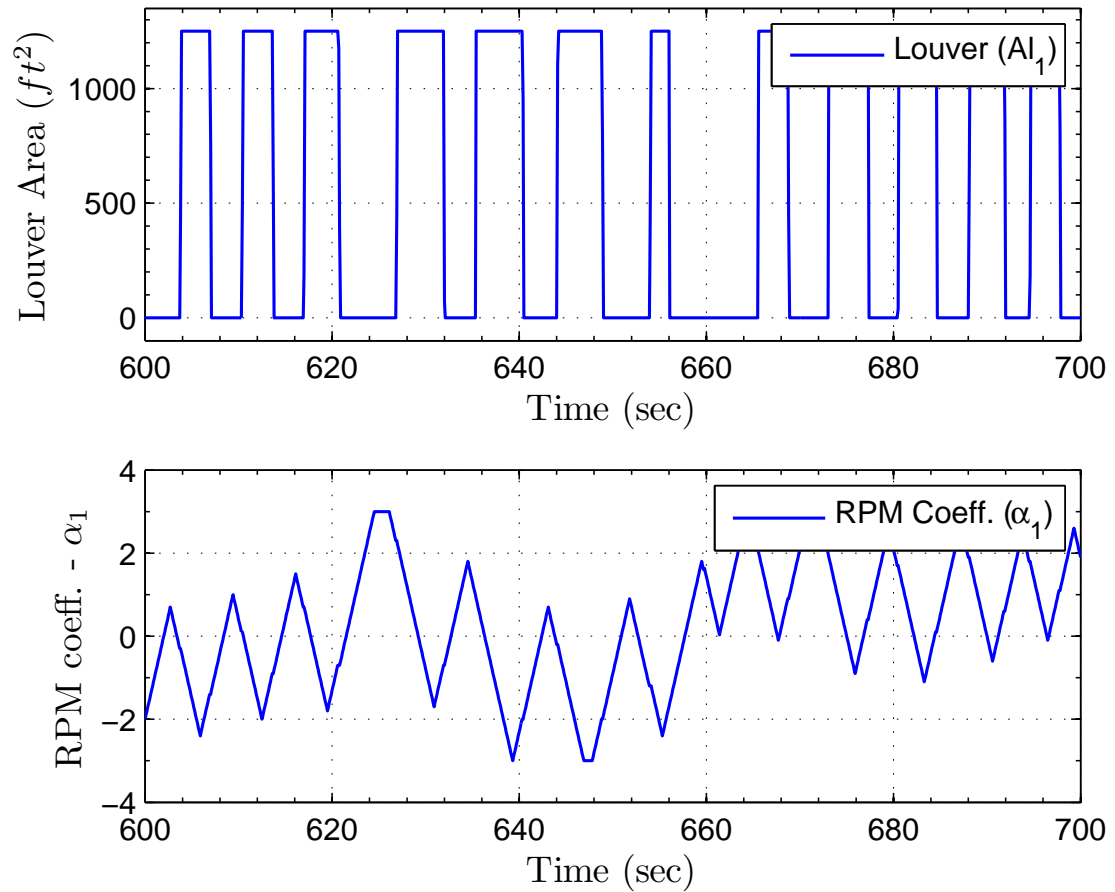


Figure 5.5: Louver area, A_{1L} , and rpm coefficient, α_1 , of the chamber one of SES between 600–700 seconds. Louver area, A_{1L} , and rpm coefficient, α_1 , are saturated at 0, 1250 ft^2 and $-3, 3$, respectively.

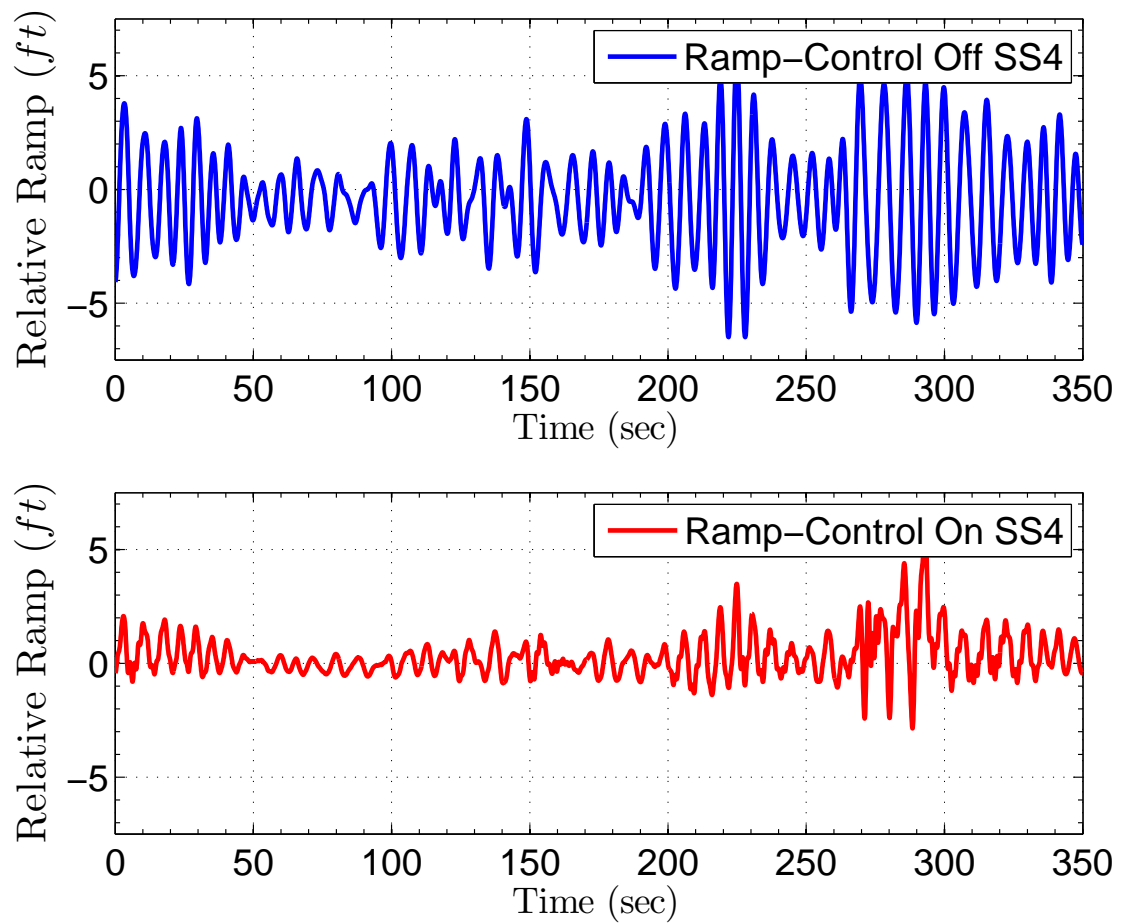


Figure 5.6: Simulation results for tracking algorithm by state feedback. Both with and without control results are shown. The developed tracking algorithm provides significant stability on the ramp.

Chapter 6

Implementation of the Developed Controller on a Scale Model Surface Effect Ship

We implement here our developed controller to a scale model SES which is designed at National Technical University of Athens and is brought to Florida Atlantic University at Boca Raton, FL. We have collaborated the hydrodynamic research group which is directed by Prof. Manhar Dhanak. The experiments have been done with the help of Michael Kindel and Quintin Du Plessis from Florida Atlantic University. We perform several experiments in a wave tank at FAU to test the performance of the controller. It is shown that the experiment results which we have obtained are consistent with the developed theory.

This chapter is organized as follows: We introduce the scale model SES in Section 6.1. Design of the controller with a dead-zone modification is given in Section 6.2. In Section 6.3, we present the experiment set-up and the result.

6.1 Scale Model SES - AirCat

A scale model SES, named AirCat, is developed for the purpose of a beacon approach project at the National Technical University of Athens and is brought to Florida Atlantic University at Boca Raton, FL. The basic AirCat equipment

Table 6.1: Dimensions of the scale model SES, named AirCat are given in millimeter (mm) .

Length overall	1210 mm
Length between perpendiculars	1030 mm
Breadth	400 mm
Depth	135 mm

consists of; hull-superstructure, rubber skirt, air-blower system. The dimension of the model is given in Table 6.1

Different views of AirCat are given in Figure 6.1. Air cushion of AirCat with side hulls and rubber skirts are shown in Figure 6.1(d). As shown in Figure 6.1(a), AirCat contains a system box with a blower system and a pressure sensor. The details of the system box is shown in Figure 6.2.

The hull and superstructure is made by epoxy rein reinforced with fiberglass. The material used to construct rubber skirt is a flexible foam material. There are several supporting struts and mounts which help to fit the skirt in the proper way. The air-blower system of AirCat consists of an electric motor foxed onto stationary fan blades, a rotational fan and a duct. The motor with two fans is assembled to the duct. We implement a 40A NAVY motor driver which is used to amplify pulse-width modulation signal from a μC and regulate a motor's angular rate.

The installed micro-controlled (μC) belongs to ARM7 family, and more specifically, is LPC2388 from NXP Semiconductors. The μC is placed on a KEIL MCB2300 development board. An inertial measurement unit (IMU) is a complex sensor that consists of multiple sensors and a μC which collects data from various sensors. The selected IMU is a VN-100 from VectorNav. It provides 3-axis linear accelerations and 3-axis angular rates. A differential pressure sensor SDP2000-L from Senirion with a range $0 - -3500 Pa$ and resolution of $\pm 1 Pa$ is placed in the system box to measure the pressure of the air-cushion chamber. Two rechargeable battery packs of NiMH cells are installed to the model to provide necessary energy to the system. One pack is connected to the micro-controller and the other one is used to drive the blower system.

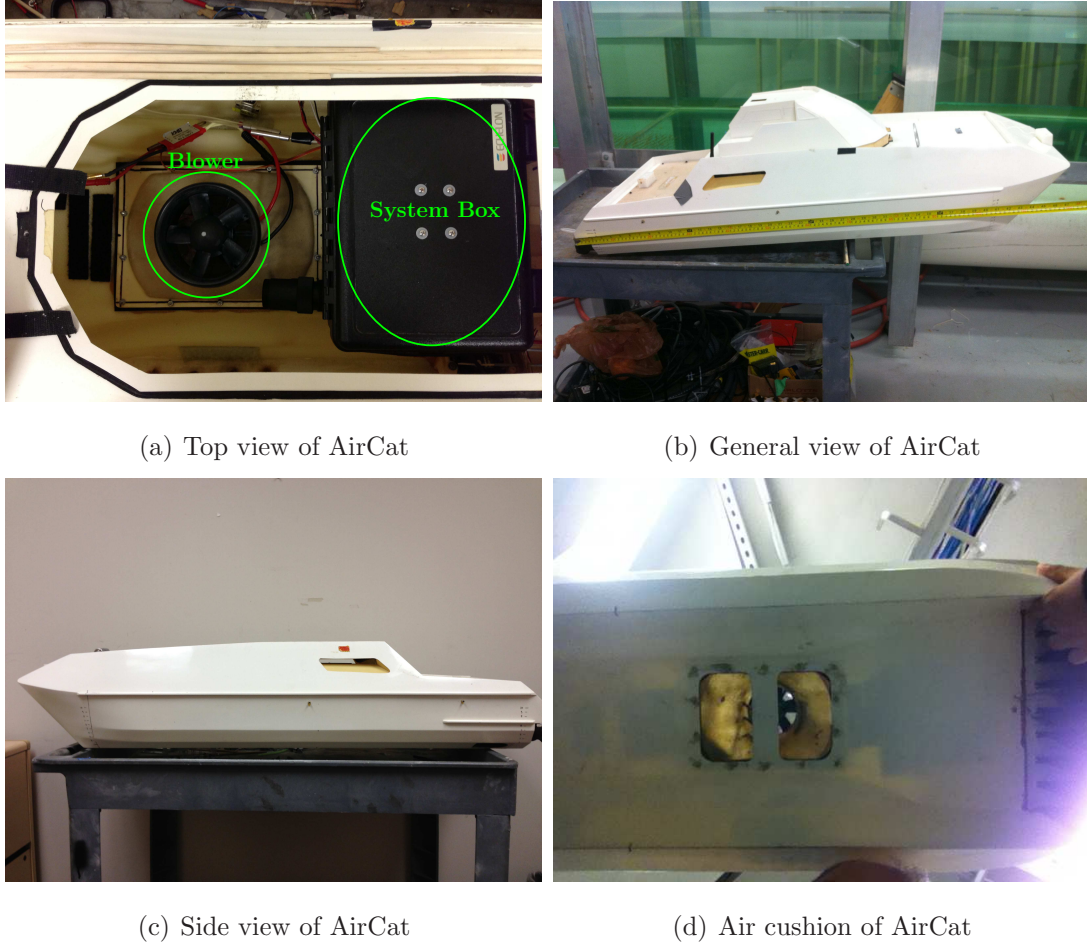


Figure 6.1: Top view with blower and system box, side view and general view of AirCat are presented with air-cushion at the bottom.

6.2 Control Design

6.2.1 Controller

We consider a linear model for pressure to design a controller for AirCat. Following [2] and [11], the air-cushion pressure dynamics are given by

$$\dot{P}_c = -\frac{\rho_0 A_0}{C_c} \dot{\zeta}_3 - \frac{1}{C_c R_L} P_c + \frac{1}{C_c} q \quad (6.1)$$

where ρ_0, V_0, P_0 are the initial values of air density, volume and pressure of the air-cushion, respectively and $C_c = \frac{\rho_0 V_0}{P_0}$. The term R_L is air resistance of hulls and skirts. It represents the air leakage from air cushion. The input q represents mass

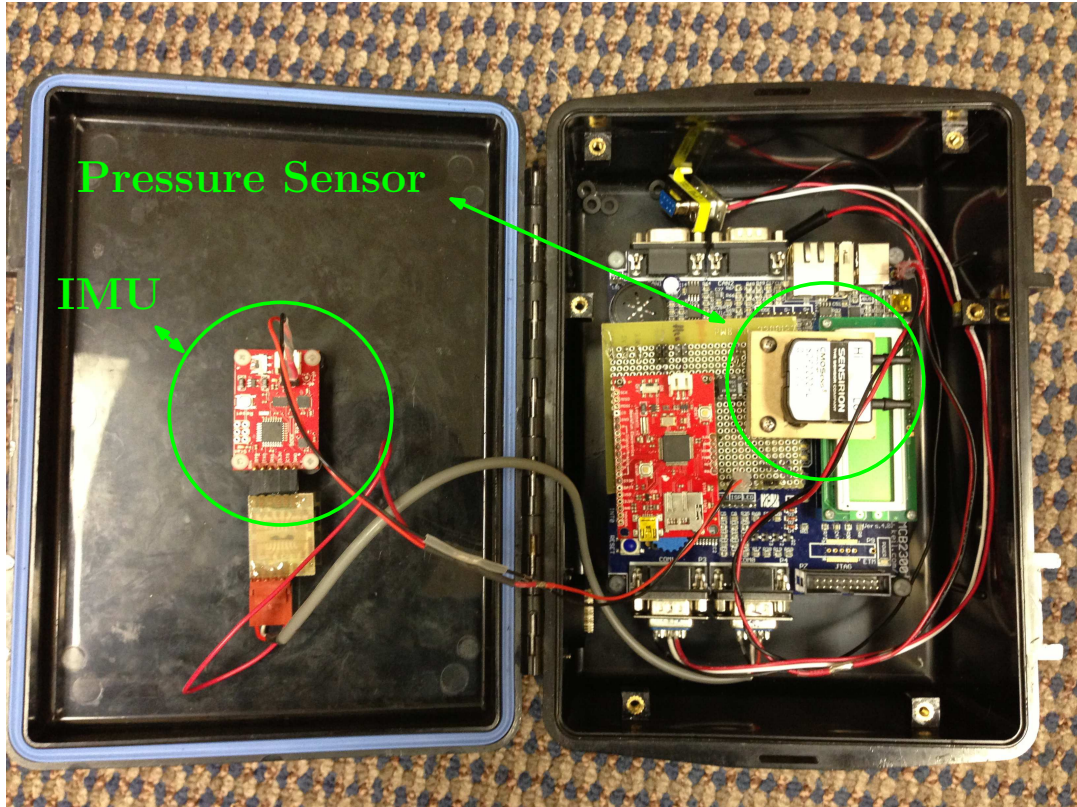


Figure 6.2: System box of AirCat. It has microcontroller inside with sensors and actuator driver. The box is placed in the scale model.

air flow rate in to the cushion. In our scale model, the main input is duty cycle. Thus, q can be represented by coefficient as follows $q = b_{\text{blower}}u$ where u is the duty cycle of the DC motor driver.

Using heave dynamics given in (4.1) and air-cushion pressure dynamics (6.1), we obtain following state-space model,

$$\dot{x} = A_0x + B(a_{11}x_1 + a_{12}x_2 + \nu(t) + \bar{b}_p p), \quad (6.2)$$

$$\dot{p} = a_{21}x_2 + \bar{b}_1 p + \bar{b}_2 u, \quad (6.3)$$

where

$$a_{21} = -\frac{\rho_0 A_0}{C_c}, \quad (6.4)$$

$$\bar{b}_1 = -\frac{1}{C_c R_L}, \quad (6.5)$$

$$\bar{b}_2 = \frac{b_{\text{blower}}}{C_c}, \quad (6.6)$$

$A_0 = \begin{bmatrix} 0 & 1 \\ 0 & 0 \end{bmatrix}$, $B = \begin{bmatrix} 0 \\ 1 \end{bmatrix}$, $x = \begin{bmatrix} x_1 \\ x_2 \end{bmatrix}$ and x_1, x_2, p, ν and u correspond to heave, heave rate, pressure, wave disturbance and duty cycle of the blower system respectively. Wave disturbance is given by

$$\nu(t) = g \sin(\omega t + \phi), \quad (6.7)$$

We make the following assumptions regarding the plant

Assumption 6.1 $a_{11}, a_{12}, a_{21}, \bar{b}_1, \bar{b}_2, \bar{b}_p$ are unknown.

Assumption 6.2 $a_{11} < 0$, $\bar{b}_p, \bar{b}_2 > 0$ and $|\bar{b}_p| \geq \bar{\tau} > 0$.

Assumption 6.3 x and ν are not measured but \dot{x} are measured.

Using the control design given in Chapter 3, the adaptive controller for system (6.2), (6.3) with disturbance $\nu(t)$ is given by

$$u = \frac{\hat{b}_2}{1 - \hat{b}_p(\hat{b}_p - \hat{\rho}k_n)} \bar{u}, \quad (6.8)$$

where k_n is the second element of the control gain $K \in R^{1 \times 2}$ which is chosen so that $(A_0^T + \bar{B}K)$ is Hurwitz and the positive definite matrix P is a solution of the matrix equation $(A_0^T + \bar{B}K)^T P + P(A_0^T + \bar{B}K) = -4I$, with $\bar{B} = \begin{bmatrix} 1 & 0_{n-1} \end{bmatrix}^T$, and

$$\begin{aligned} \bar{u} = & \hat{\gamma}_3^T (\hat{b}_p - \hat{\rho}k_2) \varphi - \hat{\gamma}_p^T \varphi + \hat{b}_p \dot{x}_2 - (\hat{\gamma}_1^T + \hat{\rho}K) A_0 \dot{x} - \left(\hat{\gamma}_1^T R + \hat{\rho}K - \hat{\rho} \bar{B}^T P \right) \dot{x} \\ & - \hat{\theta}_t^T \eta_t - \hat{\theta}_t^T \dot{\eta}_t - \hat{\beta}_{1p}^T \eta_p - \hat{\beta}_{1p}^T \dot{\eta}_p - \left((\hat{b}_p - \hat{\rho}k_2)^2 + c \right) e, \end{aligned} \quad (6.9)$$

with $c > 0$, $R = \text{diag}\{1, 0\}$. and

$$e(t) = p - \left(- (R\hat{\gamma}_1)^T \dot{x} + \hat{b}_p \dot{x}_2 - \hat{\varrho} K \dot{x} - \hat{\theta}_t^T \eta_t - \hat{\beta}_{1p}^T \eta_p \right). \quad (6.10)$$

We use projection operator to avoid singularity in (6.8). The update laws are given by

$$\dot{\hat{\gamma}}_1 = -\kappa_{\gamma_1} \text{sgn}(\bar{b}_p a_{11}) \dot{x} \bar{B}^T P \dot{x}, \quad \kappa_{\gamma_1} > 0, \quad (6.11)$$

$$\dot{\hat{\gamma}}_p = \kappa_{\gamma_p} \varphi e, \quad \kappa_{\gamma_p} > 0, \quad (6.12)$$

$$\dot{\hat{\gamma}}_3 = -\kappa_{\gamma_3} \varphi \left(\hat{b}_p - \hat{\varrho} k_2 \right) e, \quad \kappa_{\gamma_3} > 0, \quad (6.13)$$

$$\dot{\hat{b}}_2 = -\kappa_{b_2} \text{sgn}(\bar{b}_2) \bar{u} e, \quad \kappa_{b_2} > 0, \quad (6.14)$$

$$\dot{\hat{\theta}}_t = -\kappa_{\theta_t} \text{sgn}(\bar{b}_p a_{11}) \eta_t \bar{B}^T P \dot{x}, \quad \kappa_{\theta_t} > 0, \quad (6.15)$$

$$\dot{\hat{\beta}}_{1p} = -\kappa_{\beta_{1p}} \text{sgn}(\bar{b}_p a_{11}) \eta_p \bar{B}^T P \dot{x}, \quad \kappa_{\beta_{1p}} > 0, \quad (6.16)$$

$$\dot{\hat{\varrho}} = -\kappa_{\varrho} e \bar{B}^T P \dot{x}, \quad \kappa_{\varrho} > 0, \quad (6.17)$$

$$\dot{\hat{b}}_p = \begin{cases} \tau_{\bar{b}_p}, & \hat{b}_p \text{sgn}(\bar{b}_p) > \bar{\varsigma} \text{ or } \tau_{\bar{b}_p} \text{sgn}(\bar{b}_p) \geq 0 \\ 0, & \hat{b}_p \text{sgn}(\bar{b}_p) \leq \bar{\varsigma} \text{ and } \tau_{\bar{b}_p} \text{sgn}(\bar{b}_p) < 0 \end{cases}, \quad (6.18)$$

$$\begin{bmatrix} \dot{\hat{b}}_p \\ \dot{\hat{\varrho}} \end{bmatrix} = \begin{cases} \tau_{b_p, \varrho}, & \text{sgn}(\bar{b}_p) (\hat{b}_p - \hat{\varrho} k_2) > \frac{1}{\bar{\varsigma}} \\ & \text{or } \mathcal{P}^T \tau_{b_p, \varrho} \leq 0 \\ \left(I - \Gamma \frac{\mathcal{P} \mathcal{P}^T}{\mathcal{P}^T \Gamma \mathcal{P}} \right) \tau_{b_p, \varrho}, & \text{sgn}(\bar{b}_p) (\hat{b}_p - \hat{\varrho} k_2) \leq \frac{1}{\bar{\varsigma}} \\ & \text{and } \mathcal{P}^T \tau_{b_p, \varrho} > 0, \end{cases} \quad (6.19)$$

where

$$\tau_{\bar{b}_p} = -\kappa_{\bar{b}_p} \text{sgn}(\bar{b}_2) \left(\hat{b}_p - \hat{\varrho} k_2 \right) u e, \quad \kappa_{\bar{b}_p} > 0, \quad (6.20)$$

$$\tau_{b_p, \varrho} = \kappa_{b_p, \varrho} \begin{bmatrix} \text{sgn}(\varrho) \dot{x}_n \bar{B}^T P \dot{x} \\ -\text{sgn}(\varrho) K \dot{x} \bar{B}^T P \dot{x} \end{bmatrix}, \quad \kappa_{b_p, \varrho} > 0, \quad (6.21)$$

$$\mathcal{P} = \begin{bmatrix} -\text{sgn}(\bar{b}_p) & k_n \text{sgn}(\bar{b}_p) \end{bmatrix}^T, \quad (6.22)$$

$$\varphi = [\dot{x}^T, p, \eta_t^T, \eta_p^T]^T, \quad (6.23)$$

with $\eta_t = [\eta_0^T, \eta_1^T, \dots, \eta_n^T]^T$ and Γ belongs to the set of all positive definite sym-

metric 2×2 matrices. The observer filters are given by

$$\dot{\eta}_i = G\eta_i - l\dot{x}_i, \quad 1 \leq i \leq 2, \quad (6.24)$$

$$\dot{\eta}_0 = G(\eta_0 + N\dot{x}), \quad (6.25)$$

$$\eta_p = G(\eta_p - lp), \quad (6.26)$$

where $G \in \mathbb{R}^{2 \times 2}$ is a Hurwitz matrix with distinct eigenvalues, (G, l) is a controllable pair and $N = \frac{1}{B^T B} l B^T$.

6.2.2 Dead-Zone Modification

As it is discussed in Remark 4.1, in order to maintain stability in case of existence of unmodeled uncertainties and measurement noise, there are various modification is proposed in [26]. We consider a dead-zone modification to counter-attack the destabilizing effects of bounded disturbances and of a class of dynamic uncertainties. We modify the update laws by using continuous dead zone.

The modified robust update laws for γ_1 and γ_p are given by

$$\dot{\gamma}_1 = -\kappa_{\gamma_1} \text{sgn}(\bar{b}_p a_{11}) \dot{x} \left(\bar{B}^T P \dot{x} + g_x \right), \quad (6.27)$$

$$\dot{\gamma}_p = \kappa_{\gamma_p} \varphi(e + g_e), \quad (6.28)$$

where

$$g_x = \begin{cases} g_{x0} & \text{if } \bar{B}^T P \dot{x} < -g_{x0} \\ -g_{x0} & \text{if } \bar{B}^T P \dot{x} > g_{x0} \\ -\bar{B}^T P \dot{x} & \text{if } |\bar{B}^T P \dot{x}| \leq g_{x0} \end{cases}, \quad (6.29)$$

$$g_e = \begin{cases} g_{e0} & \text{if } e < -g_{e0} \\ -g_{e0} & \text{if } e > g_{e0} \\ -e & \text{if } |e| \leq g_{e0} \end{cases}. \quad (6.30)$$

The modification is applied to all update laws given in (6.11)–(6.19). The values for g_{x0} and g_{e0} depend on the size of the uncertainties. The principal idea behind the dead zone is to monitor the size of the estimation error and adapt only when the estimation error is large relative to the modeling error [26]. The updating stops

if $|e|$ and $|\overline{B}^T P \dot{x}|$ less than predefined values g_{e0} and g_{x0} , respectively. Since the update law does not trust the measured values and treat them as noise.

By using a dead-zone modification, we loose the convergence of the signals. However, we are able to maintain the stability of the equilibrium in spite of bounded disturbances and dynamic uncertainties.

6.3 Experiment Setup and Results

The designed adaptive controller is implemented to a Matlab code on a PC. The communication between PC and μC is established through serial ports. AirCat is placed in a wave tank which is shown in Figures 6.3 and 6.4. The wave tank is first developed as a laboratory arrangement for a surface wave study at Florida Atlantic University. The tank is 77 cm deep, 77 cm wide and 767 cm long. A mechanism which generates imperfect sinusoidal wave patterns with 0–3 cm range of wave amplitude and 7–13 rad/sec range of circular frequency, is placed at one end of the tank. In order to prevent the reflection of waves, an attenuator is developed and placed to the other end of the tank. The heave rate of AirCat for feedback is obtained by filtering unbiased heave acceleration which is measured by IMU, with a bandpass filter (a low pass filter in conjunction with a high pass filter). The overall experiment setup is illustrated in Figure 6.5. Time and frequency domain heave results are given in Figures 6.6 and 6.7, respectively.



Figure 6.3: Picture of the wave tank located in Hydrodynamic Lab at Florida Atlantic University.

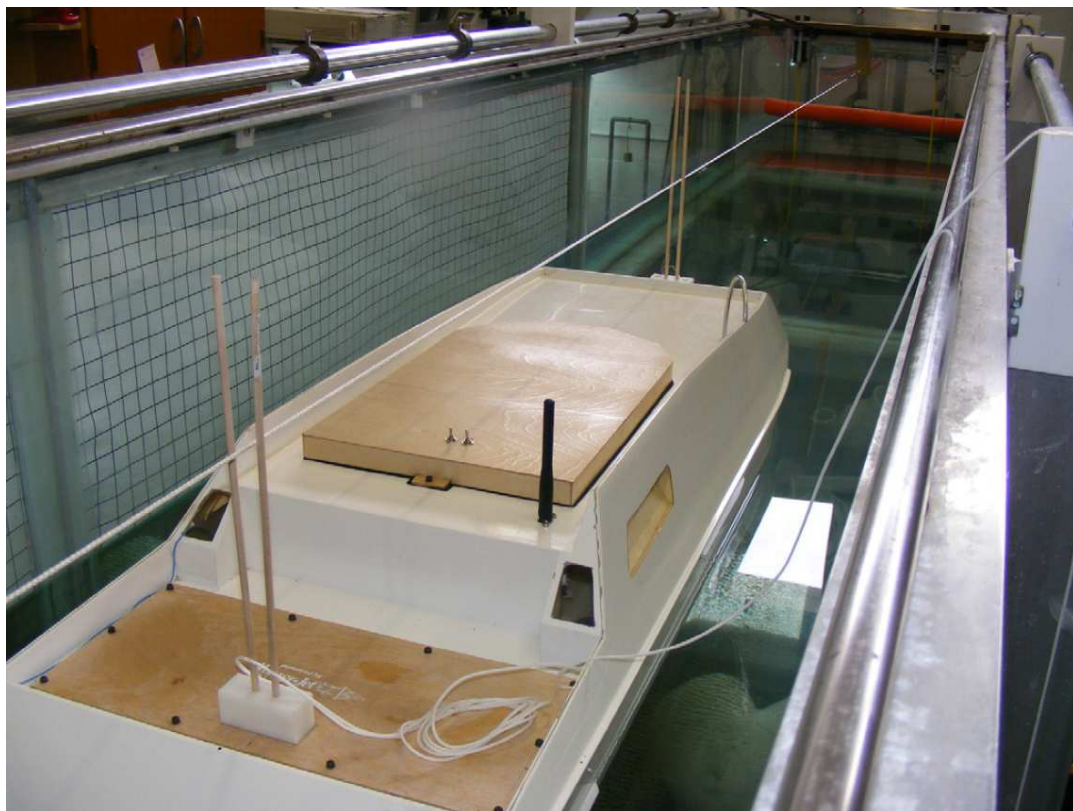


Figure 6.4: Picture of the AirCat taken in the wave tank while heading to the wave generator.

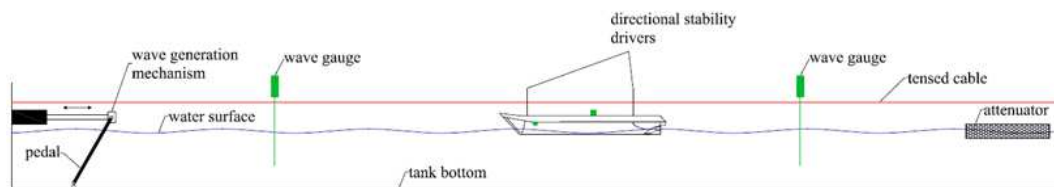


Figure 6.5: Illustration of the experiment setup located in Hydrodynamic Lab at Florida Atlantic University.

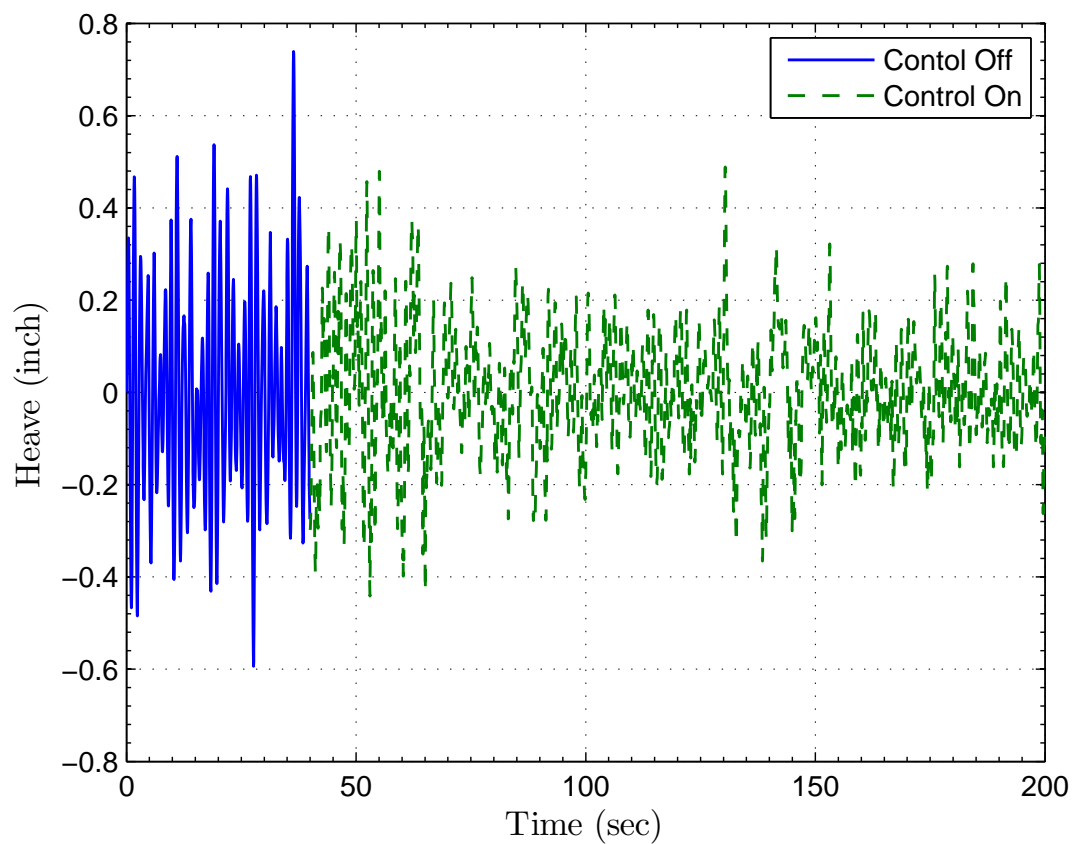


Figure 6.6: Heave of AirCat in the wave tank. The controller is turned on at 40 seconds.

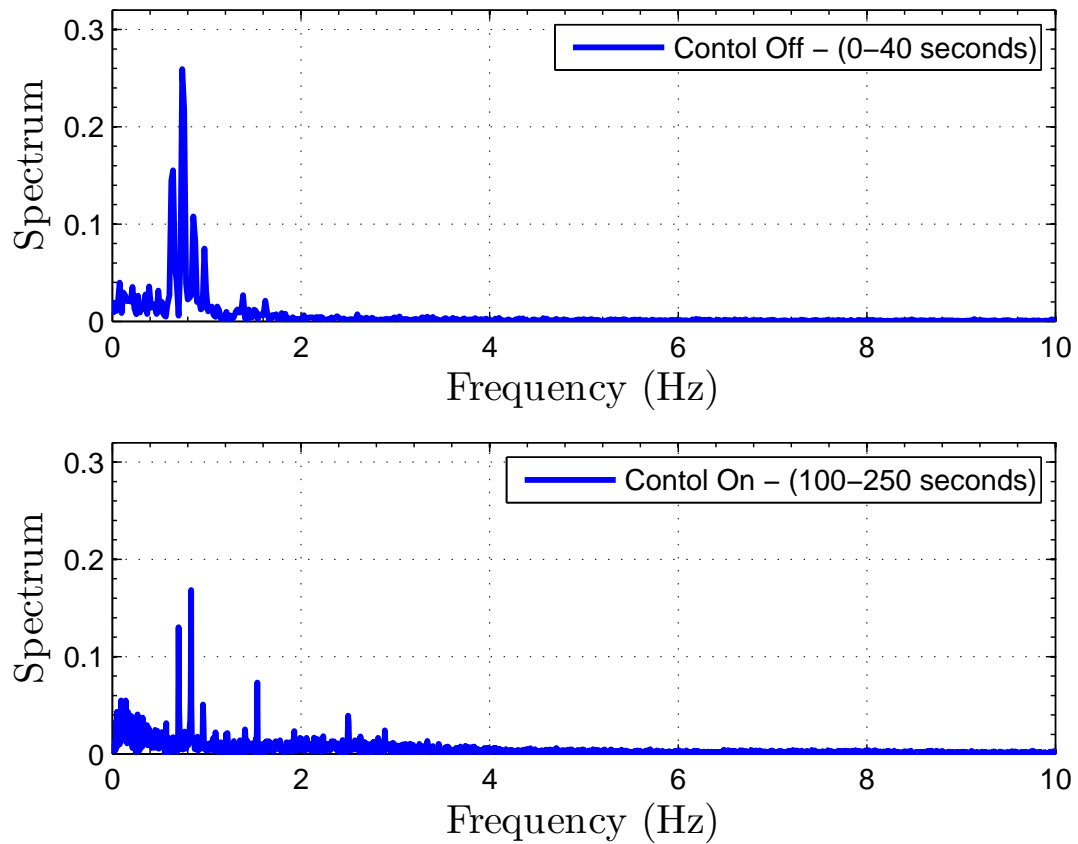


Figure 6.7: Heave response of AirCat in frequency domain. First figure in the plot represents the response heave when the control is off (0-40 sec), the second figure represents the steady state response of heave when the controller is on (100-250 sec).

Bibliography

- [1] A. A. Bobtsov, and A. A. Pyrkin, “Compensation of unknown sinusoidal disturbances in linear plants of arbitrary relative degree,” *Automation and Remote Control*, **70**, pp.449–456, 2009.
- [2] A. J. Sorensen, and O. Egeland, “Design of ride control system for surface effect ships using dissipative control,” *Automatica*, **31**, pp. 183–199, 1995.
- [3] A. L. Silver, and M. J. Hughes, “A method of evaluating multi-vessel surface effect ship motion prediction codes,” *Proceedings of Conference on Grand Challenges in Modeling and Simulation*, 2010.
- [4] A. Serrani, and A. Isidori, “Global robust output regulation for a class of nonlinear systems,” *Systems and Control Letters* , **39**, pp. 133–139, 2000.
- [5] A. Serrani, A. Isidori, and L. Marconi, “Semiglobal nonlinear output regulation with adaptive internal model,” *IEEE Transactions on Automatic Control*, **46**, pp. 227–236, 2001.
- [6] A. Serrani, “Hybrid external models, and the rejection of harmonic disturbances at the controller input,” *Proceedings of the 43rd IEEE Conference on Decision and Control*, pp. 668–673, 2004.
- [7] B. S. H. Connell, W. M. Milewski, B. Goldman and D. C. Kring “Single and multi-body surface effect ship simulation for T-Craft design evaluation,” *Proceedings of 11th International Conference on Fast Sea Transportation*, 2011.
- [8] C. C. Fang, H. S. Chan and A. Incecik, “Investigation of motions of catamarans in regular waves-I,” *Ocean Engineering*, **23**, pp. 89–105, 1996.
- [9] C. D. Johnson, “Accommodation of external disturbances in linear regulator and servomechanism problems,” *IEEE Transactions on Automatic Control*, **16**, pp. 635–644, 1971.
- [10] D. A. Francis, and W. N. Wonham, “The internal model principle for linear multivariable regulators,” *Applied Mathematics and Optimization*, **2**, pp. 170–194, 1975.

- [11] D. Bertin, S. Bittani and S. M. Savaresi, "Decoupled cushion control in ride control systems for air cushion catamarans," *Control Engineering Practice*, **8**, pp. 191–203, 2000.
- [12] D. Vassalos, N. Xie, A. Jasionowski and D. Konovessis, "Stability and safety analysis of the air-lifted catamaran," *Ships and Offshore Structures*, **3**, pp. 91–98, 2008.
- [13] E. de Souza and S. P. Bhattacharyya, "Controllability, observability and the solution of $AX - XB = C$," *Linear Algebra and Its Applications*, **39**, pp. 167–188, 1981.
- [14] H. I. Basturk, and M. Krstic, "Adaptive cancelation of matched unknown sinusoidal disturbances for LTI systems by state derivative feedback," *Journal of Dynamic Systems, Measurement, and Control*, **135**, 2013.
- [15] H. I. Basturk, and M. Krstic, "Adaptive cancelation of unmatched unknown sinusoidal disturbances for LTI systems by state derivative feedback," *Proceedings of the 5th ASME Dynamic Systems and Control Conference*, 2012.
- [16] H. I. Basturk, and M. Krstic, "Adaptive cancelation of matched unknown sinusoidal disturbances for unknown LTI systems by state derivative feedback," *Proceedings of the American Control Conference*, 2012.
- [17] H. I. Basturk, and M. Krstic, "Adaptive cancelation of unmatched unknown sinusoidal disturbances for unknown LTI systems by state derivative feedback," *Proceedings of the 2012 IEEE Conference on Decision and Control*, 2012.
- [18] K. S. Narendra and A. M. Annaswamy, *Stable Adaptive Systems*, Prentice Hall, 1989.
- [19] L. Marconi, A. Isidori, and A. Serrani, 2002, "Autonomous vertical landing on an oscillating platform: an internal-model based approach," *Automatica*, **38**, pp. 21–32.
- [20] L. Marconi, A. Isidori, and A. Serrani, "Non-resonance conditions for uniform observability in the problem of nonlinear output regulation," *Systems and Control Letters*, **53**, pp. 281–298, 2004.
- [21] M. Bodson, and S. Douglas, "Adaptive algorithms for the rejection of sinusoidal disturbances with unknown frequency," *Automatica*, **33**, pp. 2213–2221, 1997.
- [22] M. Krstic, I. Kanellakopoulos and P. Kokotovic, *Nonlinear and Adaptive Control Design*, Wiley, 1995.

- [23] N. Khaled, and N. G. Chalhoub, "Guidance and control scheme for under-actuated marine surface vessels," *Proceedings of the American Control Conference*, 2010.
- [24] N. Khaled, and N. G. Chalhoub, "A dynamic model and a robust controller for a fully actuated marine surface vessel," *Vibro-impact Dynamics of Ocean Systems*, **44**, pp. 135–148, 2009.
- [25] O. M. Faltinsen *Hydrodynamics of High-Speed Marine Vehicles*, Cambridge University Press, 2005.
- [26] P. Ioannou and J. Sun, *Robust Adaptive Control*, Prentice-Hall, 1996.
- [27] P. J. Willard, and L. Moskowitz, "A proposed spectral form for fully developed wind seas based on the similarity theory of S. A. Kitaigorodskii" *Journal of Geophysical Research*, **69** (1964): 5181-190
- [28] R. Marino, and P. Tomei, "Adaptive tracking and disturbance rejection for uncertain nonlinear systems," *IEEE Transactions on Automatic Control*, **50**, pp. 90–95, 2005.
- [29] R. Marino, and G. L. Santosuosso, "Global compensation of unknown sinusoidal disturbances for a class of nonlinear nonminimum phase systems," *IEEE Transactions on Automatic Control*, **50**, pp. 1816–1822, 2005.
- [30] R. Marino, and P. Tomei, "Robust adaptive regulation of linear time-varying systems," *IEEE Transactions on Automatic Control*, **45**, pp. 1301–1311, 2000.
- [31] R. Marino, G. L. Santosuosso, and P. Tomei, "Robust adaptive compensation of biased sinusoidal disturbances with unknown frequency," *Automatica*, **39**, pp. 1755–1761, 2003.
- [32] S. K. Kwak, G. Washington, and R. K. Yedavalli, "Acceleration-based vibration control of distributed parameter systems using the 'reciprocal state-space framework'," *J. Sound and Vibr.*, **251**, pp. 543–557, 2002.
- [33] T. Perez, and G. C. Goodwin, "Constrained predictive control of ship fin stabilizers to prevent dynamic stall," *Control Engineering Practice*, **16**, pp. 482–494, 2008.
- [34] T. Perez, and M. Blanke, "Ship roll damping control," *Annual Reviews in Control*, **36**, pp. 129–147, 2012.
- [35] T. Perez, and T. I. Fossen, "A Matlab toolbox for parametric identification of radiation-force models of ships and offshore structures," *Modeling, Identifications and Control*, **30**, pp. 1–15, 2009.

- [36] T. Perez, and T. H. Fossen, "Practical aspects of frequency-domain identification of dynamic models of marine structures from hydrodynamic data," *Ocean Engineering*, **38**, pp. 426–435, 2011.
- [37] T. I. Fossen, *Guidance and Control of Ocean Vehicles*, Wiley, 1994.
- [38] V. O. Nikiforov, "Observers of external deterministic disturbances. II. objects with unknown parameters," *Automation and Remote Control*, **65**, pp. 1724–1732, 2004.
- [39] V. O. Nikiforov, "Observers of external deterministic disturbances. I. objects with known parameters," *Automation and Remote Control*, **65**, pp. 1531–1541, 2004.
- [40] Z. Zhang, and A. Serrani, "The linear periodic output regulation problem," *System and Control Letters*, **55**, pp. 518–529, 2006.
- [41] X. Guo, and M. Bodson, "Analysis and implementation of an adaptive algorithm for the rejection of multiple sinusoidal disturbances," *IEEE Transactions on Control Systems Technology*, **17**, pp. 40–50, 2009.
- [42] K. B. Ariyur, and M. Krstic, "Feedback attenuation and adaptive cancellation of blade vortex interaction on a helicopter blade element," *IEEE Transactions on Control Systems Technology*, **7**, pp. 596–605, 1999.
- [43] Bodson, M., Jensen, J. S., and Douglas, S. C, "Active noise control for periodic disturbances," *IEEE Transactions on Control Systems Technology*, **9**, pp. 200–205, 2001.
- [44] L. Gentili, and L. Marconi, "Robust nonlinear disturbance suppression of a magnetic levitation system," *Automatica*, **39**, pp. 735–742, 2003.
- [45] A. Salem, and K. Said "A simple proof of Sylvester's (Determinants) Identity," *Applied Mathematical Sciences*, **32**, pp. 1571–1580, 2008.
- [46] V. O. Nikiforov, "Nonlinear servocompensation of unknown external disturbances," *Automatica*, **37**, pp. 1617–1653, 2001.
- [47] Z. Ding, "Universal disturbance rejection for nonlinear systems in output feedback form," *IEEE Transactions on Automatic Control*, **48**, pp. 1222–1227, 2003.
- [48] T. H. S. Abdelaziz and M. Valášek, "Pole-placement for SISO linear systems by state-derivative feedback," *IEE Proceedings of The Control Theory and Applications*, **151**, pp. 377–385, 2004,.

- [49] T. H. S. Abdelaziz, “Robust pole assignment for linear time-invariant systems using state-derivative feedback,” *Journal of Systems and Control Engineering*, **223**, pp. 187–199, 2008.
- [50] W. Michiels, T. Vyhlídal, H. Huijberts, and H. Nijmeijer, “Stabilizability and stability robustness of state derivative feedback controllers,” *SIAM Journal on Control and Optimization*, **47**, pp. 3100–3117, 2009.